SYSTEMS ANALYSIS
OF INOTROPIC INTERVENTIONS
IN
ISOLATED HEART MUSCLE

A thesis submitted to

The University of London

for the

Doctor of Philosophy Degree

by

MICHAEL OWEN TOLL, B.E.Sc.

Department of Physiology

University College, London

and

Department of Electrical Engineering

Imperial College of Science and Technology

January 1973

ABSTRACT

Calcium as an inotropic agent is an important factor in determining the contractility of the heart. Although the myofilaments in both skeletal and cardiac muscle appear to be activated by a rise in intracellular calcium concentration, the calcium movements involved in activation are thought to be quite different for the two types of muscles.

The purpose of this research project was to try to determine calcium dynamics at the cellular level by using a systems analysis approach. It was felt that if this objective could be achieved, then this approach could be extended to study the dynamics of other inotropic agents.

The preparation used was isolated kitten papillary muscle. As the isometric tension produced by the heart is directly related to the extracellular calcium concentration, the papillary muscle was considered as a system with calcium concentration as input, and peak isometric tension as output. The two methods of analysis chosen were step-response and impulse-response, the latter being determined by pseudo-random analysis.

A computer-based data acquisition and analysis system was developed that was capable of measuring a number of parameters for each muscle contraction in real-time, and on a beat-to-beat basis. In addition, the computer generated the pseudo-random binary sequences, and controlled the switching of a set of superfusion valves.

Computer simulated step-responses based on diffusion and experimentally derived dose-response curves were found to match the experimental data quite well. The non-linear dose-response curve introduced direction-dependent dynamics into the system. This was reflected as discontinuities in the impulse-response curve and could be seen in the step-response curves.

Because the isolated papillary muscle system is severely diffusion limited, it is difficult to separate the diffusion effects from those that may be physiological in origin. Therefore, it can be concluded that step-response or impulse-response methods of analysis are not likely to yield suitable physiological dynamic information in the study of drugs acting as inotropic agents.

ACKNOWLEDGMENTS

First I would like to express my gratitude to Dr. B.R. Jewell, who supervised this project with the assistance of Professor B. McA. Sayers. The work was begun during the tenure of an Athlone Fellowship, provided by the Department of Trade and Industry, and completed during the tenure of a Canadian Heart Foundation Fellowship. I would like to take this opportunity of thanking both organisations for their generous support, and the British Heart Foundation, who met the costs of the laboratory work through a research award to Dr. Jewell.

I would also like to express my appreciation to Professor D.R. Wilkie, F.R.S. and to the members of the Department of Physiology at University College for their kind hospitality; to Dr. K. Kedzior for his generous help in the preparation of some of the diagrams; to Dr. D. Allen for assisting in the transcription of hundreds of numbers; and to Mr. G. Read, Mr. E. Chappell, and Mrs. J. Davis for skilled technical assistance.

Finally, I would like to thank Professor A.F. Huxley, F.R.S. for his comments on the section on diffusion; to Dr. P.A. Lynn for his comments on the digital signal processing section; and to Dr. K.R. Godfrey and Mr. P.A.N. Briggs for providing me with a pre-publication copy of their paper on direction-dependent dynamics in relation to pseudo-random analysis.

M.O. Toll

1 December 1972

TABLE OF CONTENTS

		Page
ABSTRACT		2
ACKNOWLEDGMENTS		4
TABLE OF CONTENTS		5
CHAPTER 1	CALCIUM AND MYOCARDIAL CONTRACTILITY	8
	1.1 Introduction	8
	1.2 Excitation-Contraction Coupling in Cardiac Muscle	9
	1.3 Rationale of Present Work	14
CHAPTER 2	ANALYTICAL METHODS	17
	2.1 Introduction	17
	2.2 Step-Response Analysis	20
	2.2.1 Some basic assumptions for papillary muscles	22
	2.2.2 A diffusion model for papillary muscles	24
	2.3 Impulse Response Analysis	31
	2.3.1 The input-output relationship of a system	32
	2.3.2 Correlation as a measure of the input-output relationship	33
	2.3.3 Pseudo-random binary signals	35
	2.3.4 Correlation properties of pseudo-random sequences	40
CHAPTER 3	THE EXPERIMENTAL SYSTEM	43
	3.1 Introduction	43
	3.2 Data Acquisition and Computer Control	44

3.3 Digital Signal Processing System 46

3.4 Force Transducer 48

3.5 Muscle Clamp 51

3.6 The Superfusion System 51

3.6.1 Introduction 51

3.6.2 Superfusion control valves 52

3.6.3 Principle of operation 54

3.6.4 Flow regulation and temperature control 55

3.6.5 Fluid Delivery and switching 58

3.6.6 The electronic control system 60

CHAPTER 4 EXPERIMENTAL METHODS 62

4.1 Experimental Preparation 62

4.2 Dissection and Mounting of the Papillary Muscle 63

4.3 Experimental Protocol 65

CHAPTER 5 RESULTS 69

5.1 Introduction 69

5.2 The Steady-State Dose-Response Curve 70

5.3 Step-Response Analysis 73

5.3.1 The influence of calculation methods and the shape of the dose-response curve on tension transients 73

5.3.2 Comparison between experimental and theoretical step-responses 78

5.4 Pseudo-Random Analysis 86

5.4.1 Determination of the pseudo-random sequence length 86

5.4.2 Experimental pseudo-random results 87

CHAPTER 6 DISCUSSION 94

6.1 Steady-State Relationship Between Calcium Concentration and Isometric Tension 94

6.2 Step-Response 97

6.3 Impulse Response 102

CHAPTER 7 CONCLUSIONS AND RECOMMENDATIONS 107

BIBLIOGRAPHY 109

APPENDIX A PHYSICAL FACTORS AFFECTING MYOCARDIAL CONTRACTILITY 115

APPENDIX B ANALYSIS OF EXPONENTIAL CURVES 122

APPENDIX C THE COMPUTER INTERFACE 125

APPENDIX D DIGITAL SIGNAL PROCESSING 144

APPENDIX E FLOW CHART OF DATA ACQUISITION AND PROCESSING PROGRAM 167

APPENDIX F PSEUDO-RANDOM SUBROUTINE FLOW CHART 175

APPENDIX G SUPERFUSION ELECTRONIC CONTROL SYSTEM 180

APPENDIX H SIMULATION PROGRAM FOR STEP-RESPONSES 186

APPENDIX I TRANSIENT-FREE SWITCH REPRINT

CHAPTER 1

CALCIUM AND MYOCARDIAL CONTRACTILITY

1.1 Introduction

Cardiac muscle can be considered to be a multiple input-dual output system. The inputs can be broadly classified as mechanical, electrical, and chemical (Appendix A), and the output consists of two prime variables, tension and length, both of which are functions of time.

The output variables describe the contractile state of the heart, but a thorough description of a change in contractility is not easy and usually requires the use of several of the possible relationships between the variables (Blinks & Jewell, 1972). Sometimes it is possible to use tension alone as a measure of contractility but only in the cases when the time-to-peak tension (t_{pk}) does not change appreciably with a change of one of the input variables. This condition can be met if the muscle is allowed to contract isometrically (at a constant length). Thus if the length is fixed, and the time remains constant, the only output variable

that can change is tension.

If a change in one of the input parameters causes a change in contractility then that change of input is called an inotropic intervention. By convention, an increase in contractility is called a positive inotropic effect, and a decrease in contractility is called a negative inotropic effect.

Calcium is one input variable that alters myocardial contractility but does not have a marked effect on the time-to-peak tension. Therefore the heart, or an isolated heart muscle, can be studied as a system with calcium as the input and isometric tension as the output. However, in order to be able to make an effective analysis of the calcium-tension relationship it is necessary to control the other input variables. Appendix A reviews those input parameters - length, temperature, and frequency of stimulation - that have an effect on the contractility of the myocardium.

1.2 Excitation-Contraction Coupling in Cardiac Muscle

In the late nineteenth century Sidney Ringer, working at University College London, published a paper "Concerning the influence exerted by each of the constituents of blood on contraction of the ventricle". In 1883 he published an additional paper, partly to retract his earlier work, but more important, to put forth an exciting discovery.

It appeared that in his earlier work, the saline solutions used to perfuse the hearts were made with water supplied by the New River Water Company, but when the same experiments were repeated using solutions made with distilled water different results were obtained. With judicious investigations Ringer soon discovered that it was the calcium impurities in the tap water that were responsible for his observations. In addition, he found

that the contractility of his preparation could be changed by varying the calcium concentration in the bathing medium, and by altering the temperature of the bath.

The next important discovery about excitation-contraction coupling in cardiac muscle was reported by Locke and Rosenheim in 1907. These authors reported that the electrical activity in the heart would persist for a long time after the mechanical response of the muscle had ceased as a result of perfusion with a calcium-free medium. The significance of the observations of Ringer and of Locke and Rosenheim did not become evident until much later.

It was not until the 1950s with the introduction of radioactive isotope tracer methods that the role of calcium in the heart was begun to be studied in earnest. However, parallel to these myocardial studies, experiments with skeletal muscle were yielding new insights into the structure and operation of muscle at the cellular level.

Striated muscle (skeletal and heart) is now known to consist of regularly spaced protein filaments of two types - one containing mainly actin and the other myosin. These filaments are so arranged that they overlap, and within the region of overlap the filaments interact to produce tension in the active muscle (see for example Wilkie, 1968, for a more detailed discussion of muscle structure).

In the resting state, the calcium concentration in the sarcoplasm (the region surrounding the myofilaments within the cell membrane) is about 10^{-7} M. When the muscle is stimulated, an action potential causes calcium to be released from internal stores (skeletal muscle) and the calcium concentration in the sarcoplasm rises to about 10^{-5} M. This increased calcium concentration activates the myofilaments and the muscle contracts. Relaxation is brought about by the active sequestration of calcium from the sarco-

plasm to lower the calcium concentration back to 10^{-7} M. A considerable amount of calcium is stored in the sarcoplasmic reticulum, and it is because of this that a skeletal muscle can contract at least seven times before the calcium needs to be recycled (Winegrad, private communication).

When skeletal muscle is placed into a calcium-free bath it will continue to contract for a long time. This indicates that the extracellular space (region within a muscle surrounding a muscle cell) in skeletal muscle plays a very small role in the excitation-contraction process. In heart muscle this is not the case, for without calcium in the extracellular space, the myocardium cannot contract (e.g. Ringer, 1883). Thus the presence of calcium in the extracellular space is crucial to the excitation-contraction process in heart muscle.

Isotope studies have indicated that the distribution of calcium in cardiac muscle is complex and compartmentalized. Winegrad and Shanes (1962) found kinetic evidence for three components of calcium exchange while Langer (1971) has claimed to have found five components in his Ca^{45} washout curves. In addition, Niedergerke (1957), and Shine, Serena and Langer (1971) have reported that the time course of Ca^{45} washout is much longer than the corresponding tension changes when the external calcium concentration is changed.

Niedergerke (1957) also reported that the time course of tension followed quite closely that of calcium diffusing through the extracellular space although his diffusion constant was smaller by a factor of four than what was expected for diffusion through the extracellular space. Thus it seemed likely that external calcium has a direct effect on the tension produced by a muscle, and that calcium is actively taken up by the cells, either through adsorption onto the cell surfaces or by actual uptake into the cells.

Additional weight was given to the hypothesis that calcium was bound to the surface membrane by the studies of Niedergerke and Lüttgau (1957). They showed that in frog heart muscle the tension developed depends upon the ratio of the external calcium concentration to the square of the external sodium concentration. It was felt that sodium and calcium were both active competitors for membrane binding sites, and that by increasing the sodium concentration, calcium was displaced from the membrane with a resulting diminution in the tension produced by the muscle.

Lanthanum, a rare earth element, has been shown to bind to superficial membrane sites and has been used as a stain for these sites for electron microscopy. If lanthanum is added to the bathing solution, Sanborn and Langer (1970) have shown that there is an immediate reduction in tension, and the contractile tension remains depressed until the lanthanum is removed. It can therefore be concluded that as soon as lanthanum reaches the cell surface it displaces calcium from superficial membrane-bound sites.

Further evidence that calcium is stored intracellularly can be obtained from the isotope studies of Winegrad and Shanes (1962), and Sands and Winegrad (1970). Their results, respectively, show that the influx of calcium is beat dependent, and that the total calcium content is also beat dependent, both increasing with an increase in the frequency of stimulation.

Experiments using voltage clamp techniques (Wood, Heppner, & Weidmann, 1969) indicated that the duration and magnitude of the plateau phase of the action potential is the chief determinant of the inotropic state of cardiac muscle under steady-state conditions. Beeler and Reuter (1970b) showed that a slow inward current of calcium flows during the plateau phase of the action potential, and that this current is very sensitive to the variations in the external calcium concentration. In a subsequent paper (Beeler & Reuter, 1970c), the authors described how both the magnitude of the

calcium current and the tension produced by the muscle varies in proportion to the external calcium concentration; if this concentration is reduced to zero, no calcium current flows and no tension is produced. However, they also noted that steady-state contractions were obtained only after five to eight identical depolarizations. This beat dependency for the transient to decay was also noted by Wood et al. (1969).

If one is to explain the indirect effect of calcium current on tension, one must propose some intracellular site(s) where at least a fraction of the calcium flowing into the cell during depolarization is rapidly inactivated before any appreciable activation of the contractile protein system takes place. This stored calcium can then be released from these sites during subsequent action potentials to activate contraction by some unknown mechanism that is dependent on depolarization. Beeler and Reuter also mention that during rest, calcium is transported both into and from the cell. The net calcium transport in the outward direction, and its rate are dependent upon the external sodium concentration. On the other hand, internal sodium promotes a calcium influx into the cell. Thus an equilibrium is reached where the amount of calcium entering during an action potential and while at rest is balanced by the carrier mechanism extruding calcium from the cell.

The exact pathways that calcium follows within the myocardial cell is unknown, and there is much speculation about whether calcium is recycled between intracellular storage sites and the filaments, as it is in skeletal muscle, or whether there is a one way movement of calcium from the extracellular space through some intermediate storage site, membrane or otherwise, to the myofilaments, and then back to the extracellular space possibly through another intermediate storage site.

This latter view is taken by Langer (1971). In his model the sequence of calcium movements is as follows: 1) Calcium in the extracellular space is the source of calcium on binding sites in the cell and T-system membrane. 2) The calcium at these sites is controlled, in part, by the intracellular to extracellular sodium gradient. As this gradient increases, more calcium is bound to the membrane. 3) After stimulation, calcium is released from these binding sites and diffuses to the myofilaments to initiate contraction. 4) Relaxation is accomplished by binding and storage of calcium in the sarcotubular system. This is considered to be an irreversible process. 5) The stored calcium exchanges through the lateral cisternae to the T-tubules and then back into the extracellular space.

1.3 Rationale of Present Work

From the previous discussion it is clear that the isometric tension produced by the myocardium is directly dependent upon the external calcium concentration. What is equally clear is that the way in which calcium enters the myocardial cell and the pathways taken before it activates contraction has yet to be determined.

Chapman and Niedergerke (1970a,b) have studied the time course of the transient change in isometric tension in frog heart ventricles in response to changes in external calcium concentration. They found that their step-response curves could be separated into two exponential components which they called a fast phase and a slow phase. These two phases were considered to be a measure of two hypothetical calcium compounds whose concentrations inside the heart cells changed at different rates as the influx of calcium was altered. It was felt that the strength of the contractions was determined by the co-operative action of these two compounds

inside the cells.

No comparable studies have been undertaken for mammalian heart, and as it is morphologically quite different from amphibian heart (e.g. Fawcett & McNutt, 1969; Page & Niedergerke, 1972) it is difficult to draw conclusions about mammalian heart muscle from results taken from frog heart. Therefore, it was decided to conduct similar dynamic studies on isolated kitten papillary muscles.

If the tension dynamics for mammalian heart muscle, and in particular for a papillary muscle, can be shown to exhibit separable time constants, then the next stage is to try and match these values to specific identifiable physiological structures or compartments within the muscle. In this way it is hoped that the possible compartments and pathways of calcium through the myocardium can be traced.

In addition to making step-response measurements of tension, it was felt that a more meaningful measure of the dynamics could be obtained from the impulse response of the muscle. Thus the papillary muscle was considered as a system with calcium concentration as input, and isometric tension as output. By drawing on systems analysis techniques it was felt that a worthwhile approach to the determination of the impulse response would be to inject noise into the input of the system. This could be achieved by switching the calcium concentration surrounding the papillary muscle in a pseudo-random manner. The impulse response could then be obtained directly by crosscorrelating the output signal with the input signal (see Section 2.3).

The pseudo-random approach has not been tried before for this type of investigation, and consequently suitable apparatus had to be designed from first principles. Although pseudo-random generators and correlators were available commercially, none were available in the Department of

Physiology. As a result, data acquisition, measurement, and analysis were carried out on a LINC-8 digital computer located within the department. This computer was also used to generate the pseudo-random sequences and to control the switching of the calcium concentrations.

If, by using the methods of analysis mentioned above, the dynamics of calcium at the cellular level can be determined, then this approach can be extended to study the dynamics of other drugs that act as inotropic agents.

CHAPTER 2

ANALYTICAL METHODS

2.1 Introduction

The majority of investigations into the kinetics of calcium movements in heart muscle have been made using radioactive calcium, Ca^{45} (e.g. Langer & Brady, 1963; Winegrad & Shanes, 1962). Also a number of papers have been published which describe the steady-state effects that a change in external calcium concentration has on the mechanical properties of heart muscle (e.g. Nayler, 1960; Sands & Winegrad, 1970; Shine, Serena & Langer, 1971). Usually, these results have been obtained in conjunction with isotope or other studies, and there has been only one systematic study - to the best of the author's knowledge - of the relationship between calcium concentration and mechanical response (Chapman & Niedergerke, 1970a,b).

In attempting to establish a model for the kinetics of calcium movement within the myocardium and how it influences tension, two different approaches can be used. One is to start with the ultrastructure of the

heart cell, and by identifying its constituent parts and their normal function in relation to calcium and tension production, a model can be proposed (Page & Niedergerke, 1972). As a variation to this method, one can look more at the gross structure of the muscle and form a hypothesis of calcium movement based initially on physical processes, such as diffusion, which can influence calcium transport.

The other method of modelling is to treat the muscle as an unknown system, a "black box", and by using suitable input and output signals, a model can be derived that is based on the relationship between these two signals.

If this latter method is chosen, an initial model of the system can be formed based on the theory of linear systems (see for example Lathi for a description of linear systems). The analysis can then be carried out in either the time domain or the frequency domain. If the time domain is used, the model is called the impulse response of the system, and if the frequency domain is used, the model is called the transfer function of the system.

There are three fundamental input signals that can be chosen to excite the system under test, namely sinusoidal, step, and impulse signals. Each one can be used to determine the transfer function or impulse response of the system which then defines both the steady-state and dynamic characteristics of the system provided that it is linear. If it is not linear, it is still possible to arrive at a model by obtaining a piecewise-linear approximation to the system at a number of different steady-state operating levels.

Sinusoidal analysis has been the classical method of analysis, and by its nature it is carried out in the frequency domain. This method is slow as only one frequency can be tested at a time. In this investigation, cal-

cium concentration was used as the input variable to the heart muscle system while isometric tension was the measured output. Quite clearly it is a difficult technical problem to change the input concentration in a sinusoidal manner, and therefore, consideration of this method of analysis can be eliminated. This leaves the step-response and impulse response methods to be considered.

These remaining methods have the advantage of testing more than one frequency at a time. A step input, however, does not test all frequencies uniformly as its frequency spectrum is hyperbolic in shape. On the other hand, an impulse, which contains a uniform distribution of all frequencies, can test all frequencies simultaneously.

Since an impulse has the same frequency properties as pure white noise, i.e. a uniform frequency spectrum, both signals are ideally suited for systems analysis. In conjunction with these input signals, powerful analytical methods of correlation and/or spectrum analysis can be used in the time or frequency domain respectively, to arrive at a suitable model of the system.

In order to make a comparison of our results with those of the published literature, the two approaches in modelling, as described above, were used. In the first method, the papillary muscle was considered to be a homogeneous cylinder and a model was developed, based on diffusion, to describe the tension transients obtained when the external calcium concentration was changed in a stepwise manner. These simulated step-response transient tension curves were then compared with the experimentally derived curves. For the signal analysis method, the input signal, calcium concentration, was changed in a pseudo-random manner. The resulting output signal, isometric tension, was then crosscorrelated with the input signal to obtain the impulse response of the muscle.

2.2 Step-Response Analysis

A step function input to a system yields the step-response which is the integral of the impulse response. Therefore, it is possible to obtain the impulse response directly by differentiating the step-response. However, to obtain reliable results in this way, large steps must be applied at the input, which, if the system is not linear, can drive it into the non-linear region distorting the results. If the magnitude of the step is reduced to overcome the problem of non-linearity, the inherent noise within the system may be sufficient to completely mask the results.

The step-response method is the one which has been used in all of the isotope and mechanical dynamic studies published to date. In these experiments the calcium concentration or radioactivity was changed in a stepwise manner and the resulting transient curve was then measured and analyzed using the method of "curve stripping" (Appendix B). It was found that these curves could be best described by a sum of exponential terms, and consequently the results were compartmentalized as to the various rate constants (time constants^{-1}) contained within the transient curve (Winegrad & Shanes, 1962; Langer & Brady, 1963). Attempts were then made to relate each one of the compartments to some physiological compartment within the muscle.

Langer (1971) has claimed to have resolved four to five compartments from his Ca^{45} washout curves while Winegrad and Shanes (1962) have resolved three components in their isotope studies. On the other hand, Chapman and Niedergerke (1970a,b) mention only two components in their mechanical transient curves, and Shine et al. (1971) state that they were able to fit only one exponential term to their tension transient curve even though they claim four components in their Ca^{45} washout curves.

Although claims as to the number of physiological compartments

present in their experimental preparation vary, there has been no attempt to form a mathematical model of the myocardium and to relate the results of the model to those found experimentally.

Diffusion has, at one time or another, entered into the discussion of calcium kinetics. For example, in the radioactive study of Langer and Brady (1963) they indicate that diffusion of Ca^{45} from the extracellular space should be 2.8 times as rapid as for sucrose. Yet for their washout curves of sucrose and Ca^{45}, the half-time for the Ca^{45} fast phase was five times longer than the corresponding value for the sucrose washout curve. Thus, there was a factor of fifteen difference between the half-time of Ca^{45} based on diffusion (0.4 min), and the measured half-time (6 min).

Niedergerke (1957) showed similar results when he compared the time course of the average calcium concentration within a muscle, determined from the average concentration diffusion equation of Hill's (1928, Eq. 47), to the time course of the tension transient curve obtained experimentally, and assuming a linear dose-response curve. He found a value for the diffusion constant that was a sixteenth of the free solution value for calcium.

One could reasonably expect the diffusion constant, determined by this method, to be reduced to about one-quarter of the free solution value (Harris & Burn, 1949), but not by a factor of sixteen. The expected reduction in value is probably due to the fact that, in reality, a muscle is not a homogeneous structure, but consists of tightly packed cells, connective tissue, etc., which act as mechanical obstructions to slow down the movement of calcium ions as they diffuse through the extracellular space. Any further reduction in the diffusion constant could be accounted for by the adsorption of calcium onto the surface of the cells, or by actual uptake into the cells (Niedergerke, 1957).

Due to the fact that the movements of calcium are much less than expected for free diffusion alone, it has been concluded that diffusion is not the rate limiting process, and that these methods are reasonable approaches to the study of calcium kinetics. This conclusion is reflected in later works (Chapman & Niedergerke, 1970a,b; Langer, 1971) in which diffusion effects have been completely neglected.

However, it was decided to construct a mathematical model that treats the papillary muscle as a homogeneous cylinder, and considers diffusion as the main mechanism by which calcium enters the muscle to change the internal calcium concentration. But before diffusion through a cylinder is discussed, some simplifying assumptions about papillary muscles must be made, and the physical relationship between concentration, cross-sectional area, and tension must also be examined.

2.2.1 Some basic assumptions for papillary muscles

In attempting to model a papillary muscle a few basic assumptions must be made. The first is that the papillary muscle can be best approximated by a cylinder. From this, and by measuring the length and weight of the muscle, the cross-sectional area A (mm^2), and the diameter d (mm), can be computed as

$$A = \frac{W}{L\rho} \tag{2.1}$$

$$d = 2\sqrt{\frac{A}{\pi}} \tag{2.2}$$

where W = muscle weight in mg

L = muscle length in mm

ρ = density of the muscle which is taken to be 1 mg/mm^3

If the muscle is assumed to be homogeneous then a normalized force p, expressed as g/mm^2 and represented by a small letter "p", can be derived for the muscle. The total force P_t (g, represented by a capital letter "P")* produced by that cross-section is the product of the normalized force p and the total area A. Therefore, for a cylindrical muscle of radius R, the absolute tension dP produced by a small ring of muscle of thickness dr at radius r is

$$dP = p2\pi rdr \tag{2.3}$$

The total force P_t produced over the whole cross-section is the integral of Eq. 2.3. Thus

$$P_t = \int_0^R p2\pi rdr \tag{2.4}$$

However, the steady-state dose-response curve indicates that tension is a non-linear function of calcium concentration. This relationship can be expressed as

$$p = f(c) \tag{2.5}$$

If the concentration within the muscle is not at equilibrium, then a gradient exists which is a function of both radius and time. Thus

$$c = f(r,t) \tag{2.6}$$

Therefore, by combining Eqs. 2.5 and 2.6 and substituting into Eq. 2.4

$$P_t = \int_0^R p(c,r,t)2\pi rdr \tag{2.7}$$

---

* NOTE for convenience all force measurements are expressed in grams rather than in gram-weight.

The difficulty that now arises is to find an analytical expression that can be applied to the function p(c,r,t).

2.2.2 A diffusion model for papillary muscles

When the calcium concentration at the surface of the muscle is suddenly changed, the only way that calcium can enter, or leave the muscle is by diffusion. In the intact heart this is not the case as the cells of the heart are brought into intimate contact with the blood by the coronary arteries. Therefore, for the isolated preparation, it is necessary to consider diffusion as the main mechanism by which calcium enters the muscle.

In 1928, A.V. Hill published an article on diffusion through tissue. In Section 2 of this paper he described diffusion from or into a homogeneous cylinder, and showed that the solution of the diffusion equation for this case is

$$\frac{c}{C} = 1 - 2\left[\frac{1}{s_1 J_1(s_1)} J_o\left(\frac{rs_1}{R}\right) e^{\left(\frac{-ks_1^2 t}{R^2}\right)} + \frac{1}{s_2 J_1(s_2)} J_o\left(\frac{rs_2}{R}\right) e^{\left(\frac{-ks_2^2 t}{R^2}\right)} + \cdots\cdots\cdots\right] \qquad (2.8)$$

This equation describes the concentration c, at any radius r, and at any time t, after a step change in concentration C has been applied to the surface of a cylinder of radius R. It is important to note that this equation describes the change in concentration from an initial steady-state level. J_o and J_1 are Bessel functions of zero and first order respectively, while s_1, s_2, s_3, ... are the zero values for $J_o(x)$. The first twenty values of s_i, $J_1(s_i)$, and $(s_i J_1(s_i))^{-1}$ are tabulated in Table 2.1. k is the diffusion constant which, if the radius is expressed in cm and the time

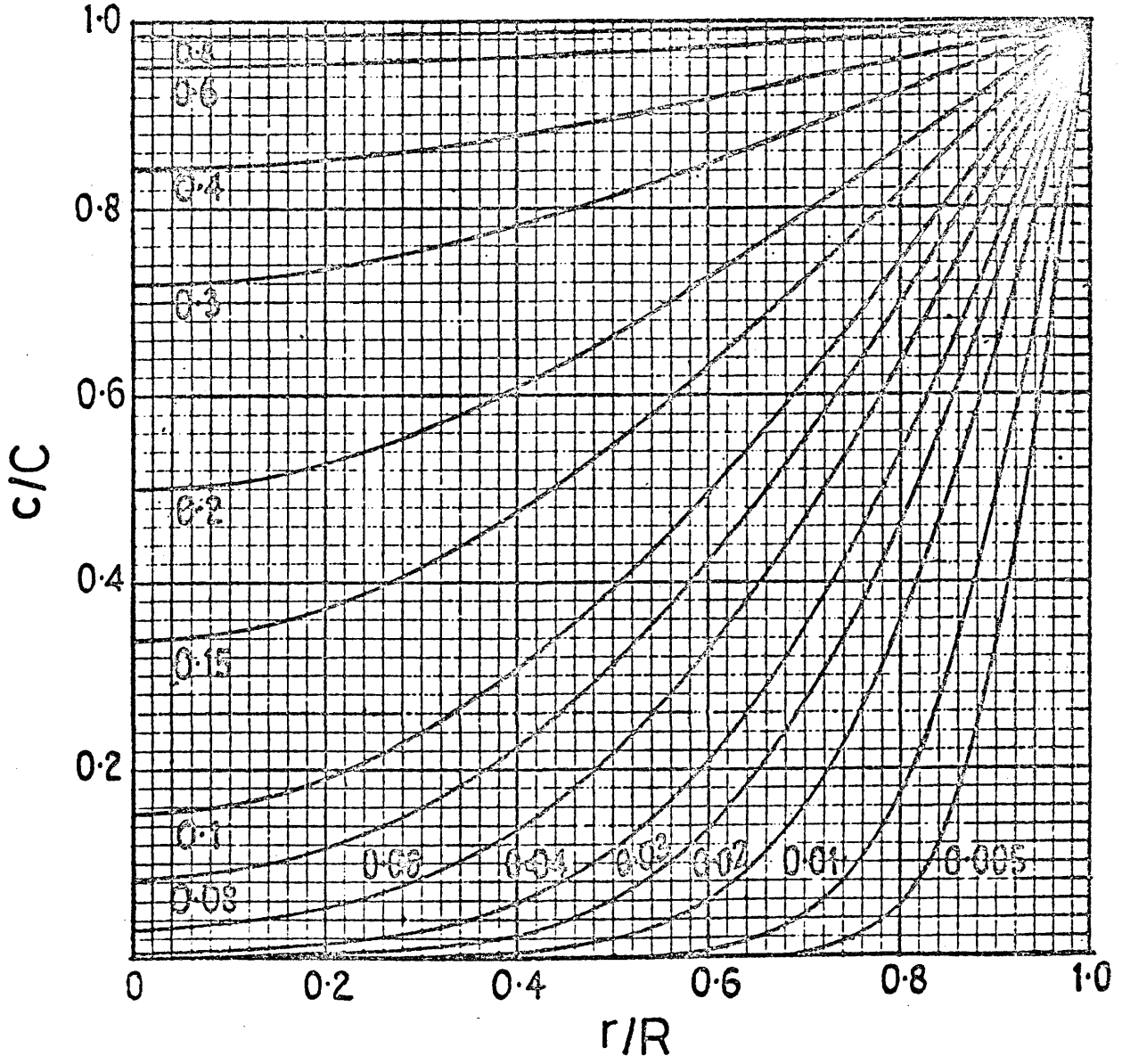

Fig. 2.1 Concentration distribution at various times in a cylinder of radius R. The numbers on the curves are the values of kt/R^2. Adapted from Carslaw and Jaeger Fig. 24.

is in seconds, has the units of cm^2/s.

A graphical representation of the solution of this equation is shown in Fig. 2.1. As can be seen, the outer shell of the muscle reaches equilibrium very quickly, but it takes much longer before the center of the muscle even begins to detect a change in concentration.

To simplify computations somewhat, Hill also showed that the average concentration $\bar{c}$, for the whole cylinder could be described as

$$\frac{\bar{c}}{C} = 1 - 4\left[\frac{e^{\left(\frac{-ks_1^2 t}{R^2}\right)}}{s_1^2} + \frac{e^{\left(\frac{-ks_2^2 t}{R^2}\right)}}{s_2^2} + \cdots\cdots\cdots\right] \qquad (2.9)$$

If this equation is substituted into the dose-response curve equation the value of tension could be computed directly for each instant of time. However, since the dose-response curve is non-linear (see Results, Section 5.2), the resulting tension transient would be in error. Therefore, it is necessary to substitute Eq. 2.8 into the dose-response curve to obtain an analytical expression for the function $p(c,r,t)$. Now to find the total tension P_t, it is necessary to integrate over the total cross-sectional area as in Eq. 2.7.

If this integration is attempted, however, it will be found to be extremely complex and unwieldy. So to overcome this difficulty, an approximation to this integration can be made if the muscle is considered to be composed of a number of concentric shells. By computing the area and concentration for each of these shells separately, the corresponding tensions can then be determined (Eq. 2.3). The total tension will be the sum of the individual tensions for each shell. Section 5.3.1 describes a comparison study of the tension transient results obtained by using the individual shell approximation and the average concentration equation for both linear and non-

i	S_i	$J_1(S_i)$	$(S_i J_1(S_i))^{-1}$
1	2.405	0.5191	0.8010
2	5.520	-0.3403	-0.5324
3	8.654	0.2714	0.4257
4	11.792	-0.2325	-0.3648
5	14.931	0.2066	0.3243
6	18.071	-0.1877	-0.2948
7	21.212	0.1733	0.2721
8	24.352	-0.1617	-0.2539
9	27.493	0.1522	0.2390
10	30.635	-0.1442	-0.2264
11	33.776	0.1373	0.2156
12	36.917	-0.1313	-0.2063
13	40.058	0.1261	0.1980
14	43.200	-0.1214	-0.1907
15	46.341	0.1172	0.1841
16	49.483	-0.1134	-0.1782
17	52.624	0.1100	0.1728
18	55.765	-0.1068	-0.1678
19	58.907	0.1040	0.1633
20	62.048	-0.1013	-0.1591

Table 2.1

i	r/R										
	0.0	0.1	0.2	0.3	0.4	0.5	0.6	0.7	0.8	0.9	1.0
1	1.0000	0.9856	0.9430	0.8740	0.7817	0.6696	0.5434	0.4075	0.2673	0.1302	0.0000
2	1.0000	0.9253	0.7177	0.4233	0.1059	-0.1684	-0.3469	-0.4026	-0.3390	-0.1880	0.0000
3	1.0000	0.9214	0.8802	-0.0950	-0.3745	-0.3563	-0.1179	0.1663	0.2989	0.2177	0.0000
4	1.0000	0.8814	0.8243	-0.7450	-0.2645	0.1299	0.2996	0.1081	-0.1628	-0.2263	0.0000
5	1.0000	0.5157	-0.2553	-0.3253	0.1429	0.2703	-0.0401	-0.2402	0.0353	0.2169	0.0000
6	1.0000	0.3359	-0.3931	-0.0339	0.2934	-0.0990	-0.1970	0.1698	0.0958	-0.1923	0.0000
7	1.0000	0.1546	-0.3704	0.2365	0.0461	-0.2270	0.1401	0.0171	-0.1727	0.1556	0.0000
8	1.0000	-0.0157	-0.2190	0.2678	-0.2764	0.0858	0.0656	-0.1651	0.1784	-0.1105	0.0000
9	1.0000	-0.1638	-0.0073	0.1098	-0.1717	0.1993	-0.1964	0.1678	-0.1200	0.0612	0.0000
10	1.0000	-0.2808	0.1941	-0.1347	0.1017	-0.0769	0.0568	-0.0398	0.0250	-0.0118	0.0000
11	1.0000	-0.3602	0.2899	-0.2495	0.2146	-0.1797	0.1478	-0.1069	0.0699	-0.0339	0.0000
12	1.0000	-0.3988	0.2804	-0.1575	0.0339	0.0702	-0.1368	0.1564	-0.1309	0.0724	0.0000
13	1.0000	-0.3968	0.1849	0.0516	-0.1770	0.1650	-0.0508	-0.0784	0.1792	-0.1011	0.0000
14	1.0000	-0.3575	0.0037	0.2039	-0.1365	-0.0650	0.1567	-0.0558	-0.0959	0.1182	0.0000
15	1.0000	-0.2873	-0.1512	0.1833	0.0832	-0.1534	0.0463	0.1363	0.0203	-0.1232	0.0000
16	1.0000	-0.1944	-0.2401	0.0175	0.1773	0.0608	-0.1187	-0.1029	0.0577	0.1162	0.0000
17	1.0000	-0.0898	-0.2346	-0.1517	0.0281	0.1439	0.1147	-0.0105	-0.1096	-0.0988	0.0000
18	1.0000	0.0191	-0.1424	-0.1900	-0.1501	-0.0573	0.0430	0.1090	0.1180	0.0731	0.0000
19	1.0000	0.1193	-0.0024	-0.0737	-0.1167	-0.1360	-0.1342	-0.1147	-0.0821	-0.0419	0.0000
20	1.0000	0.2029	0.1313	0.0956	0.0721	0.0544	0.0401	0.0281	0.0176	0.0083	0.0000

$$J_o\left(\frac{r}{R}S_i\right)$$

Table 2.2

i	r/R										
	0.0	0.1	0.2	0.3	0.4	0.5	0.6	0.7	0.8	0.9	1.0
1	0.8019	0.7894	0.7553	0.7001	0.6261	0.5366	0.4352	0.3264	0.2146	0.1043	0.0000
2	-0.5324	-0.4926	-0.3821	-0.2254	-0.0564	0.0896	0.1847	0.2143	0.1805	0.1001	0.0000
3	0.4257	0.3497	0.1518	-0.0404	-0.1594	-0.1517	-0.0481	0.0708	0.1272	0.0927	0.0000
4	-0.3648	-0.2486	-0.0089	0.1405	0.0965	-0.0441	-0.1093	-0.0394	0.0667	0.0828	0.0000
5	0.3243	0.1672	-0.0828	-0.1055	0.0463	0.0878	-0.0263	-0.0779	0.0114	0.0703	0.0000
6	-0.2943	-0.0990	0.1159	0.0100	-0.0965	0.0292	0.0581	-0.0500	-0.0282	0.0567	0.0000
7	0.2721	0.0421	-0.1008	0.0644	0.0125	-0.0618	0.0490	0.0046	-0.0470	0.0423	0.0000
8	-0.2539	0.0040	0.0556	-0.0731	0.0575	-0.0219	-0.0167	0.0419	-0.0453	0.0281	0.0000
9	0.2390	-0.0392	-0.0017	0.0262	-0.0410	0.0476	-0.0469	0.0401	-0.0297	0.0146	0.0000
10	-0.2264	0.0636	-0.0417	0.0305	-0.0230	0.0174	-0.0129	0.0090	-0.0057	0.0027	0.0000
11	0.2156	-0.0777	0.0625	-0.0538	0.0463	-0.0384	0.0310	-0.0230	0.0151	-0.0073	0.0000
12	-0.2063	0.0823	-0.0578	0.0325	-0.0070	-0.0145	0.0282	-0.0323	0.0270	-0.0149	0.0000
13	0.1983	-0.0786	0.0334	0.0102	-0.0350	0.0327	-0.0101	-0.0155	0.0276	-0.0200	0.0000
14	-0.1907	0.0682	-0.0007	-0.0389	0.0260	0.0124	-0.0299	0.0106	0.0183	-0.0225	0.0000
15	0.1841	-0.0529	-0.0278	0.0337	0.0153	-0.0282	-0.0085	0.0251	0.0037	-0.0227	0.0000
16	-0.1782	0.0346	0.0428	-0.0332	-0.0316	-0.0108	0.0211	0.0183	-0.0103	-0.0207	0.0000
17	0.1728	-0.0153	-0.0405	-0.0262	0.0048	0.0249	0.0198	-0.0116	-0.0189	-0.0171	0.0000
18	-0.1678	-0.0032	0.0239	0.0319	0.0252	0.0096	-0.0072	-0.0183	-0.0194	-0.0123	0.0000
19	0.1633	0.0195	-0.0004	-0.0120	-0.0191	-0.0222	-0.0219	-0.0187	-0.0134	-0.0068	0.0000
20	-0.1591	-0.0323	-0.0209	-0.0152	-0.0115	-0.0087	-0.0064	-0.0045	-0.0028	-0.0013	0.0000

$$J_o\left(\frac{r}{R}S_i\right)\cdot\frac{1}{S_i J_1(S_i)}$$

Table 2.3

linear dose-response curves.

If the radius is divided into ten equal sections and is expressed as a fraction of the total radius, the radius fraction can be written as

$$\frac{r_j}{R} = 0,\ 0.1,\ 0.2,\ 0.3,\ \ldots\ 1.0 \qquad (2.10)$$

where $j = 1,\ 2,\ 3,\ \ldots\ 11$

From Eq. 2.8 the factor $J_o(\frac{rs_i}{R})$ is dependent upon the radius fraction and the zero of $J_o(x)$. These values are given in Table 2.2 for $r/R = 0,\ 0.1,\ \ldots\ 1.0$, and for $s_i = 1,\ 2,\ \ldots\ 20$. In addition, Table 3.3 gives the values for $J_o(\frac{rs_i}{R}) \cdot (s_i J_1(s_i))^{-1}$. As these values are constant for any given radius the values of Table 2.3 can be used in conjunction with Eq. 2.8 to compute the concentration at any given radius r_j, for any time t. Since the first twenty exponential terms of the diffusion equation (Eq. 2.8) have been used in this simulation, and since the radius has been divided into ten, giving eleven values for the radius fraction, the values of Table 2.3 can be expressed in matrix notation as

$$D_{ij} \qquad \begin{matrix} i = 1 \ldots\ 20 \\ j = 1 \ldots\ 11 \end{matrix} \qquad (2.11)$$

To further simplify the notation let

$$b_i = \frac{k s_i^2}{R^2} \qquad (2.12)$$

Now, Eq. 2.8 can be rewritten as

$$c_j = C_s - 2C_s \left[\sum_{i=1}^{20} D_{ij} e^{-b_i t} \right] r = r_j \qquad (2.13)$$

Where c_j represents the concentration change at radius r_j for a step change C_s in concentration at the surface of the cylinder. A positive value of C_s represents an increase in concentration while a negative value represents a decrease in concentration. The values of c_j represent concentration deviations from the starting value, and to calculate absolute concentrations C_j, the starting or initial value of concentration C_I must be added to the value of c_j so that

$$C_j = C_I + c_j \tag{2.14}$$

So far all that has been calculated is the concentration at different values of the radius fraction. In order to perform the integration over the total cross-section area of the cylinder, the average concentration $\bar{C}_n$ for any annulus bounded by r_j and r_{j+1} must be calculated. Thus, if the concentration is assumed to change linearly between these two radii, the average concentration can be computed as

$$\bar{C}_n = (C_j + C_{j+1})/2 \qquad j = 1....11 \qquad n = 1....10 \tag{2.15}$$

where now C_j and $\bar{C}_n$ are expressed as absolute concentrations.

The area for each annulus a_n is

$$a_n = \pi(r_{j+1}^2 - r_j^2) \tag{2.16}$$

and the absolute force produced by each area is

$$P_n = p(\bar{C}_n)a_n \tag{2.17}$$

Therefore the total tension P_t over the whole area is

$$P_t = \sum_{n=1}^{10} P_n \tag{2.18}$$

A computer program (Appendix H) was written based on the theory just described to enable tension transient to be simulated in order that one may be able to determine how much of the experimental tension transient curve can be accounted for by diffusion into a homogeneous cylinder the same radius as the muscle. Experimentally derived parameters from the dose-response curves and muscles were used for this simulation which was done on a CDC 6400 computer at Imperial College of Science and Technology. The results of this simulation and the experimental curves are shown in Section 5.3.2.

2.3 Impulse Response Analysis

The application of an impulse to the input of a system causes the impulse response to appear at the output. The shape of the impulse-response curve is determined by the system under test, and therefore it defines the complete dynamic characteristics of the system.

The impulse input signal is also called a Dirac delta function. Theoretically, it is of infinite magnitude and infinitesimal duration such that by definition (e.g. Skilling, 1965) the area under the impulse is unity.

While the impulse function is a convenient means of studying a system mathematically, in practice, it is difficult to generate an impulse that will excite a system sufficiently to give a large and undistorted output amenable to analysis. This is particularly true for the heart muscle system which has a limited and non-linear output response (see Section 5.2). Nevertheless, by using a low amplitude input signal, such as noise, which has an autocorrelation function that approximates an impulse, it is possible to measure the impulse response of the system.

2.3.1 The input-output relationship of a system

Consider a system as in Fig. 2.2 where the response to an input x(t) is an output z(t). This output is the sum of the true output of the system y(t) and random noise n(t), and can be written as

$$z(t) = y(t) + n(t) \tag{2.19}$$

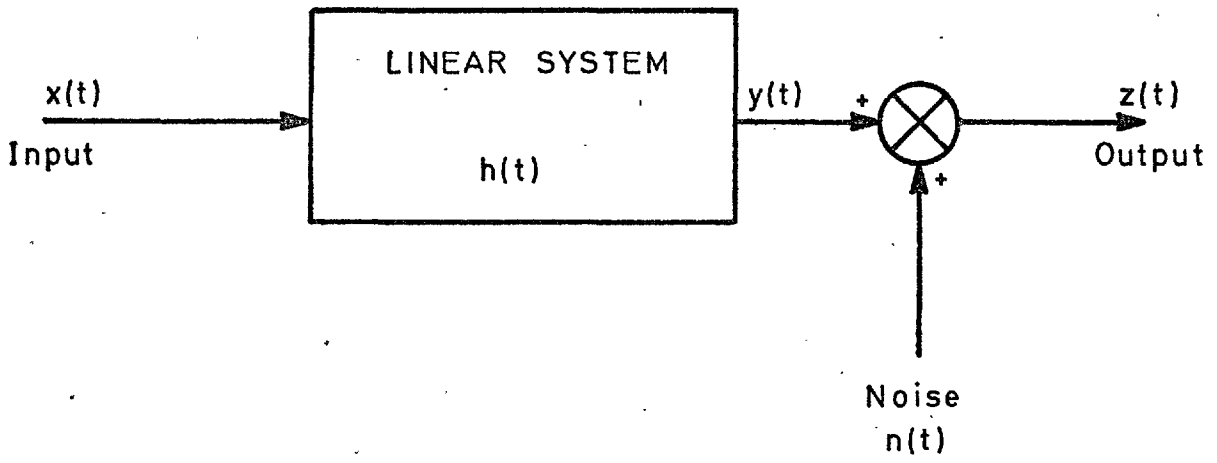

Fig. 2.2 Block diagram of a linear system

If the system under consideration is linear, the input and output signals are related by a linear transfer quantity h(t), the impulse response of the system. More precisely, the output is the result of convolution of the input signal with the impulse response (e.g. Lathi, Chapter 10), and is thus expressed mathematically as

$$y(t) = h(t)*x(t) = \int_{-\infty}^{\infty} h(t')x(t - t')dt' \tag{2.20}$$

where the symbol * denotes convolution.

A unit impulse applied to the input of a system causes the impulse response to appear at the output. Thus, for the system of Fig. 2.2 with an impulse as input, the output z(t) can be expressed as

$$z(t) = h(t) + n(t) \tag{2.21}$$

Unless the system is noise-free, the contribution of the noise term n(t) to the output may be sufficient to mask the impulse response term. By using correlation techniques however, the influence of the noise term on the output can be substantially reduced.

2.3.2 Correlation as a measure of the input-output relationship

The crosscorrelation function provides a measure of the similarity between two statistically stationary signals. In Fig. 2.2, x(t) and z(t) are the input and output signals of the system. The crosscorrelation function for these signals $R_{xz}(\tau)$, expressed as a function of the searching parameter τ, is by definition (Lee, 1960, p.341)

$$R_{xz}(\tau) = \lim_{T\to\infty} \frac{1}{2T} \int_{-T}^{T} x(t)z(t+\tau)dt \tag{2.22}$$

By substituting Eq. 2.19 for $z(t+\tau)$ Eq. 2.22 becomes

$$R_{xz}(\tau) = \lim_{T\to\infty} \frac{1}{2T} \int_{-T}^{T} x(t)y(t+\tau)dt + \lim_{T\to\infty} \frac{1}{2T} \int_{-T}^{T} x(t)n(t+\tau)dt \tag{2.23}$$

The second term in this expression represents the crosscorrelation of the noise signal with the input signal, and for convenience it will be written as $R_{xn}(\tau)$. Substituting the convolution expression (Eq. 2.20) for y(t), and changing the variable to $(t+\tau)$, Eq. 2.23 can be rewritten as

$$R_{xz}(\tau) = \lim_{T\to\infty} \frac{1}{2T} \int_{-T}^{T} x(t)dt \int_{-\infty}^{\infty} h(t')x(t + \tau - t')dt' + R_{xn}(\tau) \qquad (2.24)$$

The order of integration can be rearranged so that

$$R_{xz}(\tau) = \int_{-\infty}^{\infty} h(t')dt' \left[\lim_{T\to\infty} \frac{1}{2T} \int_{-T}^{T} x(t)x(t + \tau - t')dt \right] + R_{xn}(\tau) \qquad (2.25)$$

By comparing the first term of this equation with Eq. 2.20, one can see that this represents the convolution of the impulse response $h(t')$ with the autocorrelation of the input autocorrelation $R_{xx}(\tau - t')$. Therefore, for simplification Eq. 2.25 can be written as

$$R_{xz}(\tau) = h(t')*R_{xx}(\tau - t') + R_{xn}(\tau) \qquad (2.26)$$

The result of Eq. 2.26 shows that if a signal, whose autocorrelation represents an impulse, is applied to the input of a system, then the cross-correlation between input and output will give the impulse response of the system plus a contribution due to noise. But if the noise is uncorrelated with the input signal, the crosscorrelation of these two signals will tend towards zero, leaving only the impulse response.

White noise is thought to be generated by a random process and it has a uniform spectrum. Because of its randomness, the autocorrelation function of white noise approximates an impulse. This means that noise can be used as an input to a system, and by crosscorrelating the noise input with the resulting output signal the impulse response can be obtained directly.

The degree to which the noise autocorrelation function approximates an impulse is dependent upon the length of the signal used in the analysis,

and in the limit, as the length approaches infinity, the autocorrelation function is a Dirac delta function at zero time displacement. However, for practical situations, correlation must be carried out within a finite time, with the result that the autocorrelation function only approximates an impulse. This is because of the finite length of signal used, and as it is only a representative sample of the infinite noise signal, its statistics will, in general, be different from those of the infinite noise signal. In addition, the statistics between sample lengths will also be different, and this will introduce variability into the results. Consequently, the results from several such measurements must be averaged to reduce the variability in the data introduced by the statistical fluctuations in the noise samples.

Pseudo-random noise, on the other hand, is a periodic function, and over one period its autocorrelation function is a good approximation to an impulse function (Section 2.3.4). This type of signal is easy to synthesize, and as a result its statistics can be fixed and will not vary from one sample to the next. Thus if the measurement time of an experiment is made to correspond exactly to the length of one pseudo-random sequence, the results will be identical for every repetition provided nothing else has changed.

2.3.3 Pseudo-random binary signals

1) Maximum-length pseudo-random binary sequences

Pseudo-random binary sequences (p.r.b.s.) have levels $\pm$ 1, and can be easily generated by using either digital logic hardware, or software. The most common type of p.r.b.s. is a maximum-length (M-length) sequence. These sequences have lengths

$$N = 2^n - 1 \qquad (2.27)$$

where n is an integer, and they may be generated using an n-stage shift register (Godfrey, 1969).

In generating a p.r.b.s. the first stage of the shift register is fed with the modulo 2 (2's complement) sum of the output of the last stage and the outputs of one or more of the other stages. Modulo 2 addition is binary addition in which the end carry is discarded, and follows the rules: $0 + 0 = 0$; $0 + 1 = 1$; and $1 + 1 = 0$.

For an example, consider a 3-bit shift register (Fig. 2.3). From Eq. 2.27 the maximum length of the sequence is 7, and the sequence can be generated by feeding back to the first stage the modulo 2 sum of stages 2 and 3.

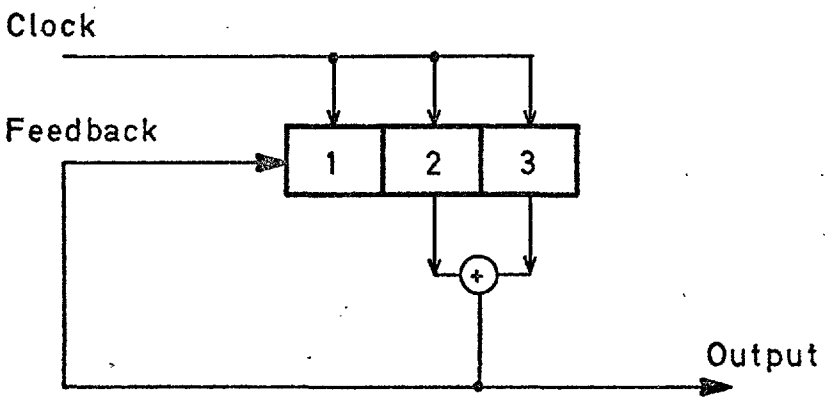

Fig. 2.3. Feedback arrangement for a 3-bit shift register to generate a 7-digit maximum-length sequence.

If one assumes that the logic values in each of the register bits is initially I_1, I_2, I_3, then upon the arrival of a clock pulse, the logic values change to

$$J_1 = I_2 + I_3$$
$$J_2 = I_1$$
$$J_3 = I_2$$

After the next clock pulse, the new levels are,

$$K_1 = J_2 + J_3 = I_1 + I_2$$
$$K_2 = J_1 = I_2 + I_3$$
$$K_3 = J_2 = I_1$$

The new output stays at the same level until another clock pulse arrives. The interval Δt between clock pulses is the interval of the sequence. Thus, the period T of the sequence is set by

$$T = N\Delta t \qquad (2.28)$$

Now if I_1, I_2, I_3, are represented by, say 0, 1, 0, then the p.r.b.s. would be

1 1 1 0 0 1 0 1 1 1 0 0 1 0 .....

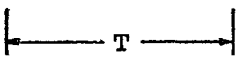

The feedback arrangements for other possible M-length sequences are given by Godfrey (1969, Table 1).

It must be noted that the binary levels (0, 1) of the p.r.b.s. only represent the perturbation levels of $\pm$ a, making it necessary to transform the p.r.b.s. output by either

1 = +a or 1 = -a

0 = -a 0 = +a

M-length sequences have the interesting property that if the sequence is shifted by a given amount, and the shifted version is then modulo 2 added to the original, the result is the original M-length sequence shifted by a specific amount. The amount of shift depends upon the internal properties of the M-length sequence, and can vary between different M-length sequences of the same period.

In the M-length sequence under consideration, the original sequence is

1 1 1 0 0 1 0

If this sequence is shifted by 1 so that it becomes

0 1 1 1 0 0 1

and then this is modulo 2 added to the original, the result is

1 0 0 1 0 1 1

Examination of this result will reveal that this is the original sequence shifted by 5. Further examination will also reveal that the value of this shift, i.e. 5, is equivalent to the number of points in the sequence that are contained from the beginning of the longest run of "0s" to the beginning of the longest run of "1s".

Godfrey and Briggs (1972) make use of this shift-and-add property of M-length sequences in predicting the location in a crosscorrelation result where discontinuities will occur if the system is linear (i.e. output proportional to input), but has direction dependent dynamics. If k_i represents the shift value for an initial shift i, then Godfrey and Briggs have shown that the first discontinuity will occur at lag $(k_1 + 1)$, the second at $(2k_1 + 1)$, the next at lag $(k_3 + 1)$, and so on.

2) Inverse-repeat pseudo-random binary sequences

The basic principle upon which pseudo-random analysis is built is that the system or process being studied is linear. Non-linear systems can be approximated to linear ones provided its operating point is kept in the linear range, or if this is not possible, the perturbation levels should be kept as small as possible.

Occasionally, even with small perturbation levels, the system is still highly non-linear. In such cases the non-linear effects show up in the crosscorrelation function as an apparent increase in the noise level, the magnitude of which is not diminished by increasing the correlation time (Godfrey, 1969). This noise can be reduced by using an inverse-repeat sequence.

An inverse-repeat sequence can be generated by inverting every other digit of a M-length p.r.b.s. . Consider the 3-bit register in the previous section that gave the 7-digit M-length sequence. Let the M-length sequence be represented by {M} and the inverting sequence by {I}. The inverse-repeat sequence {N} is the modulo 2 sum of {M} and {I}. This can be shown as follows:

```
          |------ T ------>|
{M} =  1 1 1 0 0 1 0 1 1 1 0 0 1 0 1 1 1 .....
{I} =  1 0 1 0 1 0 1 0 1 0 1 0 1 0 1 0 1 .....
{N} =  0 1 0 0 1 1 1 1 0 1 1 0 0 0 0 1 0 .....
       |---------- L ---------->|
```

As can be seen, the new inverse-repeat sequence {N} has a period L which is twice the period T of the M-length sequence. It can be further seen that the second half of the inverse-repeat sequence is the negative or

complement of the first half. It is because of this negative symmetry that the effects of all even-order non-linearities (i.e. second-order, fourth-order, etc.) cancel out.

2.3.4 Correlation properties of pseudo-random sequences

In crosscorrelating the p.r.b.s. with the output, it is necessary to correlate over exactly one period length of data, otherwise errors will be introduced into the results. Also, it is necessary to use a circular type of correlation in which the output data length is twice that of the input. As the input is periodic, the output can be assumed to be periodic as well, and therefore by repeating the output its length can be doubled. Now with the output twice the length of the input, the maximum number of lags over which the correlation can be performed is equal to N, the number of points in the sequence. The divisor, by which the lagged-product sum is divided, is also constant and equal to N.

The measured output of the heart muscle system is the peak isometric tension, and as it can only be measured when the muscle is stimulated, the expression for the correlation of continual analog functions cannot be used. The correlation equation (Eq. 2.22) must therefore be modified so that it can be used for sampled data and it can be rewritten as

$$R_{xz}(\tau) = \frac{1}{N} \sum_{n=1}^{N} x_n z_{(n+\tau)} \qquad \tau = 0, 1, \ldots (N-1) \qquad (2.29)$$

where τ represents the lag number.

Although the process of correlation is the sum of the cross-product of the corresponding input and output data points, this multiplication can be reduced to a series of additions and subtractions provided the input data has the values of $\pm$ 1.

If, by using this correlation method, an M-length sequence of period

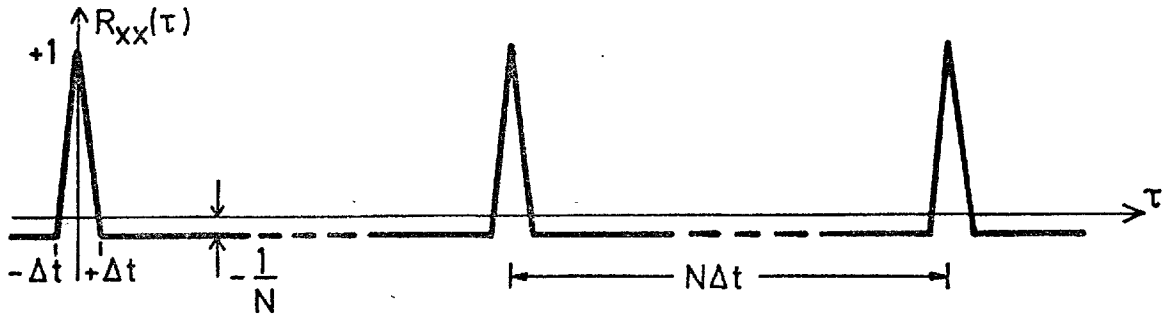

(a) Normalized autocorrelation function of a maximum-length sequence of period $N\Delta t$.

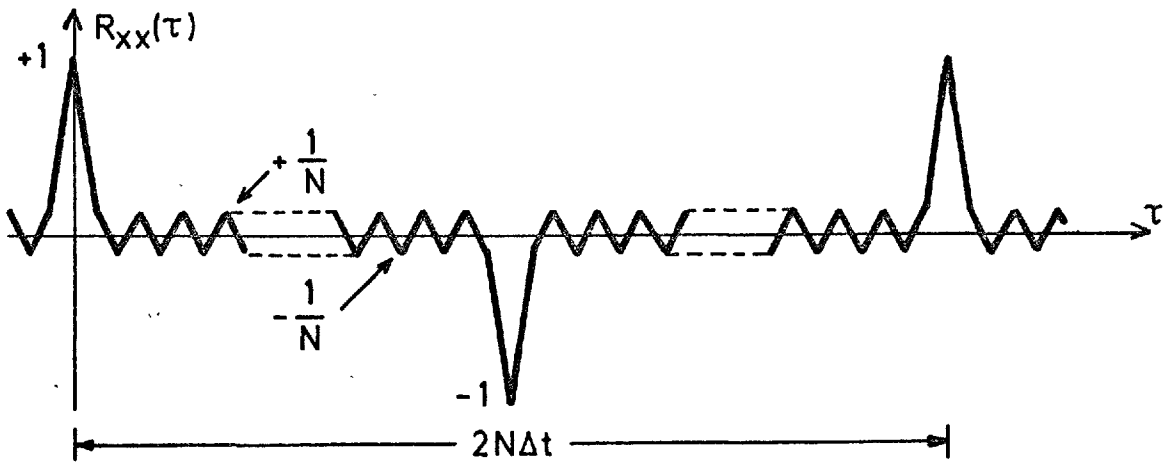

(b) Normalized autocorrelation function of an inverse-repeat sequence based on the maximum-length sequence used in (a).

Fig. 2.4 Autocorrelation of pseudo-random binary sequences

$T = N\Delta t$ is autocorrelated, the result is a series of triangular "spikes" of width $2\Delta t$ spaced by the sequence period T. If the correlation result is normalized, then the peak value is unity, and the off-peak value is constant and equal to $-1/N$ (Fig. 2.4a).

On the other hand, if an inverse-repeat sequence is used, the autocorrelation result is as shown in Fig. 2.4b. Provided the sequence is based on the M-length sequence of Fig. 2.4a, then the inverse-repeat sequence will have a period of 2T. Since the second half of this sequence is the negative of the first half (Section 2.3.3), a negative impulse occurs at time T.

Now it is possible to see the significance of using a p.r.b.s. as an input signal to the system. Since its autocorrelation represents an impulse which is applied to the system once every time T, the impulse response can be obtained directly from the crosscorrelation of the input and output signals of the system. However, because the impulse occurs every time T, the length of the p.r.b.s. must be greater than the settling time of the system T_s if the previous transient response is to have died out before the next impulse is applied to the system.

CHAPTER 3

THE EXPERIMENTAL SYSTEM

3.1 Introduction

In order to study inotropic interventions and the mechanical properties of heart muscle on a beat-to-beat basis, some form of automated or semi-automated data acquisition and measuring system is desirable. As the Department of Physiology had two LINC-8 computers available for use in on-line experiments, we decided to build in our laboratory a data acquisition system that could be interfaced to either of the computers for on-line or off-line analysis.

The computer system had to be designed for flexibility so that it could be used for different types of experiments. Consequently, the core of the system was kept constant with only the peripherals, and in particular the computer program, requiring change for different experimental purposes.

This chapter can be divided into three main sections. The first two

sections describe the hardware and software of the data acquisition and measuring system which has general application to many types of experiments. The third section describes the force transducer, muscle clamp, and superfusion system which are unique to the investigation described in the remaining chapters.

3.2 Data Acquisition and Computer Control

Before experimental signals from various transducers can be processed, they must be converted into a suitable form by some type of signal conditioning unit that is able to accept a wide range of input signals and give a standard output. It was found that a Devices DC-6 pre-amplifier could form the basis of such a unit. This type of pre-amplifier will accept a wide range of signals (5 mV to 25 V full scale), and gives a uniform output (0 - 1.25 V). In addition, it is fitted with back-off and variable filter controls. The four DC-6 pre-amplifiers used in the signal conditioning system were part of a Devices M4 recorder which was used to obtain a permanent slow speed paper record of the experiments.

To make use of the full scale analog input range ($\pm$ 1 V) of the computer and analog tape recorder (Philips ANA-LOG 7), a set of buffer amplifiers were incorporated into the computer interface to adjust the dc level and gain of the pre-amplifier outputs (Fig. 3.1).

Remote control of the computer was provided by a specially built interactive computer interface (Appendix C). Function switches were used to select the mode of operation of both the interface and the computer while status lights gave a visual indication of computer operation.

The system timing was governed by a master clock (Devices Digitimer) which controlled the rate of stimulation of the muscle (typically 20/min). It also triggered the computer to begin the sampling sequence, and set the

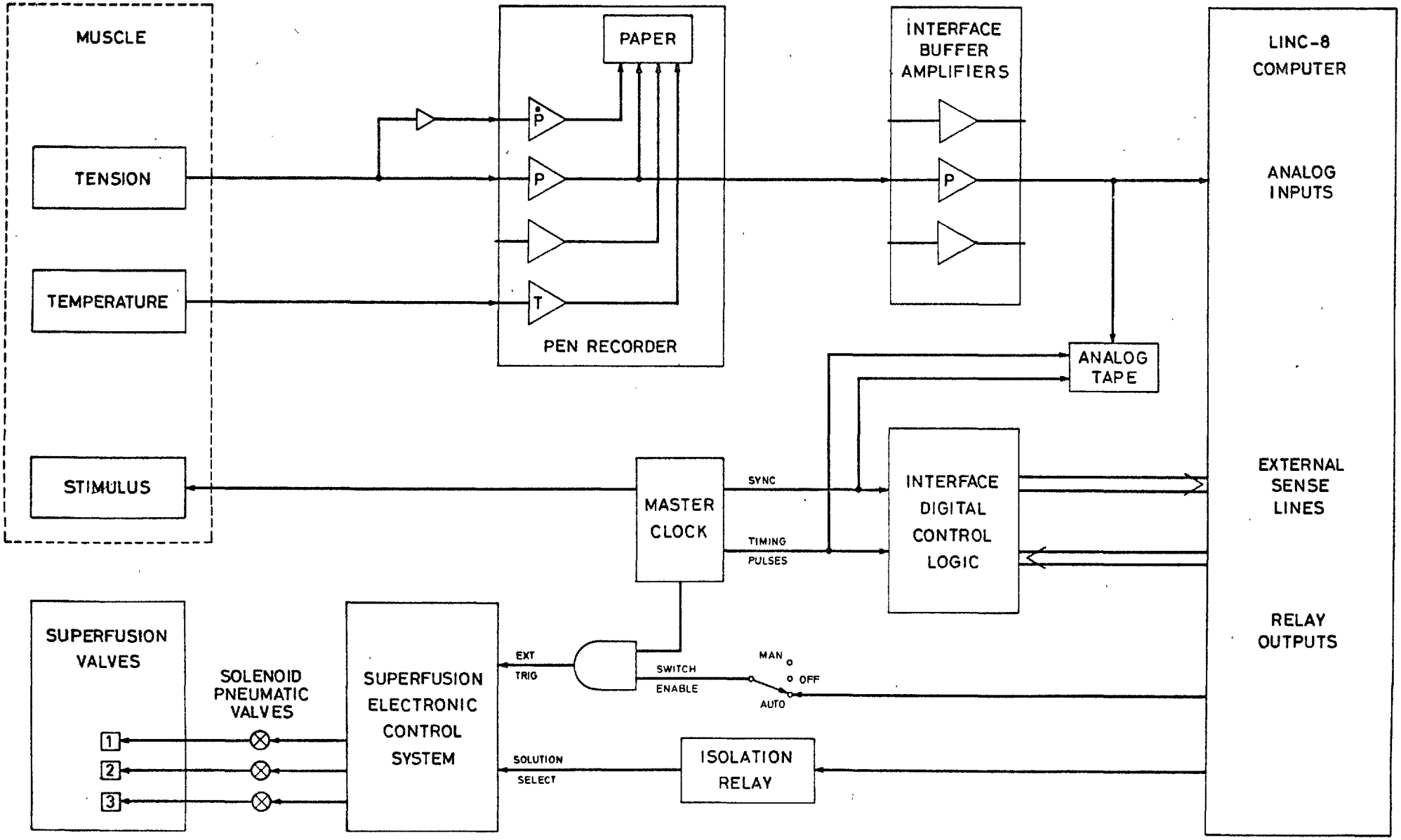

Fig. 3.1 Block diagram of the data acquisition system.

computer sampling interval of 1 ms. The Sync and Timing pulses were also recorded on the analog tape to aid in any later off-line analysis. In addition, the Digitimer was used to select the exact time during the stimulation interval when the superfusion valves could switch.

3.3 Digital Signal Processing

The LINC-8 computer was used in conjunction with the data acquisition and control system to form an on-line computer-based system capable of making measurements in real-time with the results being stored on digital magnetic tape for further off-line analysis. Fig. 3.2 illustrates the digital signal processing system.

Initialization of the sampling sequence was under direct control of the master clock and the interface. Once triggered, the computer sampled either the tension or length (for isotonic studies) signals, and passed the sampled signal through a low pass digital filter (20 point moving average) to remove any unwanted noise. Measurements were then made on the filtered signal to determine its baseline, peak value, and the time to peak value.

The filtered signal was simultaneously differentiated by a high pass digital filter (subtraction of two filtered data points spaced 20 ms apart), and values were obtained for its peak rates of rise and fall. In addition, their times of occurrence could also be measured.

When the input signal reached 25% of its peak value during the relaxation phase, the time was noted as the time to 75% relaxation, and the sampling sequence was terminated. It is of interest to note that the time over which sample points were taken was not fixed, but was a function of the duration of the muscle contraction.

If required, the measured parameters could be stored on digital magnetic tape under direct operator control at the interface. It was also

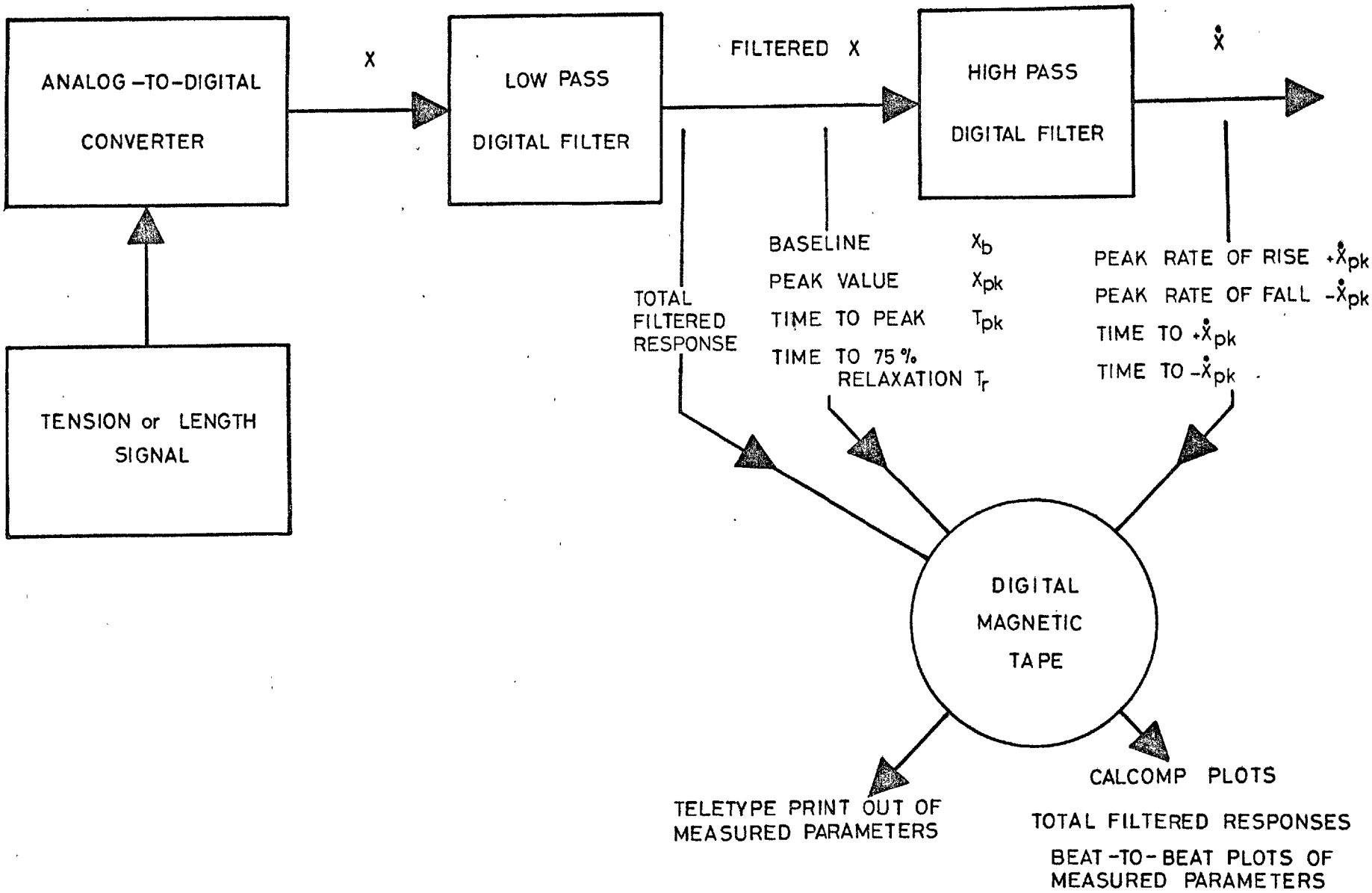

Fig. 3.2 Block diagram of the digital signal processing system.

possible to store one complete filtered sequence of the contraction cycle on a separate digital magnetic tape.

For the remainder of the time, before the beginning of the next sampling sequence, the filtered input signal and its derivatives were displayed on the computer's CRT, and this was transmitted via closed circuit television, to the laboratory where the processed signals were monitored.

Upon completion of the experiment the measured parameters could be printed off-line, on a Teletype, or they could be plotted on a beat-to-beat basis using an incremental digital plotter (Calcomp 565). The complete contraction cycle could also be plotted if required.

A detailed account of the individual software components of this system is given in Appendix D while a flow chart of the computer program is given in Appendix E. For use in pseudo-random studies, a subroutine was written which could be called by the experimenter from the computer interface. This subroutine generated a M-length pseudo-random binary sequence and sent information back to the experiment which controlled the switching of the superfusion valves. The flow chart for this subroutine is given in Appendix F.

3.4 Force Transducer

A special all-glass force transducer was designed for use in this series of experiments (Fig. 3.3). Relative movements between the ferrite slug and the coil cause a change in inductance that was detected as a phase shift of a 5 MHz carrier wave (Cambridge & Haines, 1959). The output of the phase-detector circuit was proportional to the displacement and was linear over a limited range.

Force applied to a glass tripod (1 mm diameter pyrex tubing) was transmitted along its central strut where it was brought to bear at a point

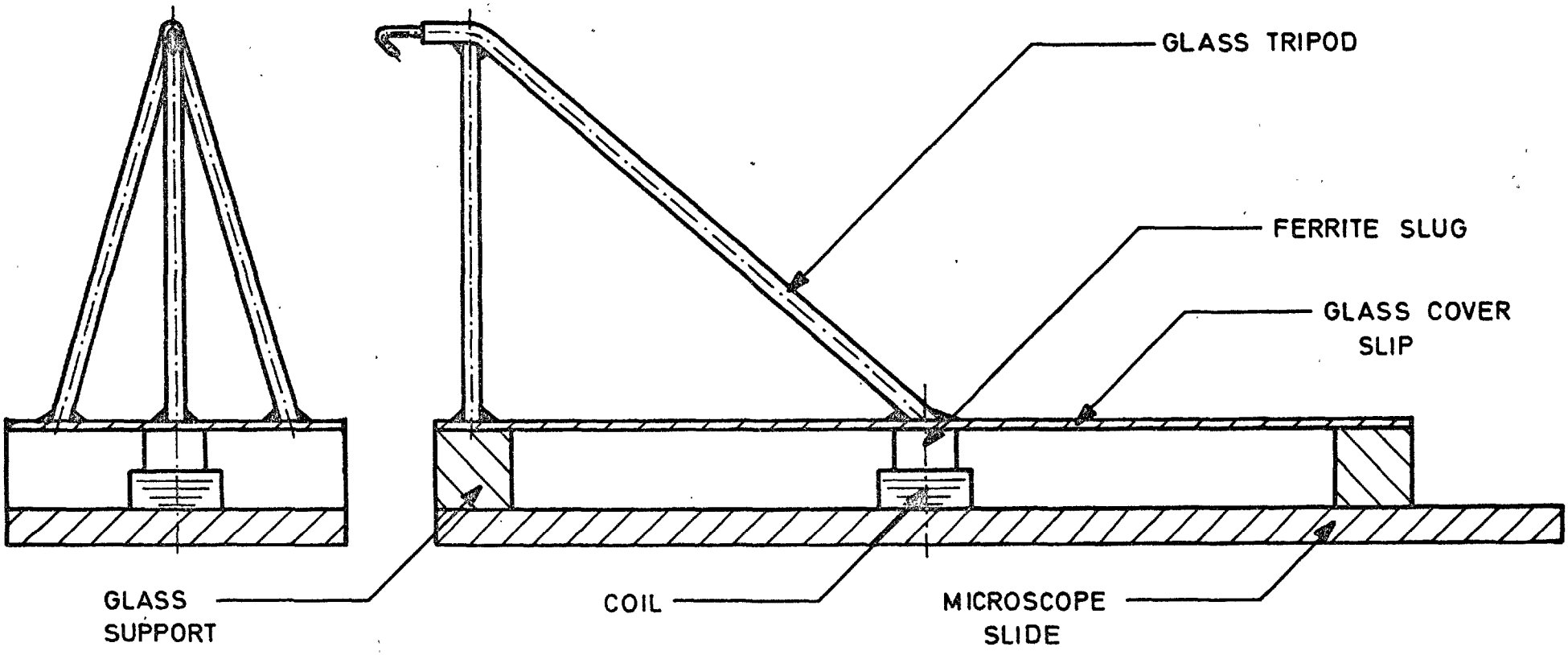

Fig. 3.3 FORCE TRANSDUCER

immediately above the ferrite slug. The amount that the slug moved was dependent upon the magnitude of the force applied at the tip of the tripod, the geometry of the tripod, and the effective stiffness of the glass cover slip. This effective stiffness was determined by the thickness of the cover slip as well as the distance between its supports. These factors also governed the distance the tip of the tripod moved for a given applied force.

The coil consisted of three layers (16, 15, and 14 turns respectively) of 36 s.w.g. enamelled copper wire wound around a number 17 drill shank. This diameter was just sufficient to allow part of a 3.5 mm length of an anti-parasitic bead (RS Components Ltd.) to move inside the coil along its longitudinal axis.

The No. 3 glass cover slip was supported by two strips of 0.635 mm (1/4") thick plate glass spaced 57.15 mm ($2\frac{1}{4}$") apart. The whole assembly, including the tripod, was fastened together using Araldite epoxy glue that had been thinned with benzene. The transducer was then mounted inside a brass box with only the tip of the tripod exposed for protection against mechanical damage as well as for isolation against temperature fluctuations (Fig. 3.6b).

The compliance of the transducer at the tip of the tripod was found to be 5.14 μ/g, and the assembly had a natural frequency of 500 Hz. The transducer was linear over the region of 0 - 5 g, and from the signal processing system the transducer was found to have a calibration of 410.8 c.u./g. This calibration, however, could be altered by changing the gain setting of both the DC-6 pre-amplifier and/or the interface buffer amplifier.

3.5 Muscle Clamp

A perspex muscle clamp was built based on a previous design of Blinks (1965). This clamp is shown in relation to the force transducer in Fig. 3.6b.

The punctate electrode was made from 25 s.w.g. platinum wire which served as the cathode of the stimulating circuit. The anode consisted of two pieces of platinum wire spaced 1.5 mm to either side of the cathode. With this arrangement the isolated papillary muscles could be stimulated with voltages less than 0.5 V with an isolated stimulator (Devices Ltd.).

3.6 The Superfusion System

3.6.1 Introduction

In order to be able to achieve a step change in calcium concentration, as seen by the muscle, one needs to be able to switch rapidly between two perfusion solutions of different concentration. In addition, if a study such as a pseudo-random study is to be conducted, the perfusion system must have the facility for remote operation.

Langer used an arterially perfused papillary muscle from dog heart in his studies (Langer & Brady, 1963). Technically this is a very difficult preparation and requires the cannulation of the papillary artery which is only some 100-200 μ in diameter. With this perfusion system, the type of perfusate could be changed within five to ten seconds by manually switching from one solution to the other, but this slow switching time is not very useful for step response studies and is out of the question for pseudo-random studies.

Another method, and the one chosen for this investigation, is superfusion, where the perfusate is allowed to flow over the preparation. One

such system was described by Chapman and Niedergerke (1970a) for a frog ventricular preparation. It also had manual switching, and the change-over of fluids could be completed within 100ms.

In both of these systems the switching is effected by a rapid turn of a two-way glass tap. Because only one solution is flowing at a time, an additional tap is required to drain the stagnant fluid in the tubing connecting the reservoir to the perfusion tap before switching the perfusion fluids. This procedure is not only wasteful of fluid, but also requires the attention of the experimenter who may be pre-occupied with more important matters. One additional disadvantage of these systems is that no provision is made for operating at any temperature other than at room temperature.

What is required is a superfusion system that has a very fast switching time, low flow rate to conserve fluid, a method of preventing fluid from becoming stagnant in the tubing, and a means of controlling the temperature of the perfusate. Also, the perfusion system must have the facility for remote control.

3.6.2 Superfusion control valves

A special set of pneumatically-actuated control valves were designed to allow for rapid changes between perfusion solutions, and to prevent the fluids from becoming stagnant in the tubing when not actually perfusing the muscle. A schematic representation of one of these valves is shown in Fig. 3.4.

The main body of the valve was made from a 6.7 cm ($2\frac{5}{8}$") length of medical grade perspex 1.6 cm (5/8") square. The body was then bored out to accept a perspex piston fitted with 3/8" O.D. x 1/4" I.D. viton o-rings. The lower end of the body was threaded and fitted with a perspex nozzle to

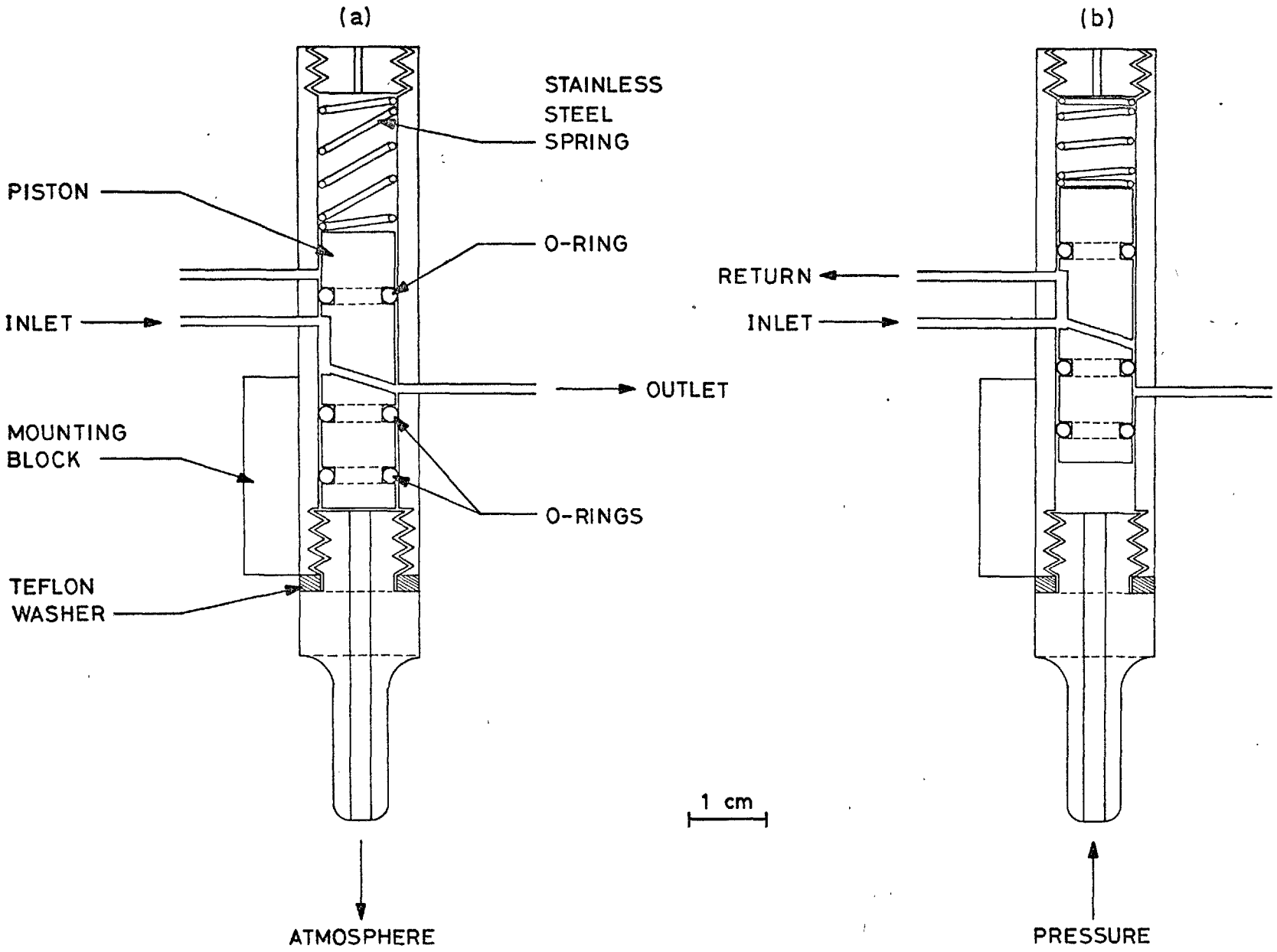

Fig. 3.4 Schematic diagram of a superfusion valve.

which was attached the pressure hose. The upper end, which was also threaded, was fitted with a perspex plug which acted as a retainer for the stainless steel spring. To facilitate cleaning, the valves were designed to be easily dismantled.

The piston was lubricated by placing small amounts of silicone oil around the o-rings. The use of grease was avoided because its high viscosity prevented rapid movement of the piston.

3.6.3 Principle of operation

The position of the piston is in one of two states. When the valve is on (Fig. 3.4a), the nozzle end is open to atmosphere through an electrically-operated two-way pneumatic valve. The stainless steel spring forces the piston down so that fluid from the inlet tube can flow along a groove in the piston, traverse the piston by means of a slightly oblique hole across its diameter, and emerge at the outlet tube. The fluid is prevented from flowing elsewhere because the lower two o-rings isolate the inlet-outlet lines from the return line.

The valve is turned off (Fig. 3.4b) by applying air pressure (30 p.s.i.) at the nozzle end of the valve. This forces the piston up against the spring compressing it. In the "up" position, the inlet and outlet tubes become separated by the middle o-ring, and consequently the fluid is forced to move along the piston groove and out the return line. The outlet tube is sealed by the lower two o-rings which prevent backflow from occurring in the outlet line.

The switching time of the valves is governed by how quickly the pressure changes in the valve cylinder, and by the amount of tension stored in the spring under compression. Unless exceptionally high pressures are used, the switching time due to spring action is quicker than that due to

pressure. With pressures of 30 p.s.i. the switching times in each direction are comparable, but not necessarily equal. Switching time will be discussed further in Section 3.6.5.

3.6.4 Flow regulation and temperature control

A Watson-Marlow MHRE-22 pump with a DELTA attachment was used to control the flow of fluid from the reservoirs to the valves and back again. The DELTA attachment consists of a triangular shaped rotor around which is wrapped a single turn of tubing. This kinks the tubing in three places, and when the rotor turns the fluid trapped between the kinks is pushed along. The flow rate is determined by two factors, the rate at which the rotor turns, and the bore of the tubing at the pump. The pump speed was set at its maximum, and the tubing used was Technicon AutoAnalyzer tubing with purple-orange coded tubing (0.100" I.D.) for fluid delivery to the valves, and purple-white coded tubing (0.110" I.D.) for fluid being returned from the valves. This combination gave a net flow rate of 5 ml/min at the muscle.

The use of slightly larger diameter tubing on the return line had the effect of creating a slight negative pressure at the superfusion valve so that when the valve was off, all the fluid being delivered to that valve was ensured of being returned to the reservoir.

To reduce the time spent by the fluid inside the delivery tubes, 1 mm bore silicone rubber tubing was used to interconnect reservoirs, pump, and valves. Because of the small diameter tubing, a large velocity was imparted to the fluid in the tubing. Fig. 3.5 illustrates, schematically, the interconnections of these elements.

Initially it was decided to place the perfusate reservoirs into a constant temperature water bath, and that this would be sufficient to deliver

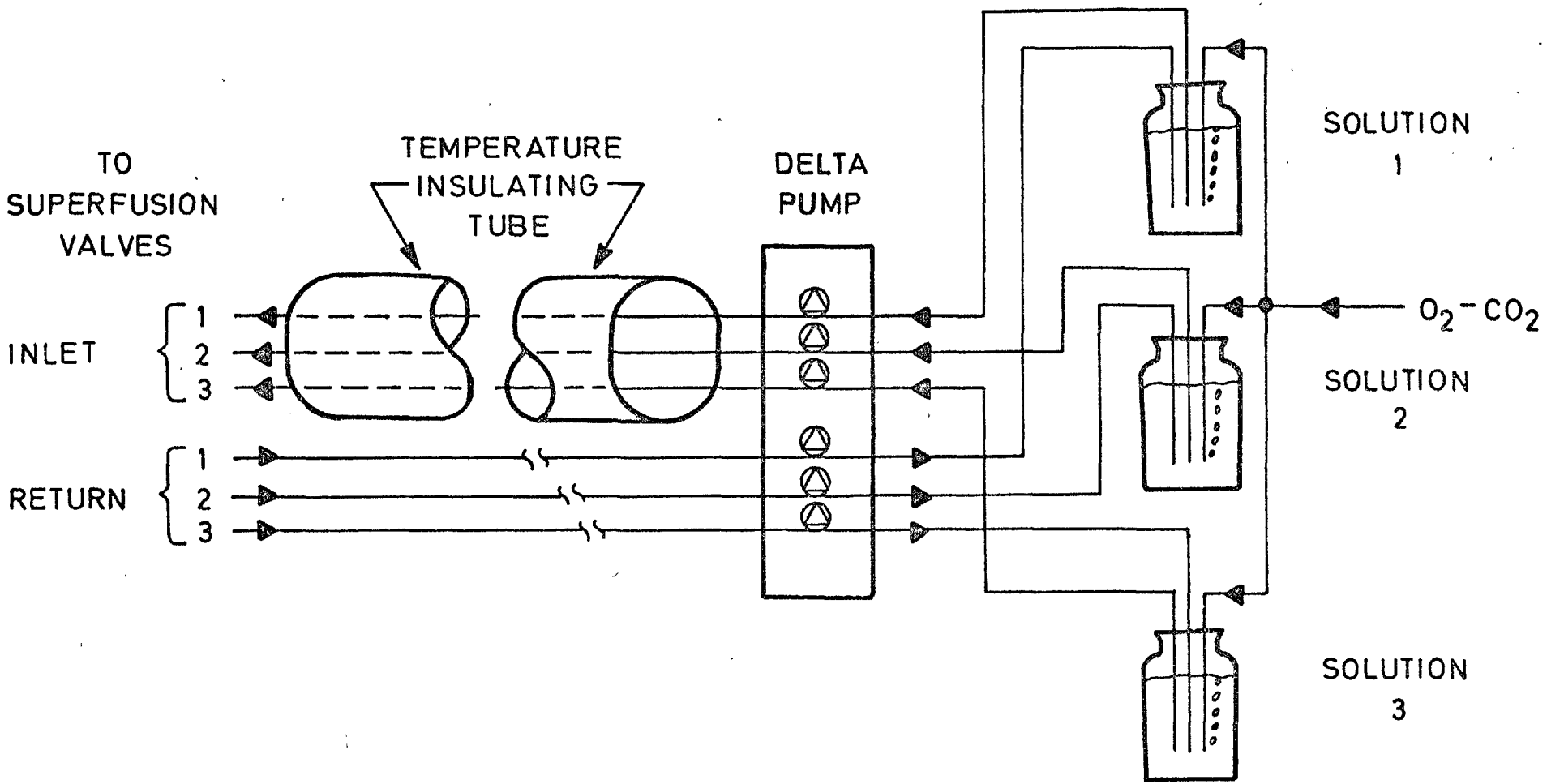

Fig. 3.5 PERFUSATE FLOW BLOCK DIAGRAM

fluid to the muscle at a constant temperature. However, this arrangement proved to be unsatisfactory, and it was necessary to enclose the complete experimental apparatus, including the water bath, inside a large heated enclosure. Heat to the box was provided by an electric fan heater whose voltage was controlled manually by a Variac. With this arrangement it was possible to maintain the temperature within the box at $30^{\circ}C \pm 1^{\circ}C$ at any one point.

Although the temperature inside the box could be maintained constant, there were enough temperature gradients present throughout the enclosure which could introduce a temperature differential between two perfusing liquids by as much as $1^{\circ}C$. This meant that not only would the muscle see a change in concentration when the solutions were switched, but also a change in temperature. It is important to keep the temperature constant if artifacts in tension changes are to be kept to a minimum (Appendix A). However, by placing all of the inlet delivery tubes inside a larger diameter tube (Fig. 3.5) this temperature effect was eliminated.

In addition, the muscle was further protected from external influences by placing a glass shroud around the muscle. This had the effect of creating a micro-environment for the muscle which was at a constant temperature. The shroud also had the additional feature of trapping the perfusate as it dripped off the muscle clamp, and through this trapped fluid an O_2-CO_2 gas mixture was bubbled to generate a suitable moist atmosphere around the muscle. A measure of the temperature of the muscle was made by placing a thermistor at the base of the muscle and measuring the temperature of the effluent as it came off the muscle.

3.6.5 Fluid delivery and switching

The three perfusion valves were mounted on a special jig so that their output tubings were convergent (Fig. 3.6a). The whole assembly was attached to a micromanipulator (not shown) for fine adjustment of flow placement in relation to the muscle.

The outlet tubings (18 gauge stainless steel needle tubing) were coupled to the delivery tubes by means of short lengths of 1 mm bore silicone tubing. The delivery tubes consisted of three pieces of 18 G stainless steel tubing bent at right-angles. Into these tubes, and up to the bends, were inserted long lengths of 23 G stainless steel tubing. The whole assembly was then fastened together using stainless steel solder.

It was found that the placement of the flow from each of the three 23 G tubes could not be made to converge at the same point, and this necessitated having to channel the three flows through one outlet. A short length of 1 mm bore silicone tubing was used to couple the three outlet tubes to a single tube, also made of 23 G stainless steel.

As each of the three flows had to go through a single outlet there was a possibility of mixing between the solutions. However, with a dead space of approximately 0.8 mm^3 at the tip of the delivery tube, and with a flow rate of 5 ml/min, or approximately 800 mm^3/s, the solutions would clear the end tubing within 1 ms.

Due to the fact that there may be a slight difference in switching time between turning the valve on and off, the electrical control circuitry was designed such that there was a delay ($\simeq$ 100 ms) between the time one valve was turned off and another was turned on. This enabled one valve to be switched off completely before the other was turned on eliminating the possibility of having two valves on simultaneously, and thus mixing the solutions.

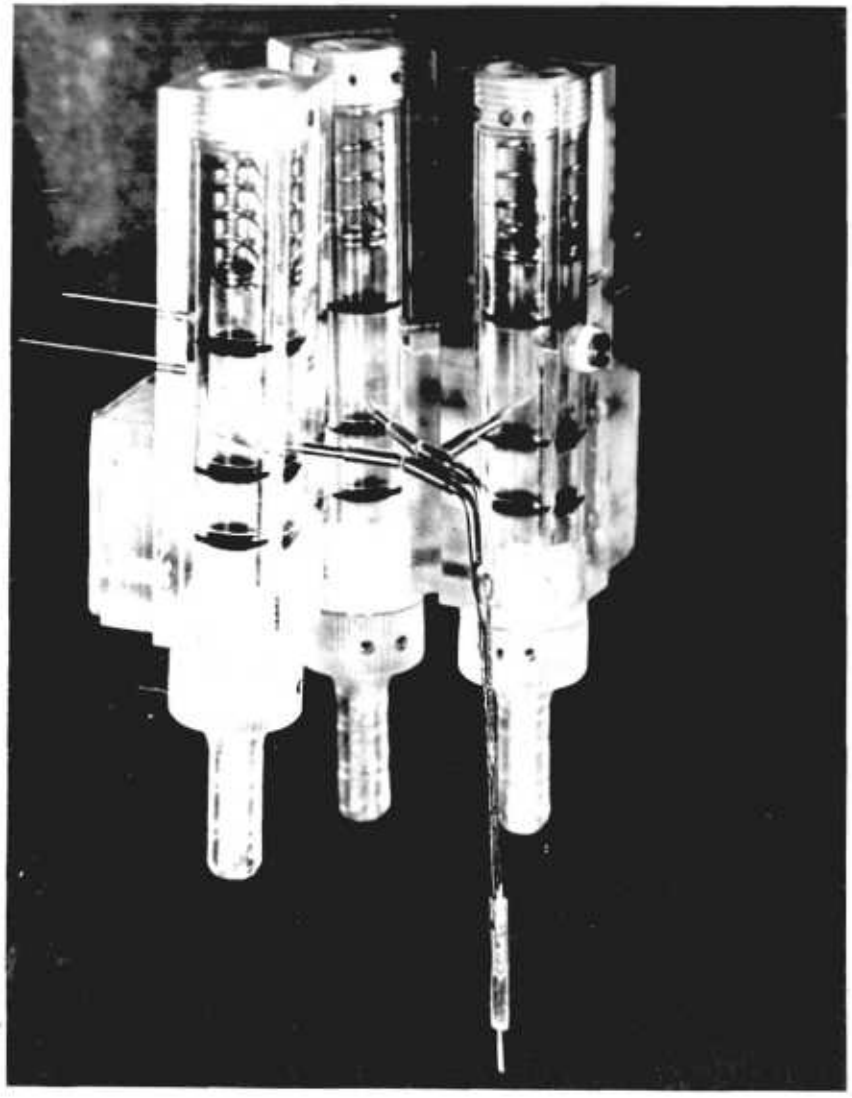

(a) SUPERFUSION VALVE CLUSTER

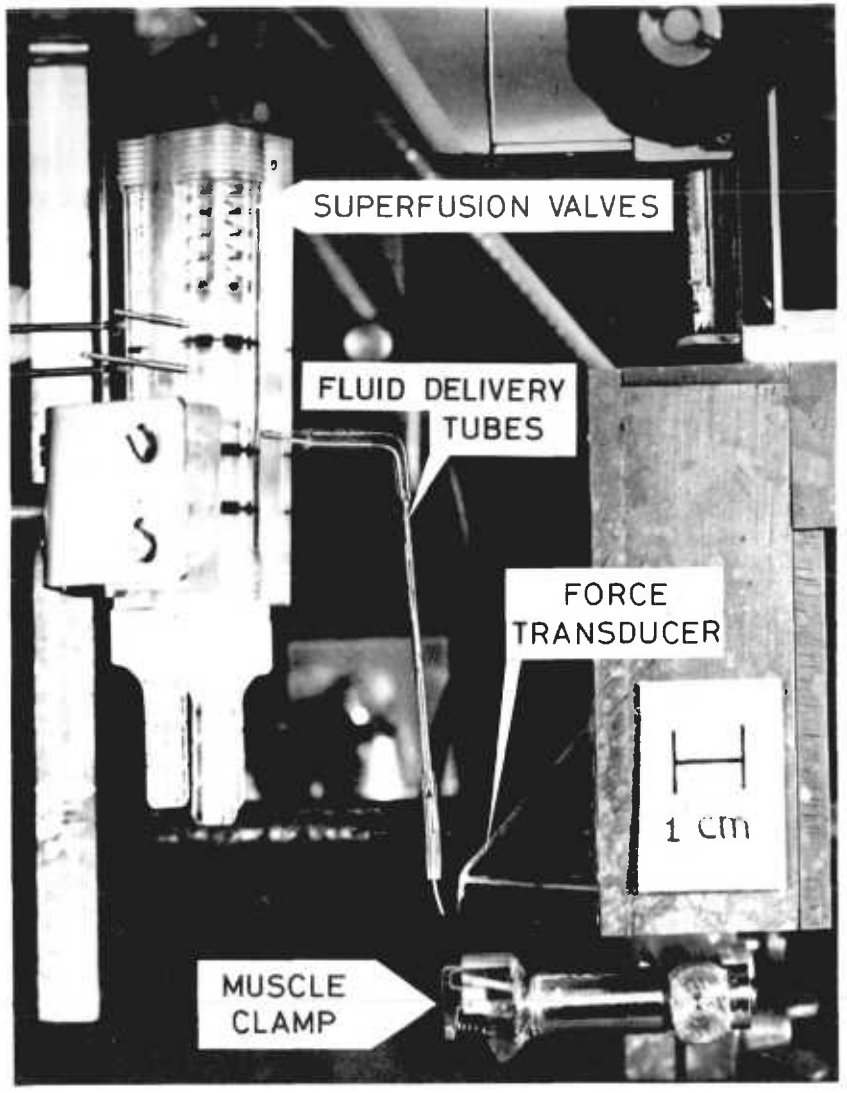

(b) MUSCLE APPARATUS

Fig. 3.6

Although one can estimate the time it takes for the dead space to be cleared, a great deal of uncertainty remains as to how quickly the solution changes around the muscle. This depends very much on the flow pattern, and whether the flow around the muscle is laminar or turbulent. If the off-on delay is adjusted such that there is a short but definite break in the flow as it emerges from the delivery tube, then the flow will become turbulent with the initial flow of the new solution. This turbulence helps to remove the old solution around the muscle and effectively increases the rise-time of the step change in concentration at the muscle. Thus, a more realistic estimate of the switching time of the solutions around the muscle is probably 100 ms or less.

3.6.6 The electronic control system

Since the superfusion system was to be used for both step-response analysis and pseudo-random analysis, a means of controlling valve action electronically was required. Mains operated solenoid valves (Kuhnke micro-solenoid valves, type 65.204) were chosen to control the air pressure required for valve action, and with suitable circuitry, switching transients could be eliminated (Appendix I).

Pseudo-random studies require the use of three solutions; one for the chosen operating level of calcium concentration, and two others at slightly different concentrations for use as the perturbation signals. Thus a means of switching between the operating solution and the perturbation solutions was required, as well as switching between the two perturbation solutions only.

With these specifications in mind, an electronic control system was designed to operate the superfusion valves. Two separate control signals were required; one to trigger the switching of the valves, and a second to

determine which valves were to be switched. Appendix G describes in detail the electronic circuitry required, and its principle of operation. Fig. 3.1 indicates the relationship between the superfusion valves, the electronic control system, and the remainder of the experimental system.

CHAPTER 4

EXPERIMENTAL METHODS

4.1 Experimental Preparation

Before commencing the experiment, the experimental enclosure was raised to the required operating temperature (30°C), and the force transducer calibrated with the pen recorder after temperature equilibrium was reached. The remaining electronics were also checked and calibrated to ensure correct levels and gains for the computer and analog tape recorder.

Concurrent with waiting for the temperature to stabilize, the physiological solutions of different calcium concentrations were prepared. It was normal practice to have the following solutions premixed and to bring these together when required to make the proper physiological salt solutions: (i) Bulk stock solution containing the following compounds: NaCl, 5.21 g/l; $NaHCO_3$, 2.02 g/l; $Na_2HPO_4.12H_2O$, 0.358 g/l; $MgSO_4.7H_2O$, 0.246 g/l; and KCl, 0.372 g/l. This solution was bubbled with an O_2(95%)-CO_2(5%) gas mixture prior to mixing the solutions. (ii) A nutritive

solution containing: sodium acetate trihydrate, 136 g/l; D-Glucose, 905 g/l; and insulin, 250 units/l. (iii) A series of $CaCl_2$ solutions, each of a different concentration.

To make the required physiological salt solution, 20 ml of the appropriate $CaCl_2$ solution, and 20 ml of the nutritive solution were pipetted into a graduated 1 litre flask. The oxygenated bulk stock was then added to make up 1 litre. The pH of this final solution, equilibrated with 5% CO_2 in O_2, was 7.3. This solution was placed in the water bath, oxygenated, and allowed to circulate through the superfusion system.

4.2 Dissection and Mounting of the Papillary Muscle

Young kittens (average weight 0.7 kg) were anesthetized with chloroform and the hearts rapidly excised after opening the chest cavity along the sternum. The pericardium was then removed and the hearts washed in three successive baths containing oxygenated physiological salt solution of 2.25 mM calcium concentration. During washing the heart was continually massaged to facilitate the removal of blood from both the ventricular cavities and the coronary arteries. After washing, the heart was placed in a dissecting dish, which also contained oxygenated solution, and the right ventricle opened to expose the papillary muscles.

Only long, thin muscles were selected (maximum diameter 1 mm, and minimum length 3 mm) to ensure that they did not become anoxic during the course of the experiment (Jewell & Blinks, 1968; Blinks & Koch-Weser, 1963). Once a suitable muscle was found, a length of silk thread with a preformed loop (diameter ≃ 1 mm) was passed under the chorda tendinea so that the base of the loop was as close as possible to the muscle-tendon junction. The thread was made secure using a reef-knot, the excess thread cut away, and the tendon cut close to the knot. The muscle was then detached from the

ventricular wall to leave a small tuft of wall at the base of the papillary muscle. During the dissection procedure, care was taken not to touch, stretch, or in any way damage the papillary muscle.

The base of the muscle was positioned over the punctate electrode in the muscle clamp, and held in place by the spring loaded clip. The assembly was transferred to the remaining apparatus, secured into position, and the free end of the muscle connected to the force transducer by passing the loop of thread around the hook at the tip of the transducer. The glass shroud was moved into position and the superfusion started. Fig. 3.6b shows the relative position of the muscle clamp, force transducer, and superfusion delivery tubes, but it does not show either the muscle or the glass shroud. On average it takes about thirty seconds to fasten the muscle to the force transducer and begin the superfusion.

Normally the muscle was stimulated at a rate of 20/min, with a pulse of 2 ms duration. The stimulation voltage was kept to within 10% of the threshold voltage (≈ 0.5 V) to reduce the effect of norepinephrine release (Koch-Weser, 1965).

Over the course of one to two hours, the muscle was slowly stretched until the optimum length was reached (Appendix A). This usually occurred with a resting tension of between 0.3 and 0.5 g. The muscle was allowed to run-in over a period of three to four hours from the time the muscle was first mounted. At the end of the run-in period the system was put on-line, and the experiment proper begun.

4.3 Experimental Protocol

The first phase of the experiment consisted of determining the steady-state and step-response of the isometric tension to changes in calcium concentration. The next phase was the pseudo-random study, normally conducted about one operating level of calcium concentration. The actual steps taken during these phases are described in detail below.

The order, in which the calcium concentrations were changed, was randomized, and the average calcium concentration was kept at about the same level throughout the first phase of the experiment. Early experiments used only three different calcium concentrations (1.25, 2.25, and 3.25 mM) to obtain preliminary step-response and pseudo-random results. In later experiments 0.5 mM and 4.5 mM were also added to obtain a better measure of the dose-response curve. For those experiments in which the pseudo-random analysis was to be attempted at low calcium concentrations, 0.75 mM and 1.0 mM were also included into the dose-response curve determination.

Since only three superfusion valves were available, two solutions only could be tested at a time; the third valve was kept for the 2.25 mM concentration which was the base from which concentration perturbations were made.

The computer would measure and record the parameters of ten consecutive steady-state contractions before the enable switch (Fig. 3.1) was placed in the MAN position by the experimenter. The solution was switched to another concentration value at the beginning of the eleventh contraction, and immediately after switching, the enable switch was returned to the OFF position. The exact time of switching was determined by the master clock (Section 3.2), and for the step-response studies was set at $t = 0$, i.e. at the time the muscle was stimulated.

The computer continued to record parameters for between 200 and 256 consecutive beats at which time, at the discretion of the experimenter, recording was stopped. The muscle was allowed to reach equilibrium before the next set of steady-state and dynamic measurements were made. It usually took between ten and fifteen minutes for the muscle to stabilize, and this was dependent to some extent upon whether the calcium concentration was increased or decreased. A typical transient for a step increase and decrease between two levels of calcium concentration is shown in Fig. 4.1, and the significance of the difference in dynamics is discussed in the next chapter.

Once the new steady-state level was reached, the same procedure was followed and the solution returned to the 2.25 mM level. After a solution had perfused the muscle, that particular superfusion valve and tubing were flushed with distilled water and then with the next solution to be tested. In this way the response of the muscle to a number of different calcium concentrations could be tested with only three superfusion valves.

Sometimes, instead of measuring the normal response on every second or alternate solution change, it was measured on every third change. In this way tension transients with a number of different concentration combinations could be measured. Also, a number of separate measurements (from 3 to 5) were made at 2.25 mM, while normally only one measurement was made at the other calcium concentrations. From this one could arrive at an estimate of the scatter in the measurements.

The duration of this phase in the experiment was about four hours, and if more repeats were required at other calcium concentrations, it would at least double the time for this phase. This fact must be kept in mind when one considers that the steady-state and step-response measurements comprise only half the experiment, and that the muscle is an ever changing system.

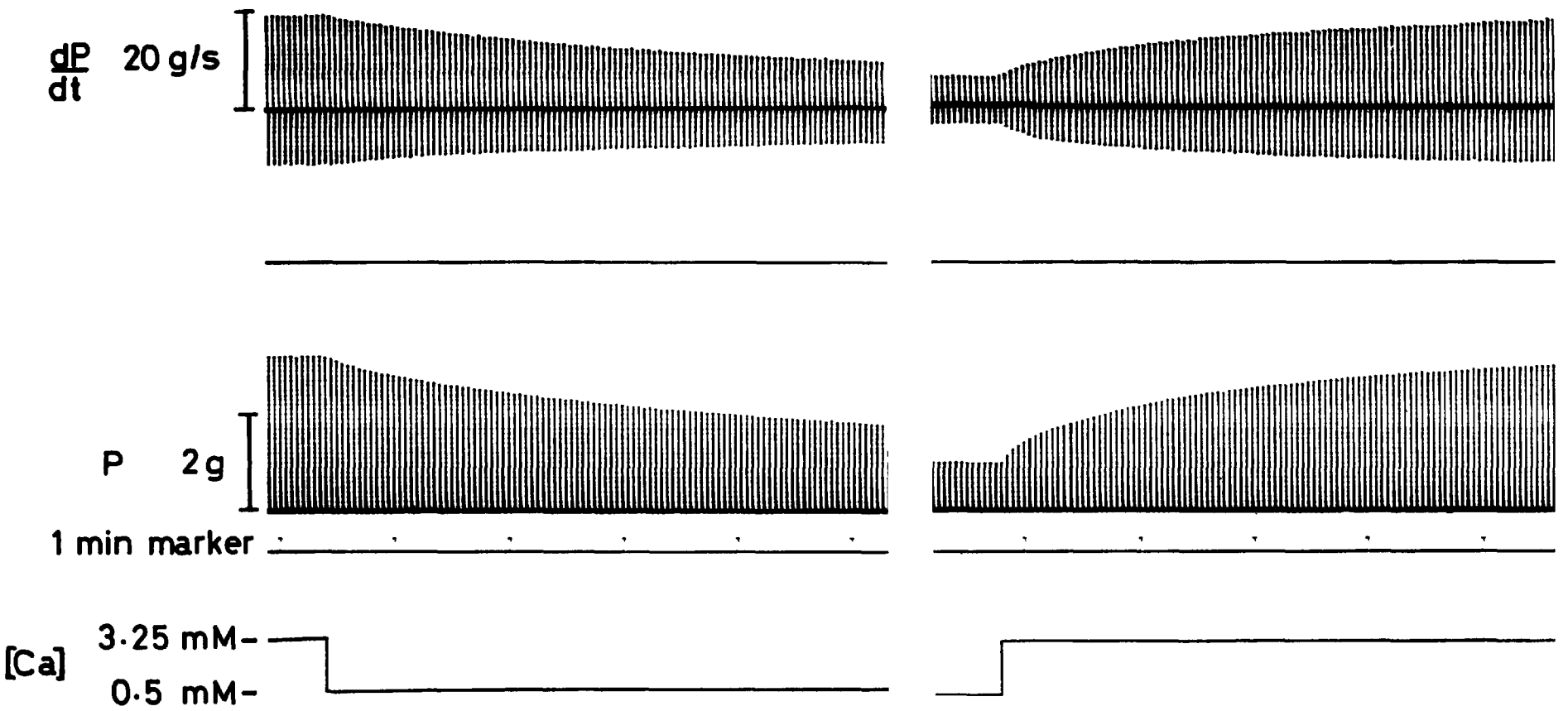

Fig. 4.1 Step-response of kitten papillary muscle to changes in external calcium concentration. Separation between records represents a time interval of 12 minutes. Muscle diameter 1·0 mm, frequency of stimulation 20/min, temperature 30°C.

After the last solution change, the concentration was at the operating level from which the pseudo-random study was to commence. Superfusion valve 3 controlled the switching of this solution, while valves 1 and 2 switched between the perturbation solutions.

To begin the p.r.b.s., the external sense line switch 3 was raised at the interface. This called the pseudo-random subroutine (Appendix F) and from then, until the end of the sequence, all operations - superfusion valve switching and data recording - were carried out automatically by the computer. At the completion of the p.r.b.s. run, the valves were returned to their initial position so that the control solution prefused the muscle. The muscle was then allowed to stabilize before the next p.r.b.s. run was begun.

Because the rate of stimulation of the muscle was 20/min, the minimum time interval permissible between the switching of the solutions was 3 s. The length of a pseudo-random run was dependent upon the type of sequence used, and allowing for initial start-up time (Appendix F) the 255 point M-length sequence lasted 20.5 minutes, and the 510 point inverse-repeat sequence lasted 30.5 minutes. The duration of this phase of the experiment was also about four hours.

At the end of the experiment - total duration of about twelve hours - the muscle length was measured with the aid of a pair of calipers before removing the muscle from the apparatus. The tuft and thread loop were then cut away and the wet weight measured on a Mettler balance (type H6T). The force transducer was also calibrated on-line before the computer and apparatus were shut down.

CHAPTER 5

RESULTS

5.1 Introduction

The results of this investigation are divided into three main groups. The first is the empirically derived dose-response curves upon which the other results depend. The next describes the validity of the shell method of modeling with a non-linear dose response curve, and this is followed by a comparison of the predicted step-response curves with those obtained experimentally. The final section describes the impulse-response curves that were obtained by using a pseudo-random change in calcium concentration as the input signal to the heart muscle system.

5.2 The Steady-State Dose-Response Curve

It was noted in Chapter 2 that there is a functional relationship between isometric tension produced by an isolated papillary muscle and the calcium concentration in the perfusion medium. This relationship can be determined empirically, and can be described by a dose-response curve. In addition to the steady-state values, the step-response of the system can be obtained as a by-product of the dose-response curve determination, provided step changes in concentration are applied to the muscle.

The average value of the peak isometric tension of ten consecutive contractions was taken as the steady-state level of tension at a given concentration. The calcium level was then suddenly changed to a new value i.e. a step change, and at least ten to fifteen minutes were allowed for the muscle to reach the new equilibrium level before the next steady-state measurements were made.

The steady-state results indicate that, in the range of 0.5 mM to 4.5 mM calcium concentration, the dose-response curve could be fitted by an exponential equation of the form

$$p = p_{max} - Ee^{-MC} \qquad (5.1)$$

where p_{max} represents the maximum possible tension that the muscle could produce even if higher calcium concentrations were applied to it. The parameters E and M represent the coefficient and "rate constant" of the exponential term, and C is the independent variable, calcium concentration. These parameters were evaluated by using the curve stripping method as described in Appendix B. The values obtained are given in Table 5.1 along with the various muscle parameters. The dose-response curves are shown in Fig. 5.1. All of these curves were obtained at a temperature of $30^{o}C$, and at a frequency of stimulation of 20/min.

Muscle	p at 2.25 mM (g/mm^2)	S.E.	N	p_{max} (g/mm^2)	E (g/mm^2)	M (mM^{-1})	Length L (mm)	Weight W (mg)	Diameter d (mm)
1	6.19	0.26	3	7.3	8.62	0.92	7	3.3	0.8
2	6.34	0.10	3	7.7	9.67	0.93	5	2.1	0.7
3	4.10	0.10	3	5.4	7.41	0.79	4.5	1.2	0.6
4	4.59	0.04	5	6.5	8.41	0.63	6	2.7	0.8
5	4.18	0.14	5	8.5	9.72	0.36	11.5	3.2	0.6
6	3.76	0.01	3	4.8	5.00	0.69	5	3.6	1.0

Dose-response curve and muscle parameters

Table 5.1

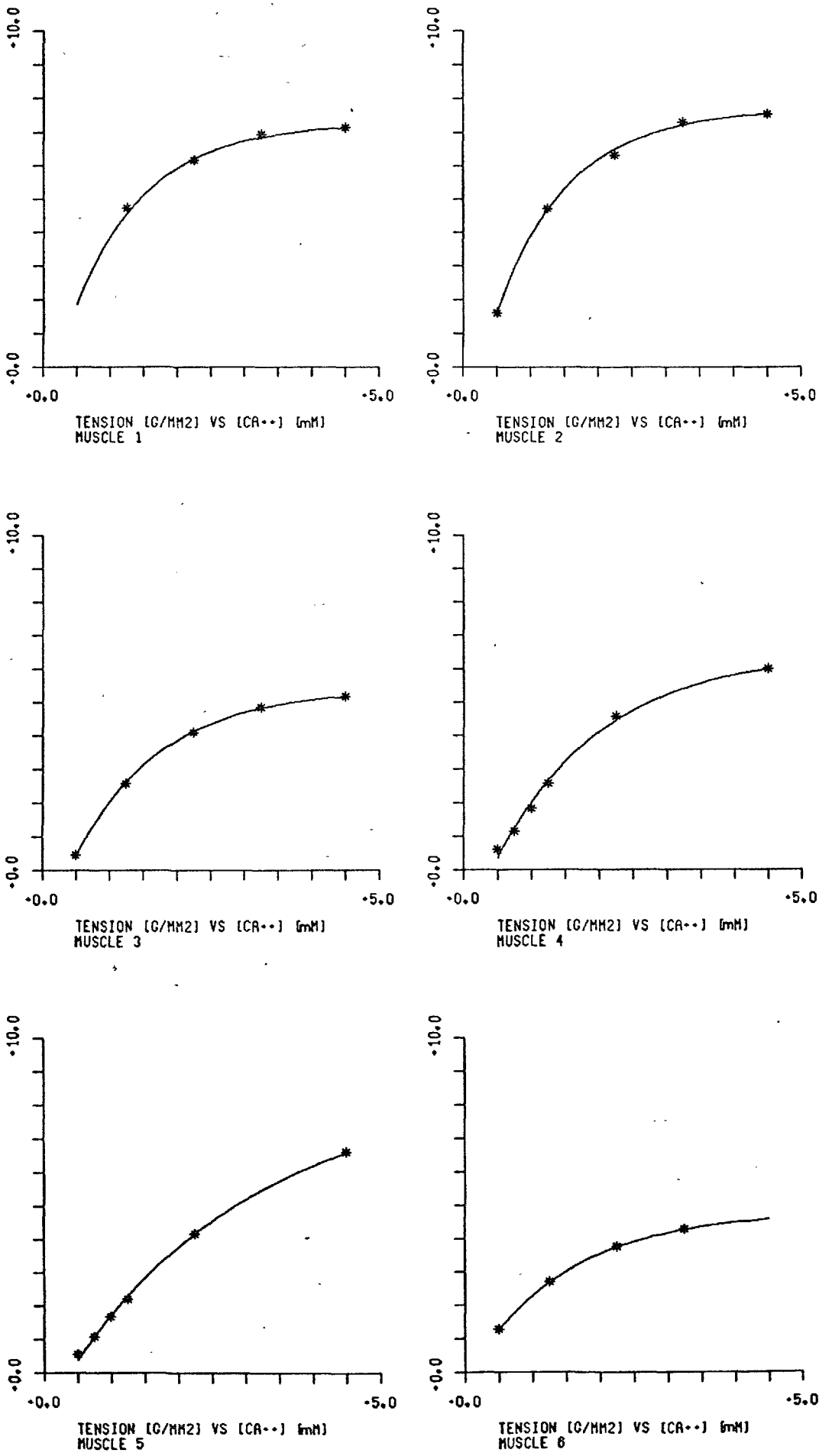

Fig. 5.1 DOSE-RESPONSE CURVES FOR KITTEN PAPILLARY MUSCLES

5.3 Step-Response Analysis

The fact that the superfusion system could be used to apply sudden changes in calcium concentration to the muscle made it ideal for step-response studies. Consequently, the tension transient curves were obtained in conjunction with the dose-response curve determination. Because the order in which the calcium concentrations were switched was random, and since the dose-response curves were non-linear (Fig. 5.1) the transients were obtained, in general, over the non-linear range of the dose-response curves. But by using the model proposed in Section 2.2, tension transients could be simulated and compared with those obtained experimentally.

5.3.1 The influence of calculation methods and the shape of the dose-response curve on tension transients

Section 2.2 described how the concentration throughout a cylinder can be computed on a point-by-point basis, (Eq. 2.8) or on an average basis (Eq. 2.9) at any instant of time. The equation for the average concentration is quite straightforward with only one variable, time, while the point-by-point equation has two variables, distance and time. These two independent variables make the implementation of Eq. 2.8 more complex, and led to the necessity of dividing the cylinder into a number of concentric shells to give the concentration at a number of points along the radius of the cylinder.

In order to determine the accuracy of the shell method of analysis, the average and shell methods were compared on a dynamic basis with a linear dose-response curve whose equation was

$$p = 1.197C - 0.200 \qquad (5.2)$$

The coefficients for this line were chosen to give the same steady-state values of tension as those given by Eq. 5.3 for concentrations of 0.5 mM and 4.5 mM.

If the two methods of computing concentration and tension are identical, then for a linear dose-response curve, the tension transients derived from each method should be identical for both a step increase, or a step decrease in concentration. An examination of Figs. 5.2a,b shows that this is indeed the case.

Next a non-linear dose-response curve was substituted in place of the linear curve and the calculations repeated. The equation for this dose-response curve was that measured for muscle 3 (Table 5.1). For convenience it is repeated here as

$$p = 5.4 - 7.41e^{-0.79C} \qquad (5.3)$$

For this case Figs. 5.2c,d show that the tension transients are different with the two methods of computing concentration.

As a further check on the validity of the shell method, and on the number of shells required to make the tension transient curves converge, the radius was subdivided into five sections instead of the ten previously used, and the analysis for the non-linear dose-response curve repeated. These results are also shown in Figs. 5.2c,d. Comparison of the five and ten shell calculations shows that the two transient curves are virtually identical, and that they are both significantly different from the result obtained by the average concentration method. Therefore, it can be concluded that there would not be any significant change in the computed results if the number of shells used in the calculations were to be increased beyond ten.

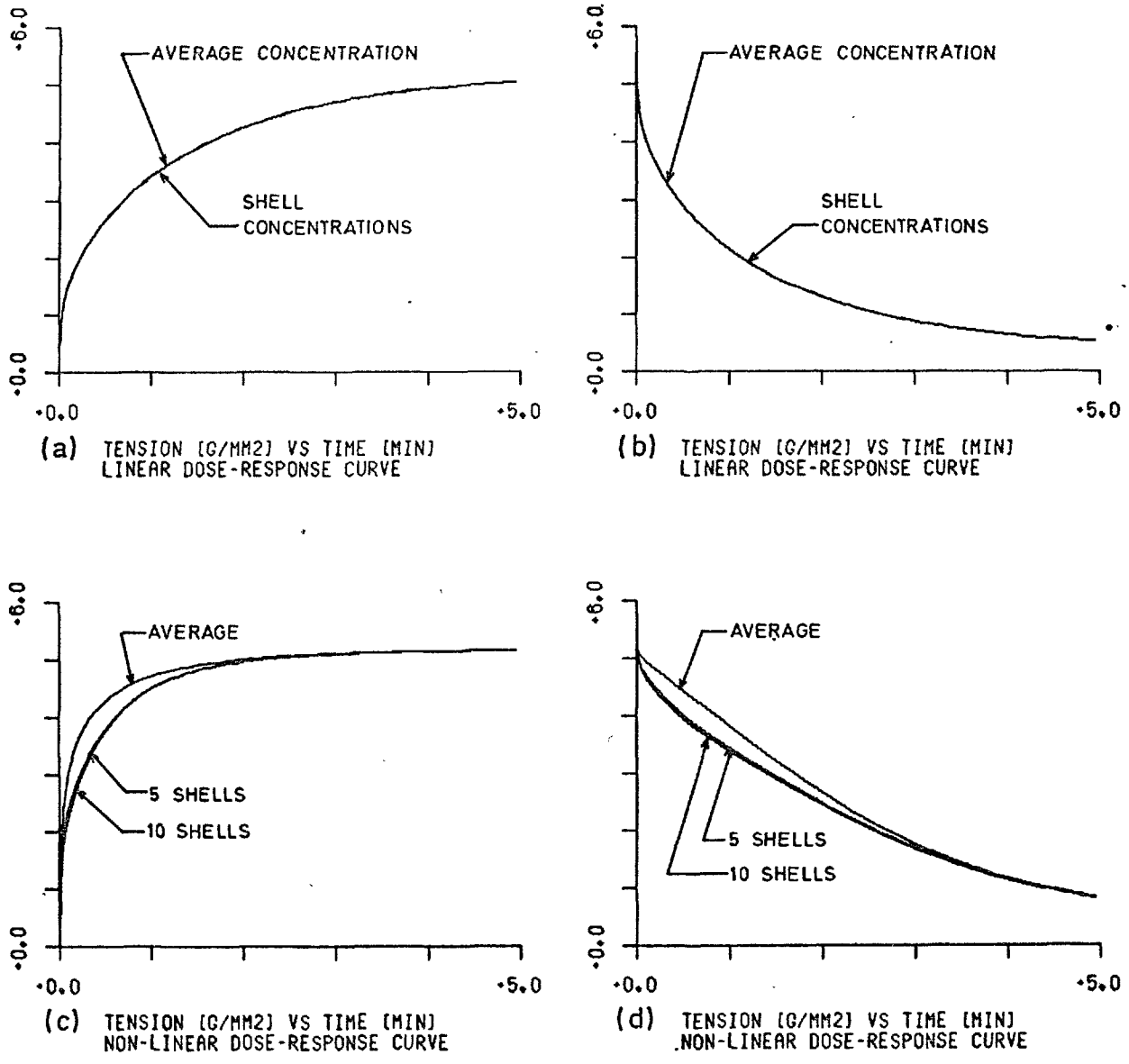

Fig. 5.2 Tension transients from different concentration calculation methods and dose-response curves.

It is also of interest to note that the time course of the transients are dependent upon the direction in which the concentration has been changed at the surface of the muscle. An increase in calcium concentration from 0.5 mM to 4.5 mM results in a tension transient that has a faster time course than the corresponding transient when the concentration is reduced from 4.5 mM to 0.5 mM. This difference in dynamics is caused by the non-linearity of the dose-response curve, and the reason for this distortion can be better appreciated from Fig. 5.3. In this figure, the time course of calcium concentration, when the external level is switched from A to B, is assumed to be identical to that when the concentration is switched from C to D, i.e. the fractional or percentage change in concentration at any time is identical in the two directions.

It can be seen (Fig. 5.3a) that initially an increase in concentration from A to B causes a rapid climb up the dose-response curve as the tension moves from A' to B'. This is because the slope of the dose-response curve is quite steep at A'. Now, if the concentration is returned to its original level, after equilibrium of tension had been reached, the tension does not decrease as rapidly as it moves from C' to D' (Fig. 5.3b). This is because the slope of the dose-response curve at C' is not as steep as it is at D'.

Thus, the amount by which the dynamics differ, is governed by the degree of non-linearity present in the dose-response curve over the region of interest. For a linear curve, there is no difference in dynamics (Fig. 5.2a,b), but for a non-linear curve there can be a marked difference (Fig. 5.2c,d).

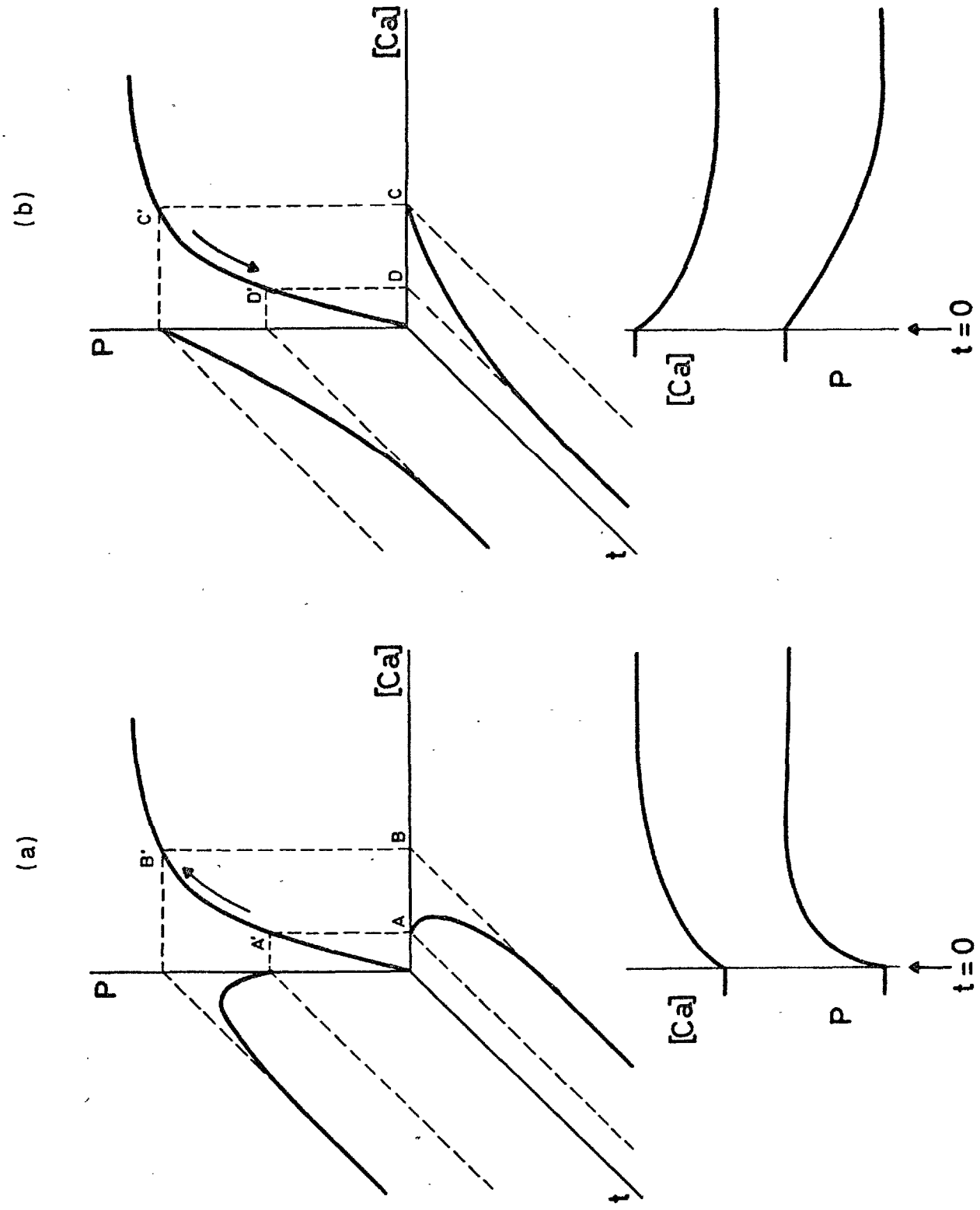

Fig. 5.3 Influence of a non-linear dose-response curve on tension transients.

5.3.2 Comparison between experimental and theoretical step-responses

Using the dose-response curves of Section 5.2 and the theoretical considerations of Section 2.2, step-responses were computed for a number of muscles with the calcium switched between different levels and in different directions. These predicted transient curves were then compared with the experimentally measured curves under the same conditions (Fig. 5.4).

In the process of matching these curves, the diffusion constant, k, was varied until a reasonable, by eye, fit was achieved. This was because the diffusion constant of a substance diffusing through the extracellular space is taken to be about one quarter the free solution value, and is not known exactly. For the curves shown in Fig. 5.4, the average value of k was found to be 1.5 ($\pm$ 0.3) x 10^{-6} cm^2/s (s.d. of 10).

It must be remembered that the shell method of computing concentration is based on the assumption that the muscle is cylindrical in shape, and that the radius remains constant along the length of the muscle. The importance of a constant radius is reflected in the diffusion equation (Eq. 2.8) where the time constants of the exponential terms vary as the square of the radius. Consequently, any errors in the determination of the radius can greatly influence the computed results.

Thus, if the muscle is tapered along its longitudinal axis, or if the cross-section of the muscle is not circular, then the use of Eqs. 2.1 and 2.2 will give only an average diameter or radius of the muscle. Thus, if the geometry of the muscle is radically different from a straight cylinder, one can expect a difference between the predicted and experimental step-response curves.

The largest single source of error in determining the radius of the muscle is in the measurement of its weight. This is done at the end of the

experiment when the muscle is "lightly" blotted to remove excess water from its surface before it is weighed. Normally the mean value, of two or more measurements, was taken as the weight of the muscle, and the results were repeatable to $\pm$ 0.1 mg using a Mettler (type H6T) balance. However, since three-quarters of the muscle's weight can be accounted for by its water content, 20-30% variations in the values obtained could be introduced, depending upon the degree of "lightness" used in blotting the muscle. With a typical weight of a papillary muscle being 2.5 mg, it can be appreciated that small fluctuations in the water content could produce large percentage changes in the estimate of the true weight. Thus weighing was a very subjective process which, although the values were repeatable, could give results significantly different from the true weight.

The length of the muscle was measured with the aid of a pair of calipers while the muscle was still suspended between the force transducer and the muscle clamp. Again inaccuracies in the length measurement (measurement error $\pm$ 0.5 mm) will cause the radius calculation to be in error.

The dose-response curve can also be in error as it is fitted by an exponential equation using the method of curve stripping. Because of this, and because of the biological variation in the muscle preparation over a period of time, it is possible that the steady-state levels of tension between the experimental and predicted results do not correspond. See for example, Fig. 5.4f in which two step-responses for the same muscle are shown along with the predicted curves. These results were obtained with the calcium concentrations switched between the same two values, but at different times during the experiment. In this example, not only are the

Fig. 5.4 Comparison of experimental and theoretical step-responses. The individual points represent the peak isometric tension for each muscle contraction while the continuous curve represents the computer simulated step-response.

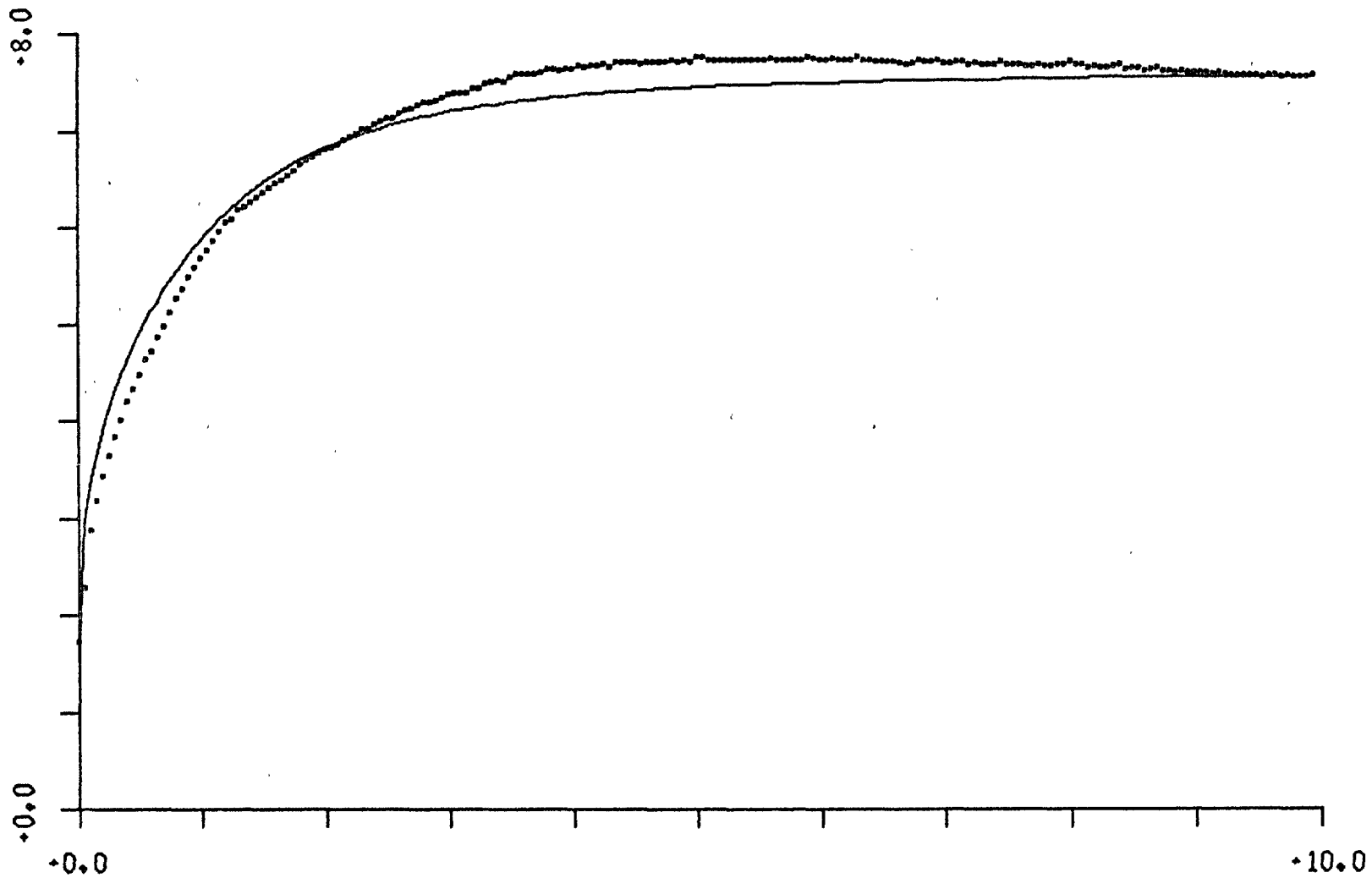

Fig. 5.4a TENSION [G/MM2] VS TIME [MIN]
[CA++] 0.5-4.5 mM . MUSCLE 2.
DIFFUSION CONSTANT 1.2 X 10E-6 CM2/S .

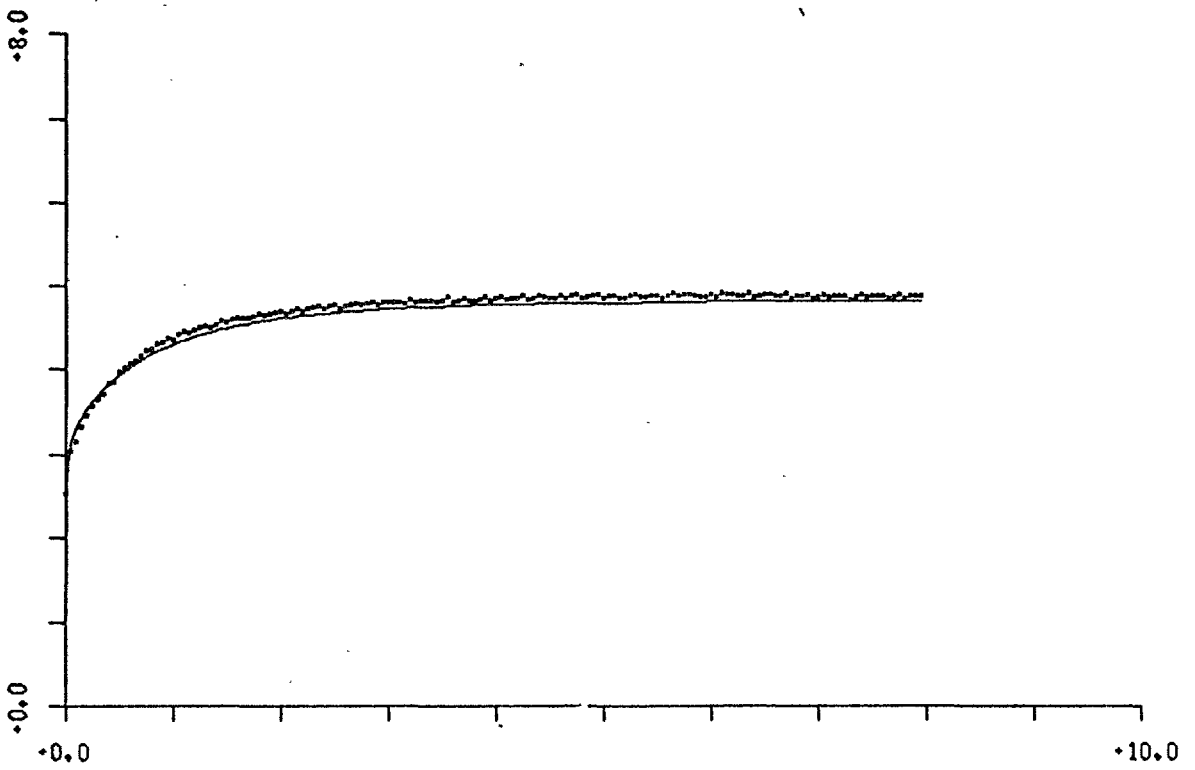

(b) TENSION [G/MM2] VS TIME [MIN]
[CA++] 1.25-3.25 mM . MUSCLE 3.
DIFFUSION CONSTANT 1.5 X 10E-6 CM2/S .

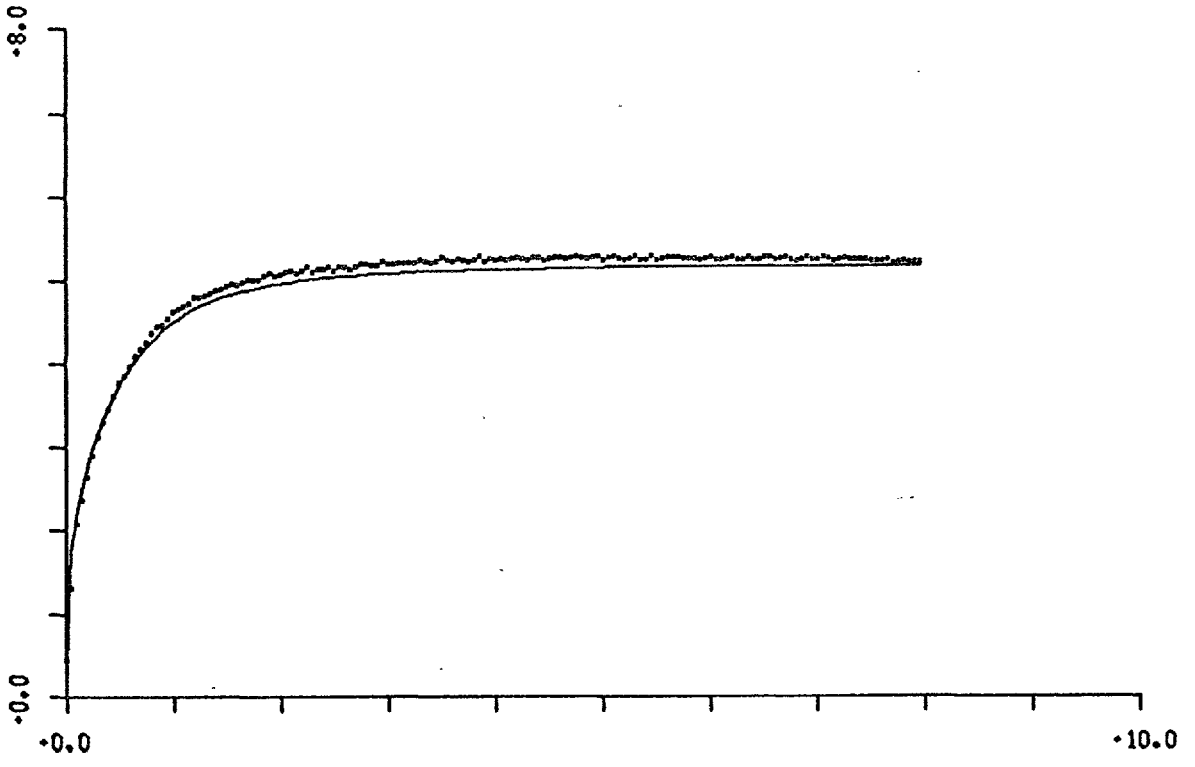

(c) TENSION [G/MM2] VS TIME [MIN]
[CA++] 0.5-4.5 mM . MUSCLE 3.
DIFFUSION CONSTANT 1.5 X 10E-6 CM2/S .

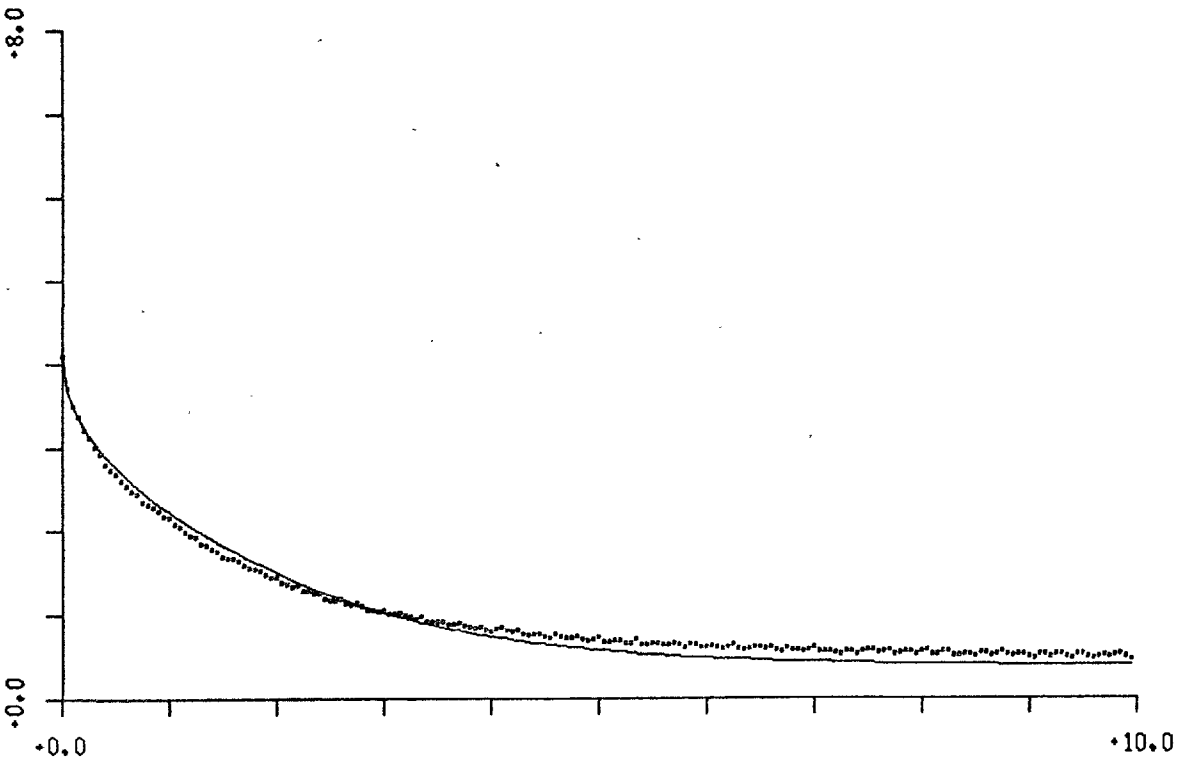

(d) TENSION [G/MM2] VS TIME [MIN]
[CA++] 2.25-0.5 mM . MUSCLE 3.
DIFFUSION CONSTANT 1.5 X 10E-6 CM2/S .

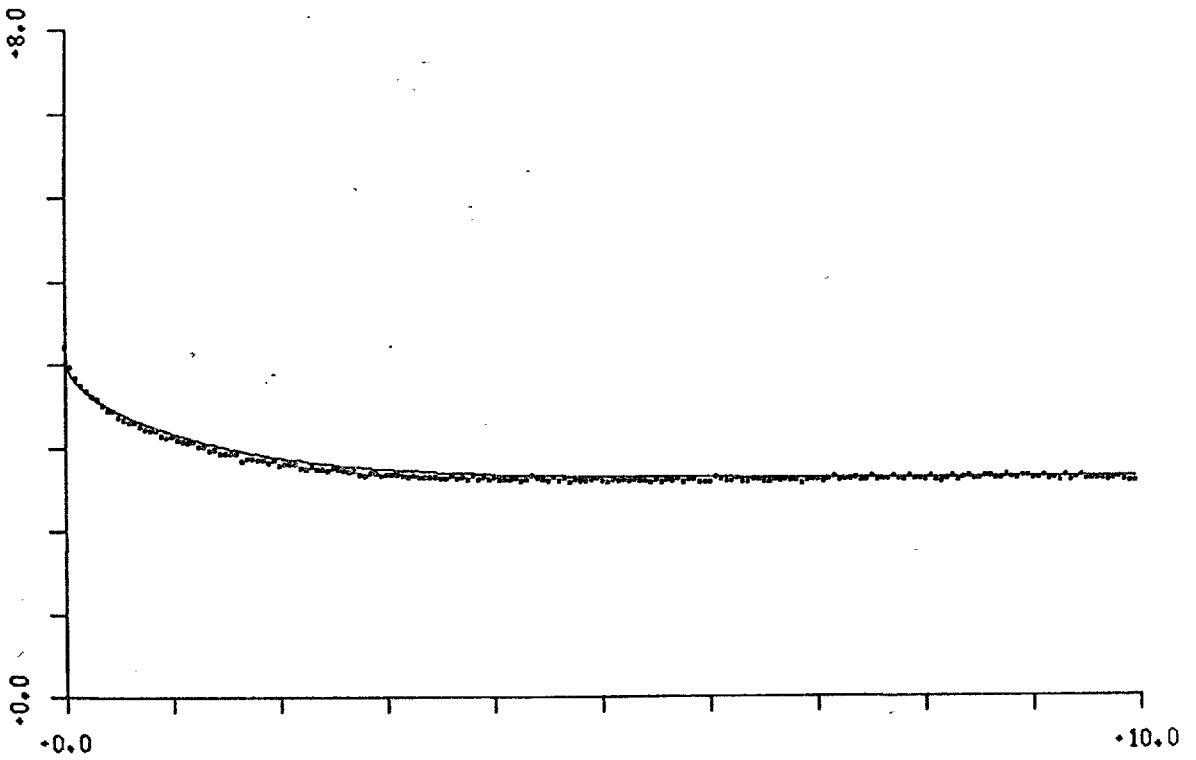

(e) TENSION [G/MM2] VS TIME [MIN]
[CA++] 2.25-1.25 mM . MUSCLE 3.
DIFFUSION CONSTANT 2.0 X 10E-6 CM2/S .

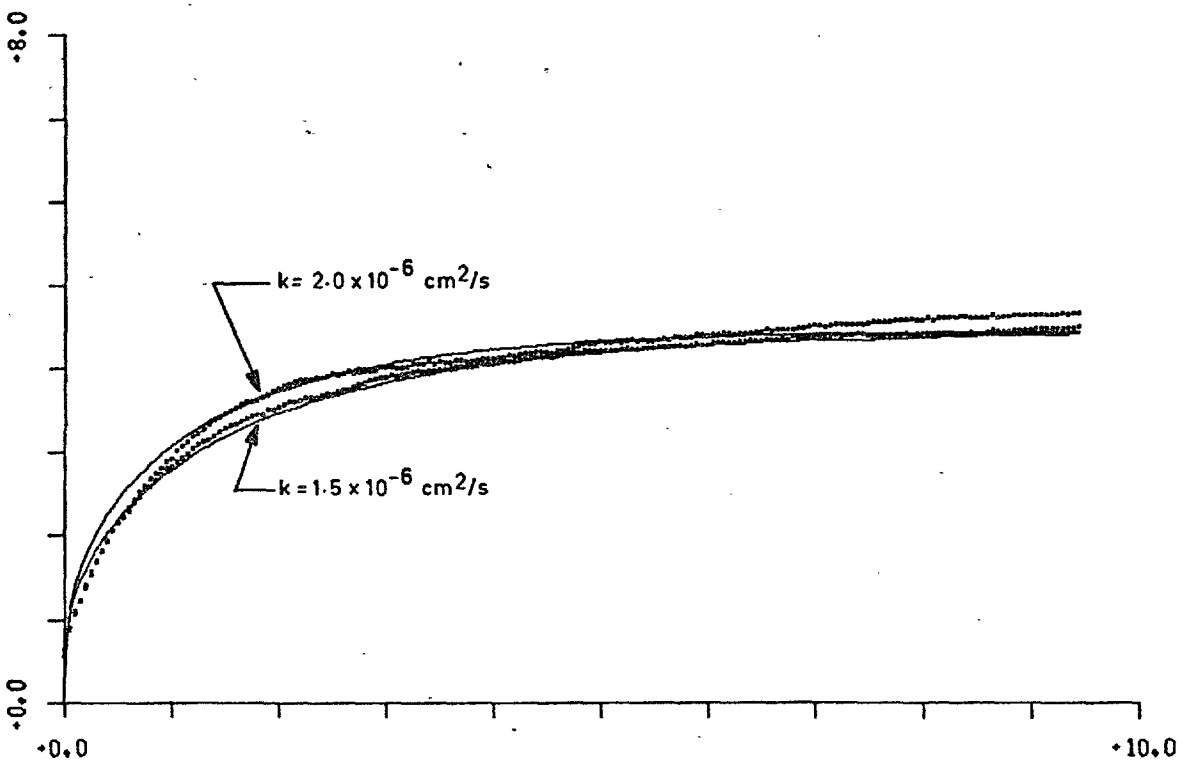

(f) TENSION [G/MM2] VS TIME [MIN]
[CA++] 0.5-2.25 mM . MUSCLE 4.

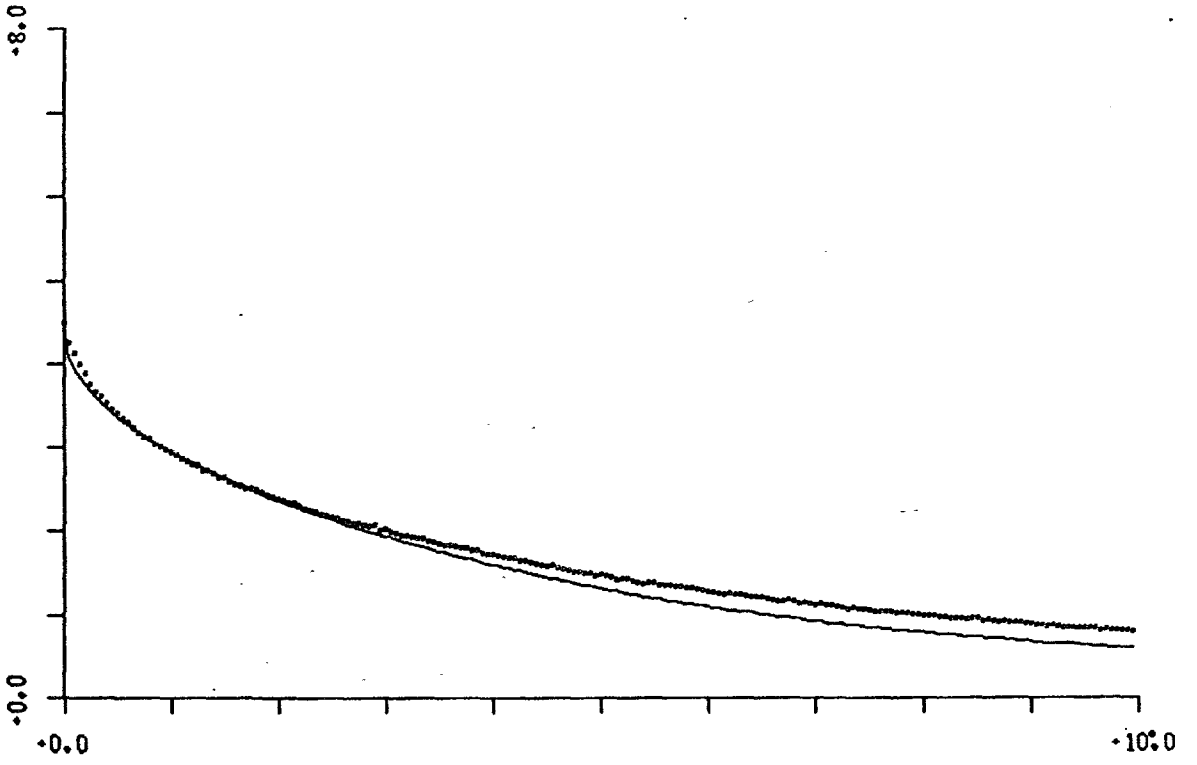

(g) TENSION [G/MM2] VS TIME [MIN]
[CA++] 2.25-0.5 mM . MUSCLE 4.
DIFFUSION CONSTANT 1.2 X 10E-6 CM2/S .

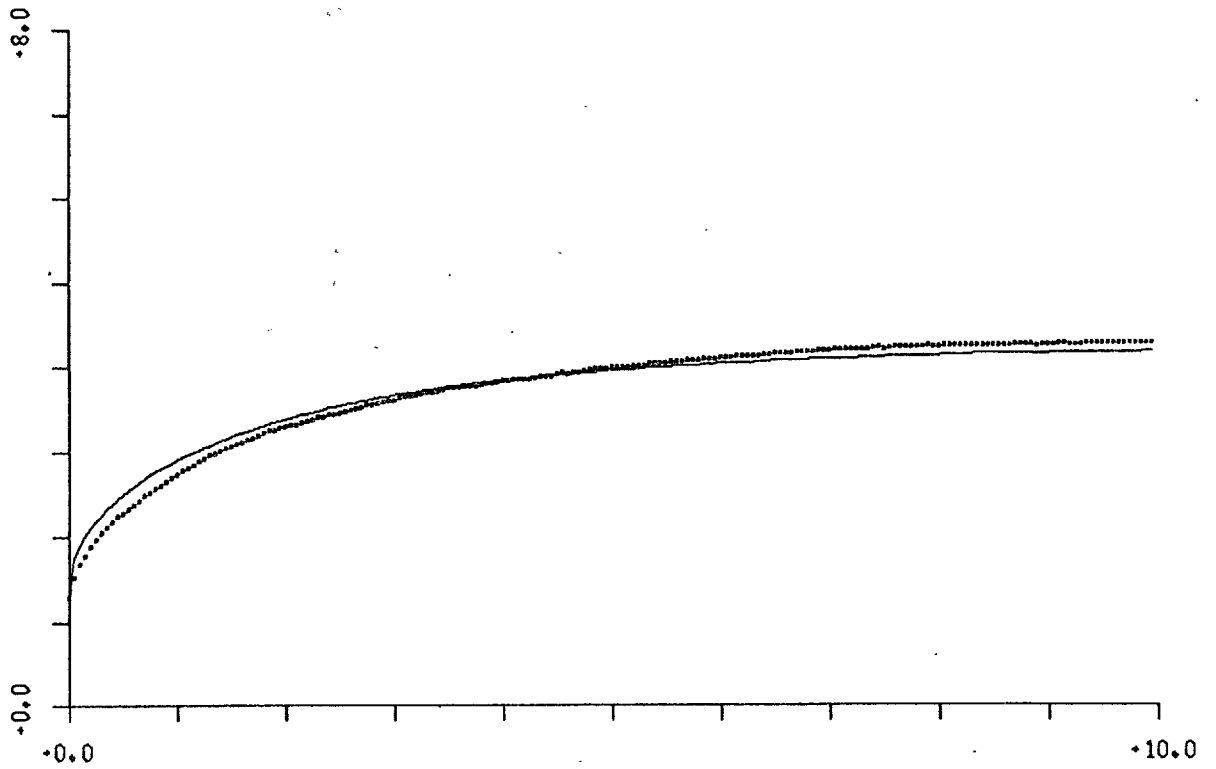

(h) TENSION [G/MM2] VS TIME [MIN]
[CA++] 0.5-3.25 mM . MUSCLE 6.
DIFFUSION CONSTANT 1.5 X 10E-6 CM2/S .

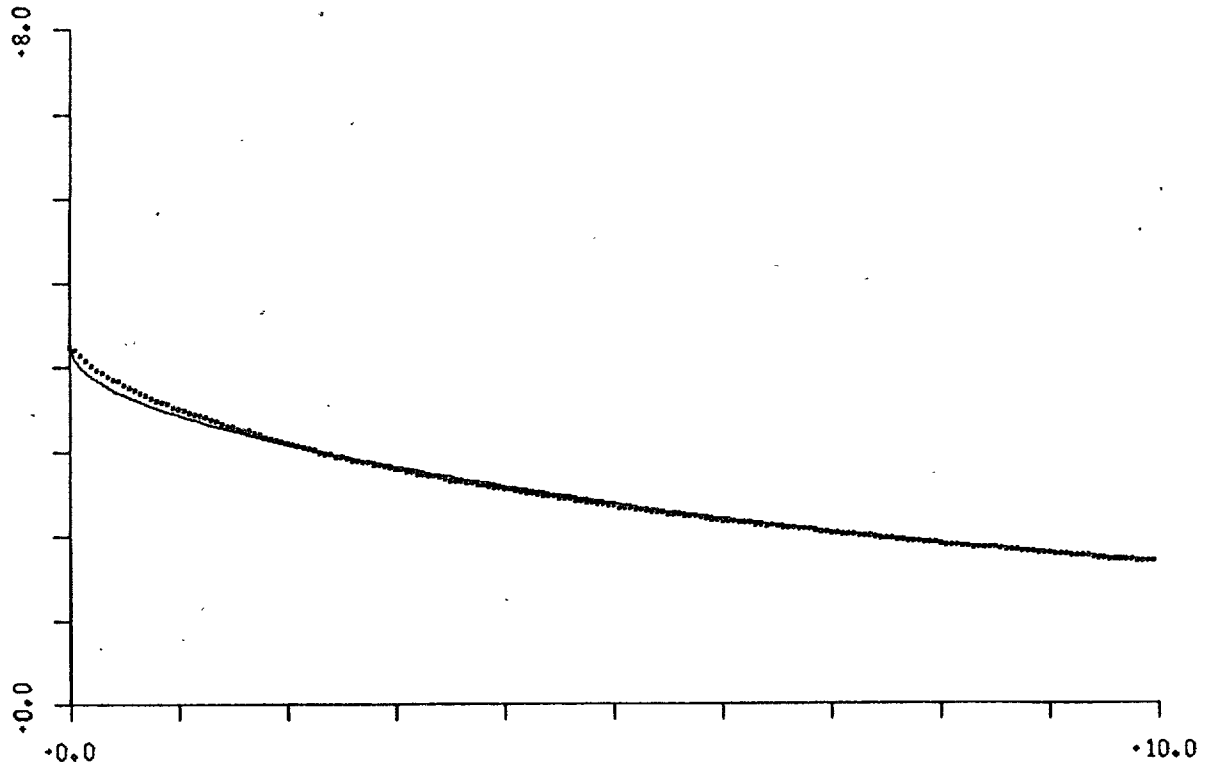

(i) TENSION [G/MM2] VS TIME [MIN]
[CA++] 3.25-0.5 mM . MUSCLE 6.
DIFFUSION CONSTANT 1.5 X 10E-6 CM2/S .

steady-state tension levels between the experimental and predicted curves different, but the time course of the two experimental curves also differ from each other. Another variation which sometimes occurred was tension overshoot (Fig. 5.4a), before the steady-state level was reached.

All of these variations must be taken into account when comparing the simulated and the experimental step-response curves. It was for these reasons that the predicted transient curves were fitted by eye to the experimental curves rather than by using a least-squares method.

In Section 5.3.1 it was shown that a non-linear dose-response curve can distort the time course of the tension transient, and that the time course is direction dependent. This direction dependency is illustrated in the paired Figs. 5.4f,g and h,i and also in Fig. 4.1. Because of this distortion, it would be meaningless to try and compute the time constants of the experimental curves. Instead, the simulated transients were taken as a measure of the true time course of calcium through the myocardium. Using the parameters for a particular muscle, and the value of k that gave the best step-response fit, the calcium movements could be described by the diffusion equation (Eq. 2.8).

5.4 Pseudo-Random Analysis

5.4.1 Determination of the pseudo-random sequence length

Initially a maximum-length (M-length) sequence was chosen for use in our experiments, but before a particular sequence could be decided upon, it was necessary to determine the settling time of the system. Preliminary analysis of tension step-responses, showed the longest time constant to be in the order of 2-3 minutes. This was determined using the curve stripping method of Appendix B. If the settling time is taken as 4-5 times the longest time constant, then a sequence length in the order of 12-15 minutes was required.

The sampling interval Δt is set by the rate at which the muscle is stimulated, and since this was selected as 20/min (sampling interval 3 s), an M-length sequence of between 240 and 300 points was required. Therefore a 255-point sequence was chosen which, from Eq. 2.28, had a period of 12.75 minutes.

Godfrey (1969, Table 1) showed that with an eight-bit shift register with the outputs from bits 2,3,4, and 8 used for the feedback arrangement, a 255-point M-length p.r.b.s. could be generated.

The computer program necessary to generate this sequence, and to control switching of the superfusion valves was written (Appendix F). The crosscorrelation analysis program was also written. As a check on both the p.r.b.s. and the crosscorrelation programs, the computer generated p.r.b.s. was autocorrelated using the crosscorrelation program. The autocorrelation result was identical to that outlined in Section 2.3.4. When the program for the inverse-repeat sequence was written, it was also checked in a similar manner. Again, the autocorrelation result was identical to that expected for an inverse-repeat sequence.

5.4.2 Experimental pseudo-random results

Fig. 5.5 shows a p.r.b.s. run performed on a muscle along with the actual sequence used. In this experiment, calcium was switched about a level of 2.25 mM with a perturbation level of $\pm$ 1 mM. The concentration changes between the two levels of 1.25 mM and 3.25 mM were abrupt, and the discontinuous ramps representing the step changes in the figure are plotting artifacts. The crosscorrelation results, averaged over three runs, are shown as the vertical crosses in Fig. 5.6.

The large discontinuities that appear at lags 26, 51, etc. were present in each of the runs, and occurred at precisely the same place. To

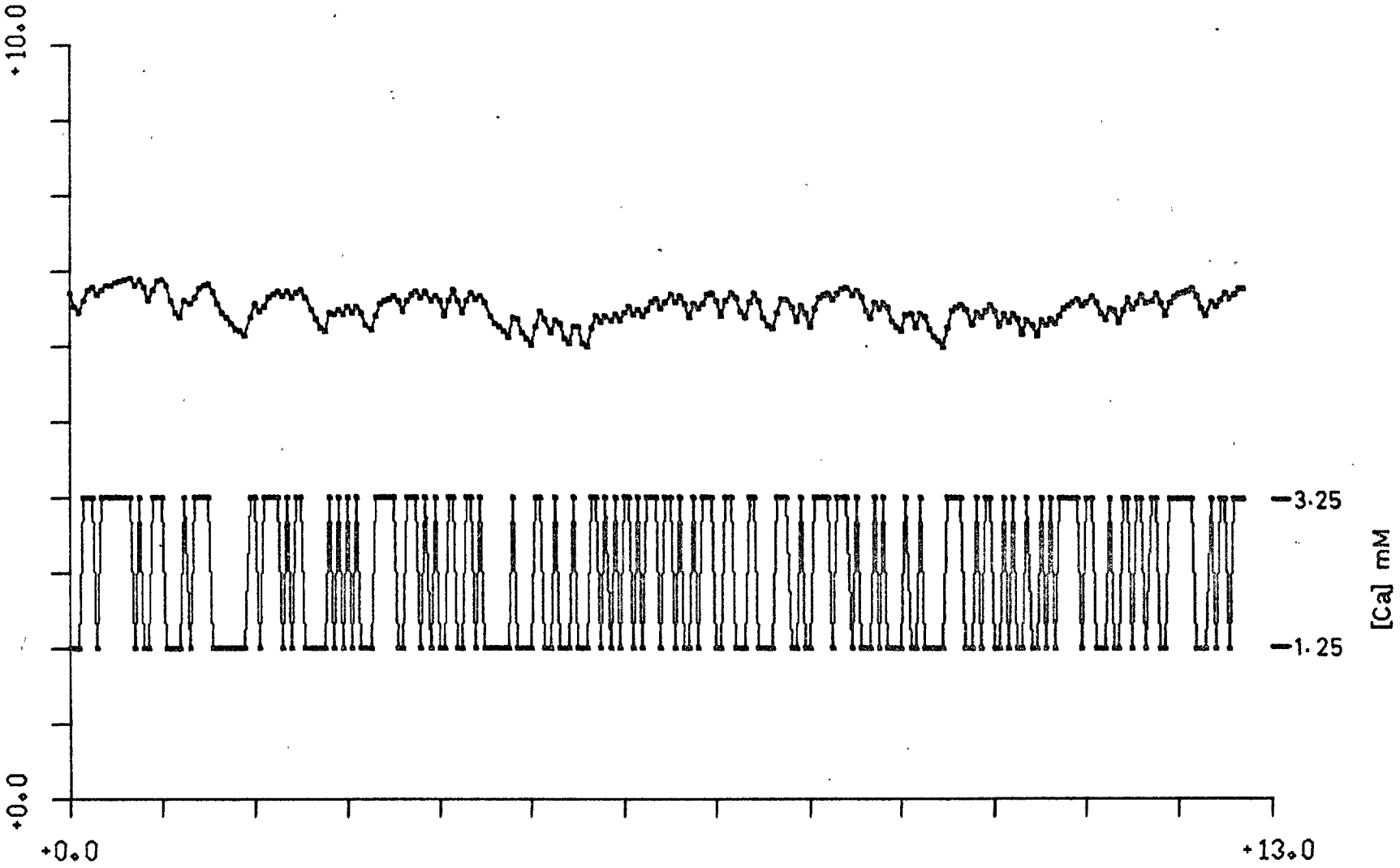

Fig. 5.5 ENVELOPE OF PEAK ISOMETRIC TENSION [G/MM2] VS TIME [MIN]
IN RESPONSE TO A PSEUDO-RANDOM CHANGE IN CALCIUM CONCENTRATION.
255 POINT PSEUDO-RANDOM BINARY SEQUENCE WITH A MINIMUM INTERVAL OF 3 SEC.

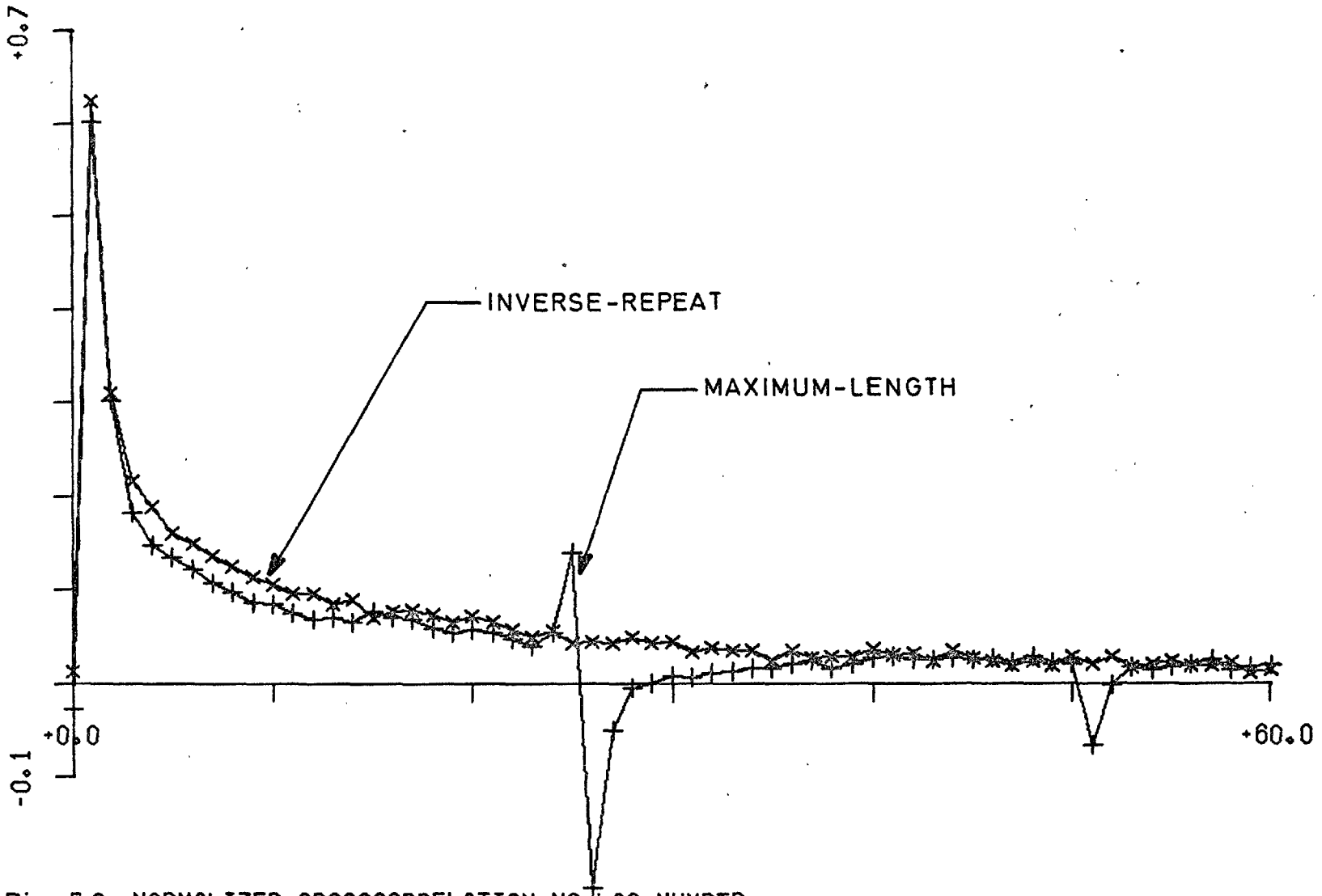

Fig. 5.6 NORMALIZED CROSSCORRELATION VS LAG NUMBER.
COMPARISON OF RESULTS FROM TWO TYPES OF P.R.B.S. BASED ON THE SAME MAXIMUM-LENGTH SEQUENCE OF 255 POINTS.

see if this noise could be eliminated, an inverse-repeat sequence based on the original 255-point p.r.b.s. was tried. The results are also shown in Fig. 5.6 for comparison and are the average of two runs obtained for the same muscle and calcium concentration levels as the M-length sequence.

The area under the impulse response curve represents the dc or steady-state gain of the system about a particular operating level. Since the dose-response curve of calcium concentration vs tension is non-linear, then impulse response measurements should vary, depending upon the steady-state operating level of the system. To test this fact, a series of impulse response determinations were made centering on 2.25 mM ($\pm$ 1 mM perturbation level) and 1.0 mM ($\pm$ 0.25 mM perturbation levels). The results from two separate experiments are shown in Fig. 5.7. This graph shows the means of four p.r.b.s. runs for each curve with the standard errors of each individual point plotted as an envelope around the mean values.

To compute the area under the curves, the corrected crosscorrelation coefficients, expressed as $(g/mm^2)/mM$, were summed over the first 255 points. The sum of the standard errors was computed in a similar manner. The results were then compared with those derived from the steady-state measurements and from differentiating the analytical dose-response curve (Section 5.2). The results of these measurements are tabulated in Table 5.2.

Muscle	Mean Calcium level (mM)	Slope from steady-state measurements $((g/mm^2)/mM)$	Slope from fitted dose-response curve $((g/mm^2)/mM)$	Slope from impulse-response curve $((g/mm^2)/mM)$	$\pm$ s.e. (n = 4)
2	2.25	1.29	1.11	1.18	0.16
5	1.0	2.29	2.44	3.11	0.99

Slope measurements of dose-response curves

Table 5.2

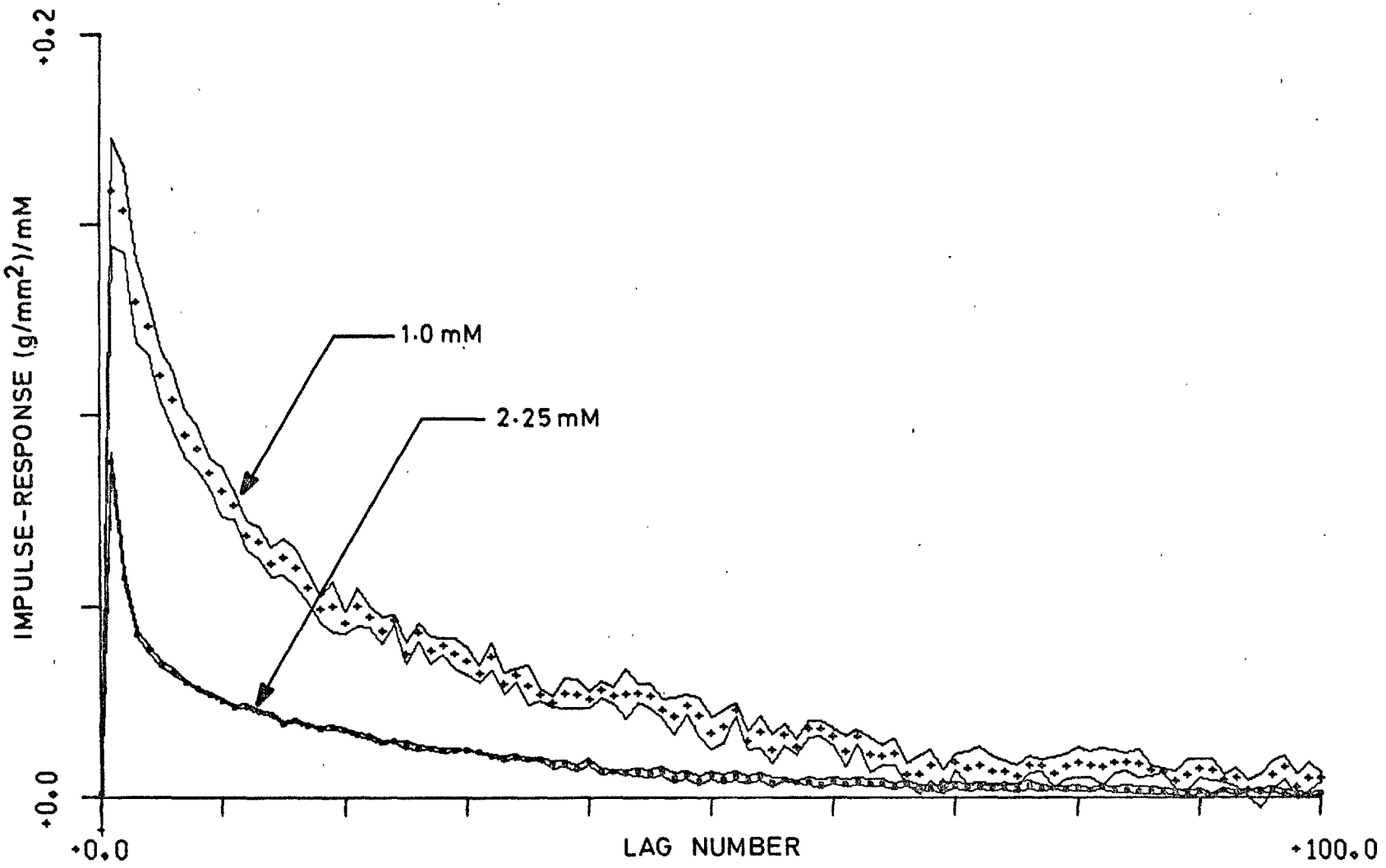

Fig. 5.7 IMPULSE-RESPONSE AT TWO DIFFERENT MEAN OPERATING LEVELS OF CALCIUM CONCENTRATION. AT 2.25 mM PERTURBATION LEVEL WAS ±1.0 mM AND AT 1.0 mM THE PERTURBATION LEVEL WAS ±0.25 mM. INDIVIDUAL POINTS REPRESENT AVERAGE OF 4 RUNS WHILE CONTINUOUS CURVE IS ±1 S.E. FROM THE MEAN.

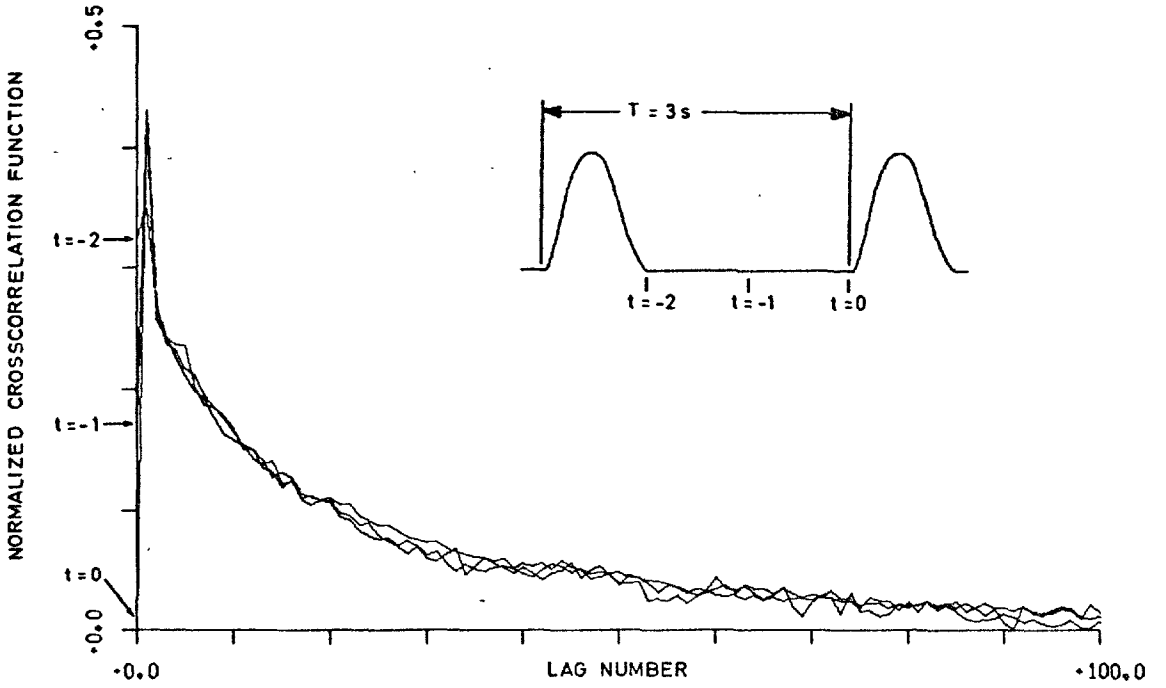

INFLUENCE ON CROSSCORRELATION RESULTS OF VARYING THE TIME INTERVAL BETWEEN SWITCHING THE SOLUTIONS AND STIMULATING THE MUSCLE.

(a)

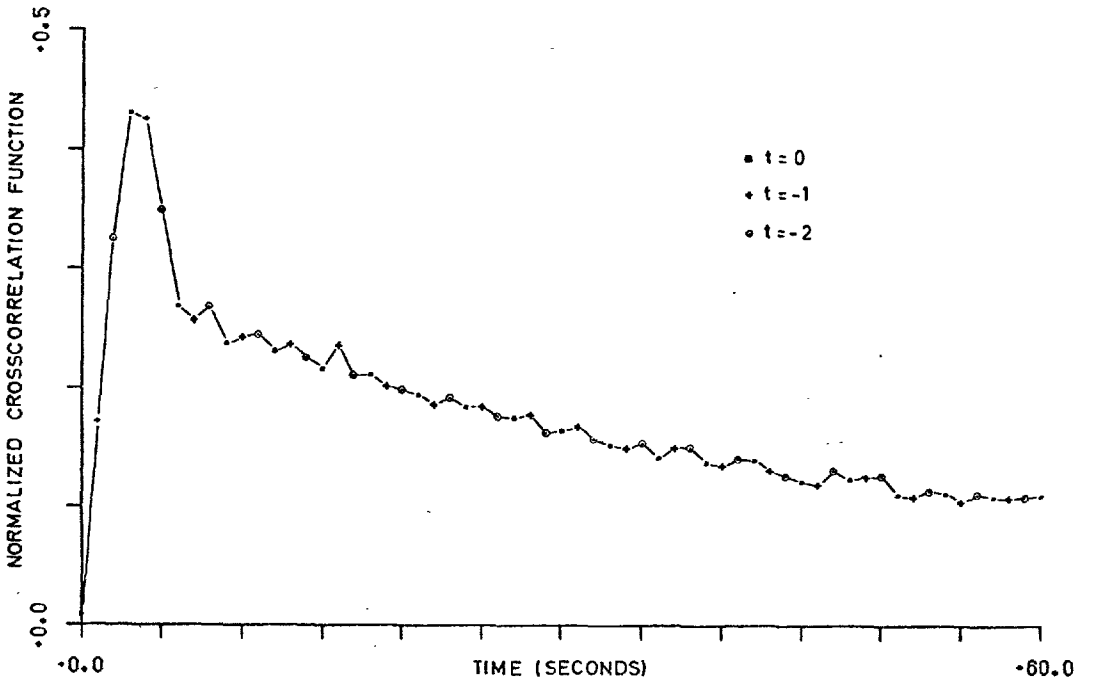

COMPOSITE CROSSCORRELATION CURVE AS A FUNCTION OF TIME (SEC) CORRECTED FOR THE INTERVAL BETWEEN SWITCHING THE SOLUTIONS AND STIMULATING THE MUSCLE.

(b)

Fig. 5.8

Because the measured output (peak tension) is intimately connected with the stimulus, and the stimulation rate, it is impossible to make the solution switching rate greater than the stimulation rate. Therefore, the resolution of the impulse response is limited by the stimulation rate, and if this is increased, the fundamental relationship between frequency and tension is altered (Appendix A) making impulse response comparisons impracticable.

To investigate if finer resolution could be obtained without altering the sampling rate, the interval between switching the solution and stimulating the muscle was varied. Fig. 5.8a shows the results of such a study. Other than the differences in the first crosscorrelation coefficients at lag 0, it is very difficult to tell one run from another. However, by plotting the crosscorrelation results as a function of time, instead of lag number, and correcting for the switching-stimulation interval, it can be seen (Fig. 5.8b) that a finer time resolution can be obtained. The origin of this graph (t = 0) represents the time that the solution was switched, and is taken as the reference for all other time measurements. Only the first minute has been plotted so that individual correlation points can be seen.

CHAPTER 6

DISCUSSION

6.1 Steady-State Relationship Between Calcium Concentration and Isometric Tension

It was noted as early as 1883 (Ringer) that the contraction of the heart was dependent upon the external calcium in the perfusing medium. The fact that this situation does not exist in skeletal muscle indicates that the myocardium is unique amongst striated muscles.

Although a number of investigators have shown that the heart has a graded tension response to calcium concentrations (e.g. Blinks, Olson, Jewell & Braveny, 1972; Nayler, 1960), their data has normally been presented as a composite photograph of a number of individual twitches at different calcium concentration. These results have not been accompanied by any quantitative analysis. In fact, it appears that this fundamental relationship has been completely ignored in the study of calcium movements and the subsequent dynamic changes in myocardial contractility.

As the dose-response curve was not the primary interest, and because of time limitations (each steady-state measurement required ten to fifteen minutes to allow for the muscle to equilibrate), the curves were evaluated, for each muscle, only in the region of 0.5 mM to 4.5 mM calcium concentration, and at irregularily spaced concentration values. This gave a sufficient number of points (from 4 to 7) to enable a single exponential curve to be fitted to the data. Certainly if a more precise curve was required, starting from zero calcium, a single exponential curve would not be adequate, and either a polynomial or a sigmoid curve would give a better description of the dose-response curve.

While the exponential curve was able to describe fairly closely the shape of the dose-response curve, it did not necessarily pass through each data point, and this led to steady-state errors between the computer generated tension transients and those found experimentally. In addition, differences in curvature between the actual dose-response curve and that described by the exponential equation could also account for differences in the time course between the two tension transient curves.

It is of interest to note the variations between dose-response curves as shown in Fig. 5.1. This is somewhat surprising as all the tensions have been expressed as force per unit cross-sectional area. In skeletal muscle such a normalizing procedure allows for comparisons to be made between muscles (Wilkie, 1968, p.31), for without it, comparisons would be meaningless. A possible explanation for this variability may be in the fact that the fibre orientation in cat papillary muscle is such that the fibre chains define a spiral angled at about 30° around the length axis of the muscle (Abbott, 1971), and thus, unlike skeletal muscle, only a component of the total force produced by a fibre is directed along the longitudinal axis of the muscle. If the geometry of the papillary muscle is

taken into account, then it may be possible to reduce this variability. However, as this has never been attempted, either here or in the published literature, it is very difficult to make quantitative comparisons between heart muscles.

Beeler and Reuter (1970b,c) have shown, using voltage clamp techniques, the existence of a slow inward calcium current that flows into the myocardial cell during the plateau phase of the action potential. This current was found to be very sensitive to the calcium concentration in the external medium such that when the external concentration was increased, both the inward current and the tension produced were also increased. If the external calcium concentration was reduced to zero, the inward current disappeared and there was no tension produced by the muscle. Thus there appears to be a strong correlation between the external calcium concentration, the slow inward current, and the ability of the muscle to produce tension.

If these facts are taken into consideration, it can be appreciated that during steady-state, there is an equilibrium between the amount of calcium entering and leaving the cells. A change in external calcium concentration upsets this balance so that the internal calcium stores are augmented or diminished depending upon whether the concentration was increased or decreased. This change in internal stores would then alter the amount of calcium available to activate the contractile system, and would cause a corresponding change in tension.

If the frequency of stimulation is changed so that the mark/space ratio is altered, i.e. the ratio of the time the muscle is contracting to the time that it is resting, this can upset the calcium balance as well. Sands and Winegrad (1970) have shown that the total calcium content of frog ventricle does depend upon the frequency of stimulation. An increase in

frequency causes an increase in the internal stores, with a corresponding increase in tension. Conversely, a decrease in frequency diminishes the calcium stores, which in turn reduces the amount of tension produced.

As either the external calcium concentration or the frequency of stimulation is increased, the internal calcium stores become saturated and the tension levels off at some maximum value.

It is important to remember that this discussion is concerned only with steady-state conditions. The dynamic situation is considered in the following sections.

6.2 Step-Response

If a system is to be studied using the step-response method, it is important that the study be conducted over the linear region of the input/output transfer characteristics. Otherwise, non-linearities will introduce distortions into the output so that any subsequent analysis, based on linear theory, is meaningless.

In addition, if the system under study is both non-linear and of a distributive nature, i.e. the input is distributed to a number of elements in the system and the outputs from each of these elements are then combined to give the system output, each of these elements must be analysed in turn rather than on an average basis. This was shown in Section 5.3.1 in which a finite-element approach to calculating concentration, and the subsequent step-response, was compared to that using an average concentration approach. Figs. 5.2c,d indicated a considerable difference in the time course between the transients computed by these two methods such that, if the calcium concentration was increased in a stepwise manner, and a predicted transient was fitted to the experimental curve by varying k, the diffusion constant, then the value of k for the average method would be found to be smaller than

that determined by the shell method of calculation. The converse is true for a decrease in external calcium concentration.

From the simulated step-responses for kitten papillary muscle an average diffusion constant for calcium was found to be 1.5 ($\pm$ 0.3) x 10^{-6} cm^2/s (s.d. of 10), and this is about one-fifth the free solution value of 7.78 x 10^{-6} cm^2/s (Wang, 1953). The fact that this value is reduced from the free solution value is to be expected, for radioisotope studies (Creese, 1954; Harris & Burn, 1949; Johnson, 1955; Keynes, 1954) have shown that the diffusion constant in muscle is reduced to about one-quarter the free solution value. This reduction is attributed to the obstructions of cells, and to the tortuosity of the pathway that a substance diffusing through the extracellular space must follow. The above mentioned studies, however, have been mainly concerned with the diffusion of sodium through the extracellular space of frog skeletal muscle.

Niedergerke (1957) had attempted the same type of calculation using strips of frog ventricular muscle, and instead of radioactivity, he used the change in tension as a measure of the calcium concentration in the muscle. He then equated the half-time of his transients to the numerical solution of the average concentration diffusion equation (Eq. 2.9) for half saturation inside a cylinder. He found that, for frog ventricular strips, calcium had an apparent diffusion coefficient that was one-sixteenth the free solution value.

This added reduction in the value of the diffusion constant led Niedergerke to the conclusion that there was an additional factor slowing down the rate of diffusion within the muscle. This added factor was thought to be adsorption of calcium onto the surface of the cells, and he showed that if adsorption did take place, this would reduce the apparent diffusion constant still more.

The method of arriving at the diffusion constant used in the present work, and by Niedergerke (1957) is based on calculations that consider the muscle to be homogeneous. This is clearly not the case, for if the high calcium concentrations (0.5 - 4.5 mM were present in the sarcoplasm, the muscle would be in a constant state of contracture (see Section 1.2). Thus the high calcium levels must be confined to the extracellular space or to a restricted part of the muscle cell, such as the sarcoplasmic reticulum.

E. Page (1962) has made a study of the extracellular space of cat papillary muscle and has found it to be quite complex with diffusion substantially altered from the free solution process. Although he did not measure the diffusion constant through this space, he did note that the first two time constants in his inulin uptake curves did not appear in the same ratio as the first two time constants in the diffusion equation for a homogeneous cylinder. From the diffusion equation, either Eq. 2.8, or 2.9, the ratio of the time constants of the first two exponential terms should be in the ratio of s_1/s_2.

It can be argued that the smaller value of the diffusion constant takes into account the extended diffusion pathways, obstructions, etc., that result from non-homogeneity in the muscle. If this is the case, then Eq. 2.9 should give a true indication of the calcium concentration in the extracellular space. From this it can be concluded that the amount of tension produced by a cell is intimately connected to the calcium concentration in the extracellular space, and that equilibrium between the cells and the calcium in this space is reached very quickly.

Shine et al. (1971) and Niedergerke (1957) have shown that tension changes with a time course significantly different from the time course of Ca^{45} in a washout curve. Therefore within the myocardial cell there must be

an internal store of calcium that is not available for excitation-contraction coupling (Shine et al., 1971; Langer, 1971). Furthermore, this calcium appears to be released into the extracellular space at a rate slower than that of calcium diffusing through the extracellular space. This slow release could increase the calcium concentration locally in the extracellular space with the result that the diffusion of calcium within this space appears to be slower than it actually is. This could account for why a fifth instead of a quarter of the free solution value of the calcium diffusion constant was found in our experiments.

Since diffusion has been shown to dominate the step-response for a papillary muscle, a number of important facts emerge. The most important is that diffusion into a cylindrical muscle for a step change in concentration can be expressed as an infinite sum of exponentials. Therefore, any subsequent analysis of the transient curve will yield time constants that are a measure of the diffusion process only, and they have no physiological significance except that their value is proportional to the square of the radius of the muscle. In addition, the values of the time constants can be severely distorted if the step change takes place over the non-linear region of the dose-response curve.

Computer simulation of the step-response has confirmed the dependence of the muscle's dynamics on the shape of the dose-response curve. Thus, if the shape is altered by changing the frequency of stimulation, one would expect the corresponding dynamics to change as well. This fact can be appreciated from Fig. 5.3. If the time course of calcium concentration remains the same for a step change from A to B, and if the dose-response curve has a greater slope than that shown between A' and B', the resulting tension dynamics must therefore become faster if the tension is to reach equilibrium in the same time that the calcium concentration stabilizes. This can apply

only for a non-linear dose-response curve whose shape changes within the region of interest, and is not valid for a linear dose-response curve.

Chapman and Niedergerke (1970a) have shown that the time constant of their fast phase is inversely proportional to the frequency of stimulation. In their second paper (Chapman & Niedergerke, 1970b), the authors have also shown that the slope of their dose-response curve is proportional to the frequency of stimulation. Therefore, from the previous discussion, one would expect their dynamics to change as they appear to be operating over the non-linear region of their dose-response curves. However, the dependence of the dynamics on the shape of the dose-response curve seems to have been overlooked, and they attribute their observations to the consecutive diminution of the intracellular concentration of two active calcium compounds that fall with two distinct time constants. It is conceivable that the effect that they are measuring is the influence of the dose-response curve on the first two time constants in the diffusion equation, that is provided that diffusion is the rate-limiting process in their frog ventricular preparation.

A related study has been reported by S. Page and Niedergerke (1972) for diffusion across the endothelial layer surrounding a single bundle of fibres in frog ventricular muscle. Their calculations show that the free solution value for the diffusion constant can be used, and that diffusion restrictions are due to the geometry of the endothelial layer. It was concluded that diffusion through this layer was responsible for the fast phase of the results of Chapman and Niedergerke (1970a). However the calculations of Page and Niedergerke do not consider calcium movements from the surface of the muscle through the myocardium, and thus diffuion through the bulk of the muscle may still be the rate-limiting process.

E. Page (1962) states in his paper that the complexity of the extracellular space in papillary muscle may be expected to influence the diffusion of ions and other substances, and that an investigation of the kinetics of extracellular diffusion should yield a clear separation of cellular and extracellular movements. If diffusion is the rate-limiting process as the present work suggests, then it will be extremely difficult to make such a separation. The possibility of diffusion limitations has certainly been ignored by Blinks et al. (1972), and their analysis of the dynamics of the onset of action of caffeine is probably not valid for this reason.

6.3 Impulse Response of Papillary Muscle

The results of Section 5.4 show that pseudo-random analysis can be used as a method of studying the dynamic relationship between calcium and isometric tension in a papillary muscle system. However, because this type of analysis is based on linear theory, its use is limited for this non-linear system.

The crosscorrelation results of an M-length sequence contains discontinuities that cannot be eliminated by ensemble averaging. But by using an inverse-repeat sequence the discontinuities can be made to disappear (Fig. 5.6). The presence of these discontinuities is attributed to direction-dependent dynamics and non-linearities in the system (Godfrey, 1969, and private communications). The elimination of this noise by the use of an inverse-repeat sequence is due to its property of "negative symmetry" which has the effect of cancelling all even-order non-linearities (Godfrey, 1969; Godfrey & Briggs, 1972).

Examination of the particular 255-point M-length sequence used revealed that the sequence shift k_1 (Section 2.3.3) was 25, and therefore

$2k_1$ was 50. From the predictions of Godfrey and Briggs (1972) the discontinuities in the crosscorrelation results should occur at $(k_1 + 1) = 26$, and $(2k_1 + 1) = 51$. From Fig. 5.6 one can see that the peak discontinuities do occur at these lags. The large positive discontinuity at lag 25 is unexplainable by the theory of Godfrey and Briggs, but it is thought that the non-linearity of the system (i.e. output not proportional to input) is the contributing factor. The discontinuities at lag 26 and 51 are due to the direction-dependent dynamics of the system.

The presence of dynamic differences was confirmed by the step-response analysis (Section 5.3). The non-linear transfer characteristics of tension and calcium concentration was illustrated in Section 5.2. It was further shown (Section 5.3.1) that the direction-dependent dynamics is a direct result of the non-linear dose-response curve.

The area under the impulse response curve gives the gain of the system at that particular operating point, and this is equivalent to computing the slope of the dose-response curve, also at that point. Comparison of the slope measurements from the area under the impulse-response curve to those obtained from steady-state measurements, and from differentiating the analytical dose-response curve are all in good agreement (Table 5.2). This indicates that the inverse-repeat sequence assumes that the system is linear between the two perturbation levels. If this sequence has a linearizing effect, then the dynamics, as given by the impulse-response, should be a measure of the average up-down dynamics. As a result, only an approximation to the true step-response could be obtained if the impulse response was used to simulate the step-response.

The increase in the noise level (increased s.e.) at the low calcium level (Fig. 5.7) can be attributed to two factors, one physical, and the

other physiological. Eq. 2.26 shows that there are two components to the crosscorrelation results. One is the true correlation between input and output, while the other is the correlation of system noise with the input signal. If the input perturbation level is a value other than 1, the input-output crosscorrelation value is increased by the square of the perturbation level, while the noise term is only proportional to this level. Thus an increase in perturbation level has the effect of increasing the signal-to-noise level. So, for Fig. 5.7 the impulse response curve at 2.25 mM and a perturbation level of $\pm$ 1 mM, the noise on the curve is minimal, but at the lower level of 1.0 mM $\pm$ 0.25 mM the noise is substantially increased.

Unfortunately, continual perfusion at low calcium levels causes alternation in tension production in successive contractions (Badeer, Ryo, Gassner, Kass, Cavaluzzi, Gilbert, and Brooks, 1967). This condition of "alternans" occurs spontaneously and may last for brief periods of time or for extended periods. These spontaneous fluctuations in tension will therefore introduce noise into the correlation measurements. In a series of six muscles perfused at 1.0 mM calcium suitable results were obtained from only one muscle. The remaining results were spoiled by severe alternation in tension.

The most interesting result in the pseudo-random study, from a physiological point of view, is that found by varying the interval between switching the solutions and stimulating the muscle (Fig. 5.8b). This study is, in effect, introducing a variable delay in the time of tension measurement with reference to when the solution is switched. The results show that the change in tension is proportional to the length of the delay interval, and this is reflected in the rising phase of the impulse response curve. The longer the interval, the larger becomes the change in tension for the

corresponding contraction.

This result supports the conclusion that the papillary muscle preparation is severely diffusion limited; by increasing the time interval between switching the solution and stimulating the muscle, more time is allowed for calcium to diffuse into the muscle and affect more cells. With more cells producing a greater tension output, due to increased calcium concentration in the extracellular space, the total tension produced by the muscle is also increased.

Consequently, one can conclude that calcium in the extracellular space has a direct influence on the amount of tension produced by a cell, and that this effect is present in the first contraction immediately after a change in the extracellular calcium level. It is difficult to assess if this effect is maximal in the first contraction or whether it takes a few contractions for the tension to stabilize.

Wood, Heppner, and Weidmann (1969) and also Beeler and Reuter (1970c) have shown that if an electrical inotropic intervention is applied to a muscle, there is a transient period of about eight contractions before the muscle response stabilizes. However, it is important to bear in mind that their transient is in response to a step change, and that the corresponding impulse response may have a similar form to those found here, except with much faster time constants.

Fig. 5.8b shows an extremely rapid time constant in the decay phase of the impulse response curve which appears to have a value of about 6 seconds, and would therefore have a corresponding settling time of between 24 and 30 seconds. With a stimulation frequency of 20/min, this settling time corresponds to 8 to 10 beats. Therefore, it is possible that the fast phase in the impulse response curve is a property of the myocardial cell, while the remaining slow time constants, which are quite different from the fast phase,

are due to extracellular diffusion effects.

Another point of interest is the peak of the impulse-response curve. Fig. 5.8b shows that the peak may be rounded, or that a definite sharp peak may be present between 3 and 4 seconds. In order to resolve this, however, it is necessary to switch the solutions during the period of tension development rather than while the muscle is at rest.

CHAPTER 7

CONCLUSIONS AND RECOMMENDATIONS

The dose-response curve of a papillary muscle is non-linear, and over the region of 0.5 mM and 4.5 mM calcium concentration it can be fitted by a single exponential equation. However, if quantitative comparisons of steady-state results between muscles are to be made, some form of dose-response curve normalization is required.

The non-linearity of the dose-response curve distorts the time course of step-responses and introduces direction dependent dynamics. The dynamic results are further complicated by the fact that movement of calcium into the muscle appears to be diffusion limited, and as a result, the time constants of the dynamics vary as the square of the radius of the muscle (assuming the muscle to be cylindrical).

In addition, diffusion into a circular muscle can be expressed as a sum of exponential terms provided a step change in concentration is made at

the surface of the muscle. Therefore, any exponentials measured in the tension step-response can be considered to be part of the diffusion process, and no physiological significance can be attached to either their value (distorted by the dose-response curve), or the number resolved (diffusion equation infinite sum of exponentials).

The response relating tension to calcium concentration can be determined for a papillary muscle by using pseudo-random analysis. But because the preparation is severely diffusion limited, it is difficult to separate the diffusion effects from those that may be physiological in origin.

There is a possibility that the fast component present in the impulse response is a characteristic of the myocardial cell, but further experiments are necessary before a more definite conclusion can be reached. If calcium concentration is to be used for the perturbation signal, the thinnest muscles, and ideally a single fibre, should be used to minimize diffusion effects.

As an alternative to using calcium as the perturbation signal, the frequency of stimulation could be changed in a pseudo-random manner. This would activate all cells simultaneously, and would circumvent the problems associated with diffusion from the surface of the muscle.

However, because of the diffusion limitations of this preparation, step response or impulse response methods of analysis are not likely to yield suitable physiological dynamic information in the study of other drugs that act as inotropic agents.

BIBLIOGRAPHY

ABBOTT, B.C., Force-frequency relationship in heart muscle. Cardiovascular Res., Supp. I, 51-54, 1971.

BADEER, H.S., RYO, U.Y., GASSNER, W.F., KASS, E.J., CAVALUZZI, J., GILBERT, J.L., and BROOKS, C. McC. Factors affecting pulsus alternans in the rapidly driven heart and papillary muscle. Am. J. Physiol. 213: 1095-1101, 1967.

BEELER, G.W. and REUTER, H. Membrane calcium current in ventricular myocardial fibres. J. Physiol. 207: 191-209, 1970b.

BEELER, G.W. and REUTER, H. The relation between membrane potential, membrane currents and activation of contraction in ventricular myocardial fibres. J. Physiol. 207: 211-299, 1970c.

BLACKMAN, R.B. and TUKEY, J.W. The measurement of power spectra. Dover, New York, 1958.

BLINKS, J.R. Convenient apparatus for recording contractions of isolated heart muscle. J. Appl. Physiol. 20: 755-757, 1965.

BLINKS, J.R. and KOCH-WESER, J. Physical factors in the analysis of the actions of drugs on myocardial contractility. Pharmacol. Rev. 15(3): 531-599, 1963.

BLINKS, J.R., OLSON, C.B., JEWELL, B.R. and BRAVENY, P. Influence of caffeine and other methylxanthines on mechanical properties of isolated mammalian heart muscle. Circulation Res. 30: 367-392, 1972.

BLINKS, J.R. and JEWELL, B.R. The meaning and measurement of myocardial contractility. Chapter 7 in Cardiovascular Fluid Dynamics, Vol. 1. ed. D.H. Bergel. Academic Press, London, 1972.

CAMBRIDGE, G.W. and HAINES, J. A new versatile transducer system. J. Physiol. 149: 2P. 1959.

CARSLAW, H.S. and JAEGER, J.C. Conduction of heat in solids. Oxford, 1947.

CHAPMAN, R.A. and NIEDERGERKE, R. Effects of calcium on the contraction of the hypodynamic frog heart. J. Physiol. 211: 389-421, 1970a.

CHAPMAN, R.A. and NIEDERGERKE, R. Interaction between heart rate and calcium concentration in the control of contractile strength of the frog heart. J. Physiol. 211: 423-443, 1970b.

CREESE, R. Measurement of cation fluxes in rat diaphragm. Proc. Roy. Soc. (B). 142: 497-513, 1954.

DEL TORO, V. and PARKER, S.R. Principles of control systems engineering, McGraw-Hill, New York, 1960.

FAWCETT, D.W. and MCNUTT, N.S. The ultrastructure of the cat myocardium I. Ventricular papillary muscle. J. Cell Biol. 42(1): 1-45, 1969.

GODFREY, K.R. The theory of the correlation method of dynamic analysis and its application to industrial processes and nuclear power plant. Measurement & Control, 2: 65-72, 1969.

GODFREY, K.R. and BRIGGS, M.A. The identification of processes with direction-dependent dynamic responses. Proc. I.E.E. in press, 1972.

HARRIS, E.J. and BURN, G.P. The transfer of Na and K between muscle and the surrounding medium. Trans. Faraday Soc. 45: 508-528, 1949.

HILL, R.V. The diffusion of oxygen and lactic acid through tissues. Proc. Royal Soc. 104B: 39-96, 1928.

JEWELL, B.R. and BLINKS, J.R. Drugs and the mechanical properties of heart muscle. Ann. Rev. Pharmacol. 8: 113-130, 1968.

JOHNSON, J.A. Kinetics of release of radioactive sodium, sulfate and sucrose from the frog sartorius muscle. Am. J. Physiol. 181: 263-268, 1955.

KEILIOR, S.A. Flow charting by interactive computer graphics. C.A.D. 4(4): 165-168, 1972.

KEYNES, R.D. The ionic fluxes in frog muscle. Proc. Roy. Soc. (B), 142: 359-382, 1954.

KOCH-WESER, J. Role of norepinephrine release in the interval-strength relationship of heart muscle. J. Pharmacol. Exptl. Therap. 150: 184-189, 1965.

KOCH-WESER, J. and BLINKS, J.R. The influence of the interval between beats on myocardial contractility. Pharmacol. Rev. 15(3): 601-652, 1963.

LANGER, G.A. Coupling calcium in mammalian ventricle: its source and factors regulating its quantity. Cardiovascular Res. Supp I, 71-75, 1971.

LANGER, G.A. and BRADY, A.J. Calcium flux in the mammalian ventricular myocardium. J. gen. Physiol., 46: 703-719, 1963.

LATHI, B.P. Signals, systems and communications, Wiley, New York, 1965.

LOCKE, F.S. and ROSENHEIM, O. Contributions to the physiology of the isolated heart. The consumption of dextrose by mammalian cardiac muscle. J. Physiol. 36: 205-220, 1907.

MILSUM, J.H. Biological control systems analysis. McGraw-Hill, New York, 1966.

NAYLER, W.G. A study of the "staircase" in ventricular muscle and its relationship to the inotropic activity of certain drugs. J. gen. Physiol. 44: 393-404, 1960.

NIEDERGERKE, R. The rate of action of calcium ions on the contraction of the heart. J. Physiol. 138: 506-515, 1957.

NIEDERGERKE, R. and LÜTTGAU, H.C. Calcium and the contraction of the heart. Nature 179: 1066-1069, 1957.

PAGE, E. Cat heart muscle in vitro. III The extracellular space. J. gen. Physiol. 46: 201-213, 1962.

PAGE, S. and NIEDERGERKE, R. Structures of physiological interest in the frog heart ventricle. J. Cell Sci. 11: 179-203, 1972.

RIGGS, D.S. The mathematical approach to physiological problems. Williams and Wilkins, Baltimore, 1963.

RINGER, S. A further contribution regarding the influence of the different constituents of the blood on the contraction of the heart. J. Physiol. 4: 29-42, 1883.

SANBORN, W.G. and LANGER, G.A. Specific uncoupling of excitation and contraction in mammalian cardiac tissue by lanthanum. J. Gen. Physiol. 56: 191-217, 1970.

SANDS, S.D. and WINEGRAD, S. Treppe and total calcium content of the frog ventricle. Am. J. Physiol. 218(3): 908-910, 1970.

SHINE, K.I., SERENA, S.D. and LANGER, G.A. Kinetic localization of contractile calcium in rabbit myocardium. Am. J. Physiol. 221(5): 1408-1417, 1971.

SKILLING, H.H. Electrical engineering circuits. Wiley, New York, 2nd ed. 1965.

SOLOMON, A.K. Compartmental methods of kinetic analysis: In Mineral Metabolism, ed. C.L. Comar and F. Bronner. Academic, New York, 1A: 119-167, 1960.

SPIRO, D. and SONNENBLICK, E.H. Comparison of the ultrastructural basis of the contractile process in heart and skeletal muscle. Circ. Res., Suppl. II, 15: 14-36, 1964.

TRAUTWEIN, W. and DUDEL, J. Aktionspotential und mechanogramm des katzenpapillarmuskels als funktion der temperature. Pflüg. Arch. ges Physiol. 260; 104-115, 1954.

WANG, J.H. Tracer diffusion in liquids. IV. Self diffusion of calcium ion and chloride ion in aqueous calcium chloride solutions. J. Amer. chem. Soc. 75: 1769-1772, 1953.

WILKIE, D.R. Muscle. Studies in Biology no. 11, Arnold, London, 1968.

WINEGRAD, S. and SHANES, A.M. Calcium flux and contractility in guinea pig atria. J. gen. Physiol. 45: 371-394, 1962.

WOOD, E.H., HEPPNER, R.L. and WEIDMANN, S. Inotropic effects of electrical currents. Circulation Res. 24: 409-445, 1969.

WORSLEY, B. Analysis of decay-type data. Commun. ACM 7(1): 39-44, 1964.

APPENDIX A

PHYSICAL FACTORS AFFECTING MYOCARDIAL CONTRACTILITY

A.1 Length-Tension Relationship

Resting muscle is elastic. It can only be stretched by applying a force, and the greater the force, the greater the extension. Examination of the resting tension curves of Fig. A.1 (from Spiro & Sonnenblick, 1964) reveals that muscles do not obey Hooke's law in that the length-tension relationship is not linear. This resting elasticity results largely from the meshwork of connective tissue within the muscle, whose fibres become progressively taut when the muscle is stretched.

When the muscle is stimulated at a given length (isometric contraction), an increase in tension (active tension) is superimposed on that already present in the resting muscle. The length at which the greatest increase in tension occurs is called L_{max}. Tension development falls off at lengths above and below this value.

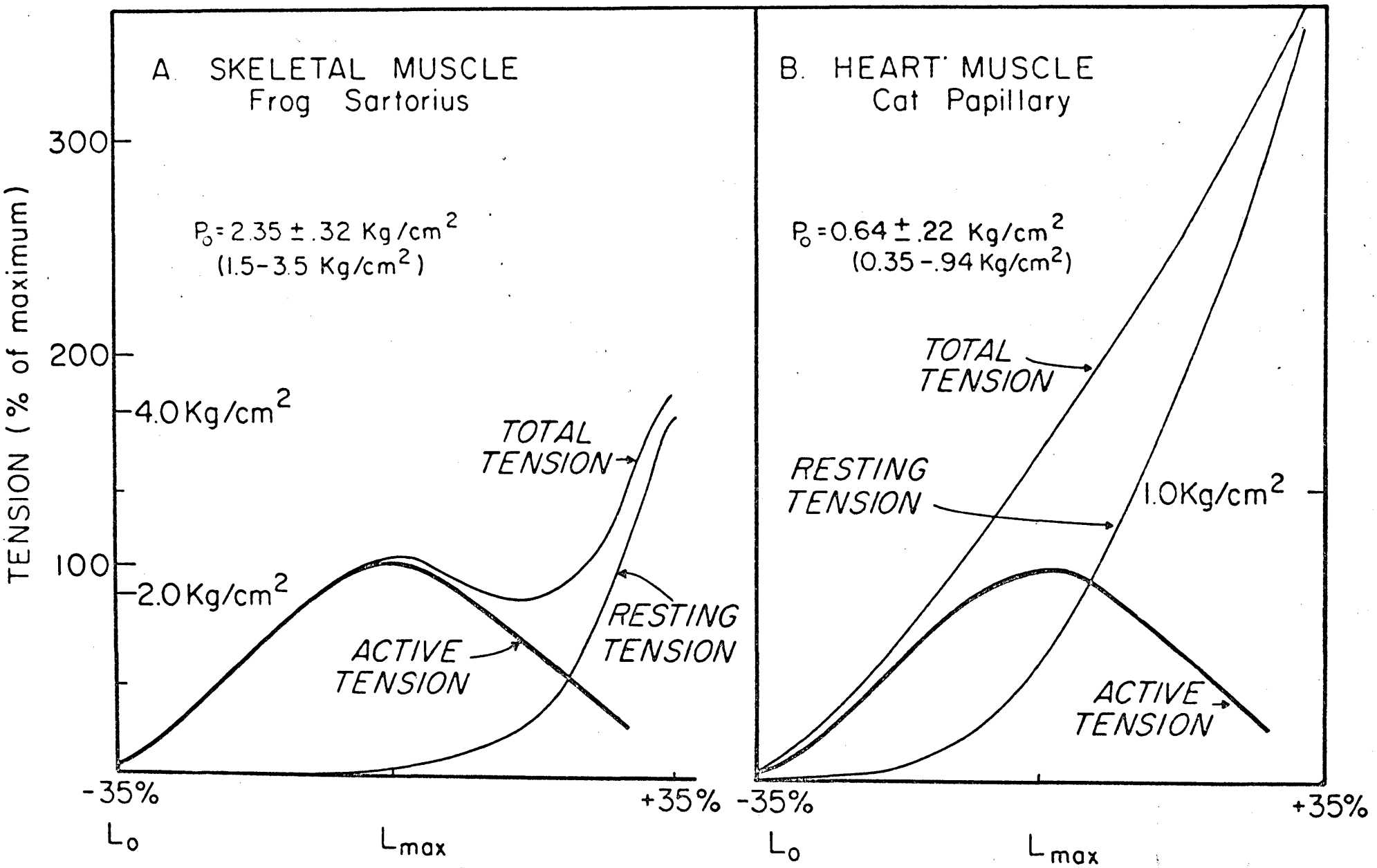

Fig. A.1 Length-tension relationship

A.2 Rate of Stimulation

Within the human body the heart contracts rhythmically about once every second. This rate is set by a group of cells within the heart which are known as pacemaker cells. Once a pacemaker cell is fired, a wave of depolarization (action potential) spreads throughout the heart causing it to contract. Alternatively, the heart can also be made to contract by passing an external electric current through it (e.g. an artificial pacemaker). In the case of isolated heart muscle, such as the papillary muscle, this form of external stimulation is required to make the muscle contract regularly at a controlled rate.

It is an important property of heart muscle that it produces one contraction each time it is stimulated. As the rate of stimulation is increased, the duration of the contraction becomes shorter, and the amount of tension produced becomes greater. Heart muscle exhibits a characteristic force-frequency relationship and this is illustrated in Fig. A.2 (from Koch-Weser & Blinks, 1963) for a kitten papillary muscle. The top diagram shows the steady-state level of isometric tension as a function of the stimulation interval, in seconds, on a logarithmic scale. The bottom diagram illustrates the positive and negative staircase phenomena that occur with an increase and a decrease in the rate of stimulation, respectively. This relationship varies greatly with the species of animal, and the region of the heart from which the muscle is taken. In addition, other factors such as drugs, temperature, and the resting tension under which the muscle is studied affect the shape of the force-frequency curve.

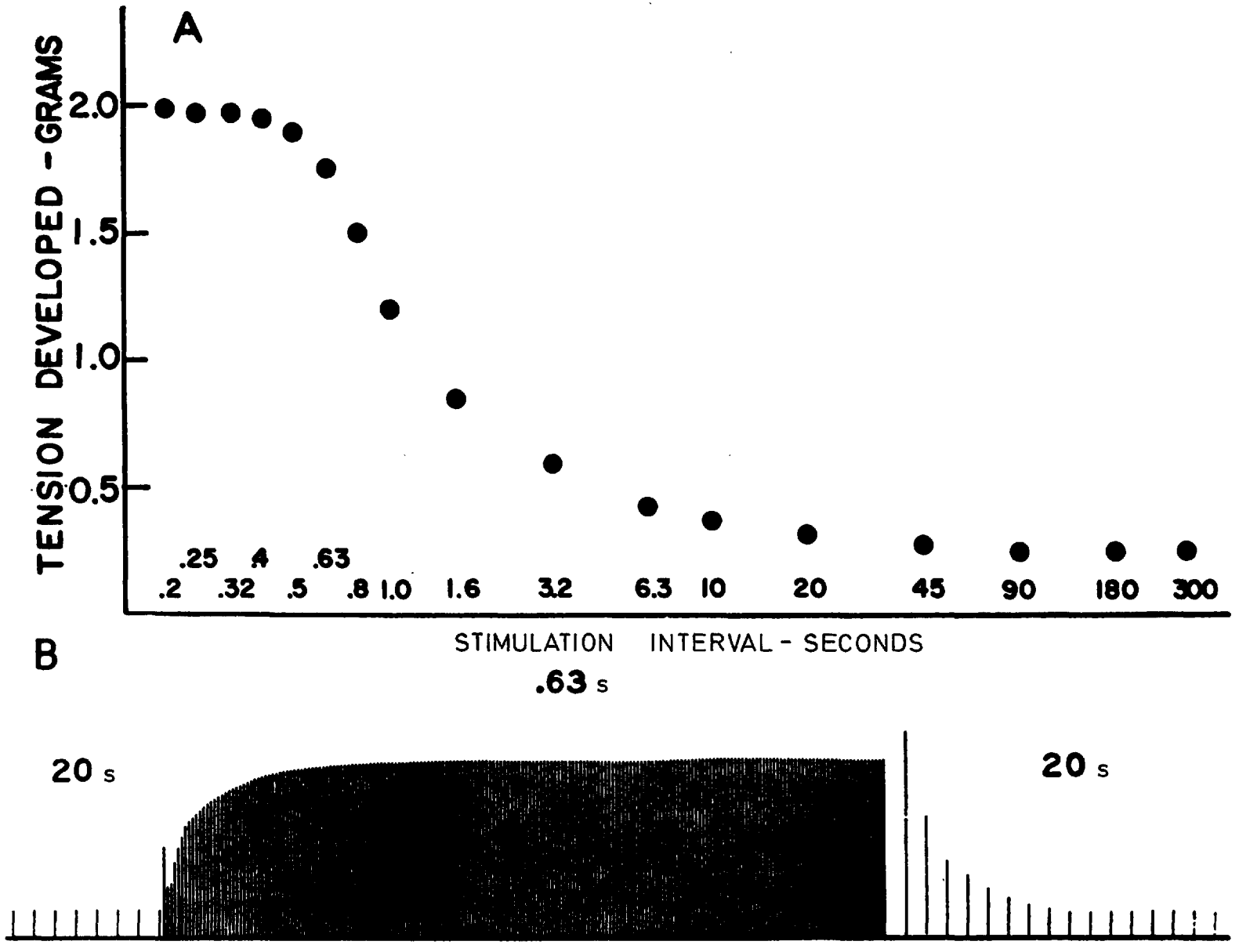

Fig. A-2 Interval-strength relationship for kitten papillary muscle, T = 38°C.

A.3 Temperature

The strength of contraction of heart muscle is markedly affected by changes in temperature; for an increase in temperature the tension becomes smaller and the duration of the contraction becomes shorter.

Fig. A.3 (derived from Trautwein & Dudel, 1954) indicates the interaction between temperature and the frequency of stimulation on isometric tension. There appears to be an optimum temperature of about 22°C at which the tension is maximal. However, this maximum value is also dependent on frequency.

The relation of temperature to the strength of contraction of isolated heart muscle is also affected by the composition of the solution, by oxygenation, and by the age of the preparation. These factors are discussed in a review paper by Blinks and Koch-Weser (1963).

A.4 Chemical

Various drugs and chemicals can alter both the time course that a contraction follows as well as the total tension produced. In a review article (Jewell & Blinks, 1968), the authors have outlined the effects that certain groups of substances, such as catecholamines and cardiac glycosides, have on myocardial contractility.

Changes in the ionic concentration of the solution bathing an isolated heart muscle preparation can also influence contractility. For example, the study described within this thesis has shown a non-linear relationship between isometric tension and external calcium concentration. Niedergerke and Lüttgau (1957) demonstrated that calcium and sodium interact to affect tension. They showed that in amphibian heart muscle the tension developed depends on the ratio of the calcium concentration to the square of the sodium concentration. This relationship was also shown to be true for

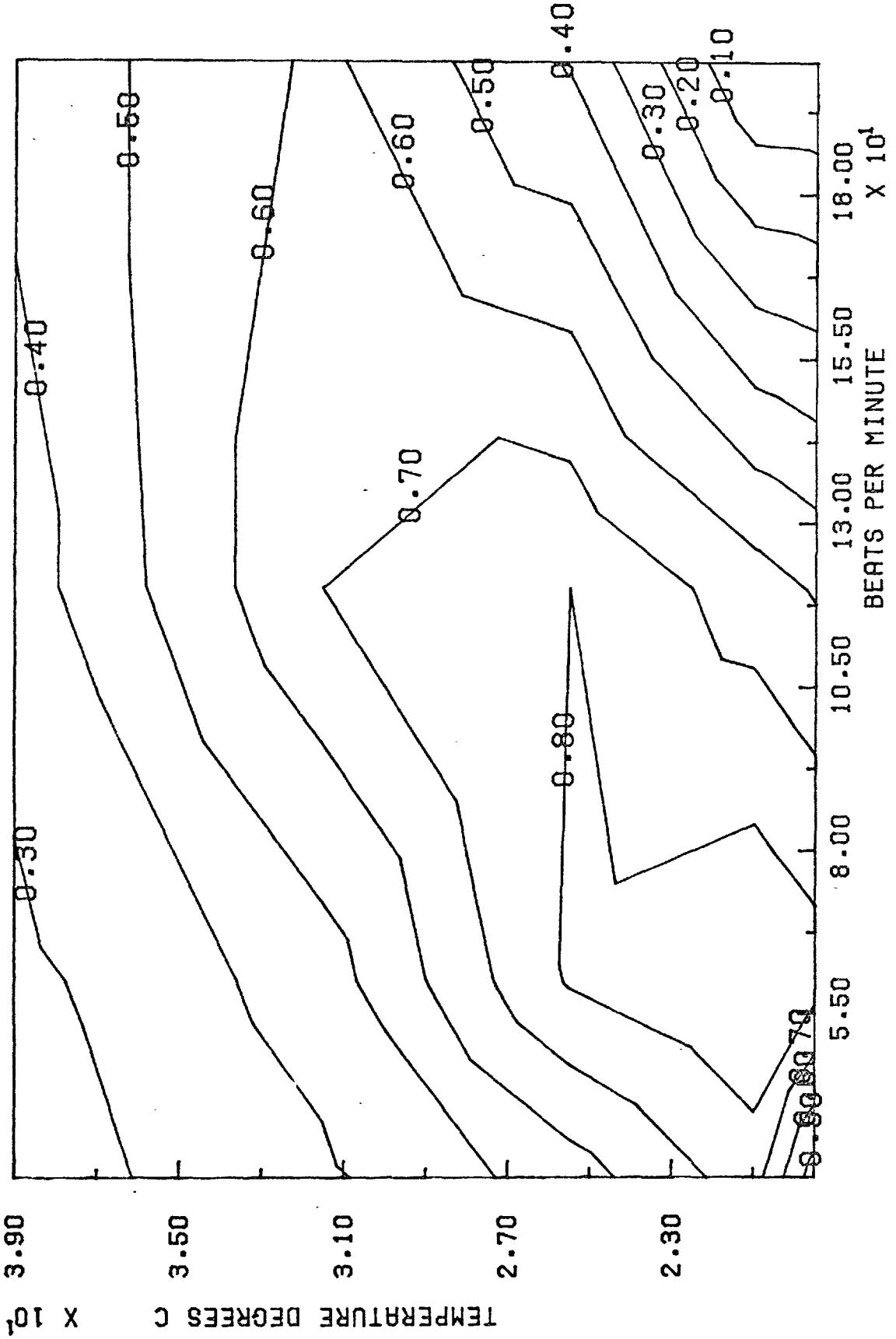

Fig. A-3 Tension as a function of temperature and frequency of stimulation. Contours represent tension in grams.

rabbit atrial muscle (Teiger & Farah, 1968).

Blinks et al. (1972) have shown the effects of caffeine and other methyxanthines on the mechanical properties of isolated mammalian heart muscle. Koch-Weser (1965) has also illustrated how norepinephrine, released from within an isolated muscle due to excessive stimulation voltage, can alter the force-frequency relationship.

A.5 Summary

From the discussion of the previous sections it is clear that isometric tension can be affected by many external factors and that these factors also interact with each other. Therefore, for meaningful experimental results, all of these parameters must be controlled, and only the one of interest allowed to vary. Even then, it is unlikely that the particular set of operating conditions chosen will correspond exactly to those used by someone else. Thus comparison of data contained within the literature is more likely to be on a qualitative basis only.

APPENDIX B

ANALYSIS OF EXPONENTIAL CURVES

Quite frequently in biological or engineering experiments in which transient response curves are obtained, it is desirable to express these results in analytical terms. One method of analysis used is a graphical method sometimes referred to as "curve stripping" (Milsum, 1966 p. 249-252; Solomon, 1960, p.137-139; Riggs, 1963, pp.146-161).

In this method, the transient curve is assumed to be composed of one or more exponential terms whose time constants are widely different. If the transient curve consists only of a single exponential term, and can be described by the equation

$$y = Ee^{-xt}$$

then the values of E and x can be obtained very easily from the intercept and slope of the straight line produced by plotting the data on semi-logarithmic graph paper. If the transient curve decays to a level other than zero, this steady-state value must be subtracted from each of the data points and the differences plotted semilogarithmically.

If, on the other hand, the transient curve can be described by the sum of two or more exponential terms, the analysis becomes more complicated because now a semi-logarithmic plot of the data does not yield a straight line. However, provided the time constants of the exponentials differ by a factor of at least five, the last portion of the semilogarithmic curve can be said to represent the exponential term with the longest time constant. This implies that all the other exponential terms have decayed to zero, and clearly the greater the differences in time constants the truer

this statement becomes.

By fitting a straight line to this last section of the difference curve the values for the exponential term with the longest time constant can be computed. This term is then subtracted from the linear transient curve and the process is repeated until all the exponential terms have been identified.

Chapman and Niedergerke (1970a,b) used this method to analyze their tension transient curves on a beat-to-beat basis. This same method has also been used in the analysis of isotope uptake and washout curves (e.g. Winegrad & Shanes, 1962; Langer & Brady, 1963; Shine et al., 1971).

When curve stripping is used as a method of compartmental analysis, a serious restriction is placed on the interpretation of the results. The assumption that the curve is a sum of exponentials implies that all the compartments are in parallel with no series compartments present. This point is mentioned briefly by Shine et al. (1971), but they assumed that the magnitude of any error introduced by a series compartment is small. For their study, each of the exponential components in their Ca^{45} washout curves is assumed to represent a pool or pools of exchangeable calcium in the tissue.

In their respective books, Riggs and Milsum have pointed out that this method of analysis can be subject to large errors, which are accumulative as more exponential terms are subtracted from the curve. What they do not mention is the fact that errors in the estimation of non-zero steady-state values can result in distortions of the semilogarithmic difference curve at late times. Under-estimation of the steady-state value causes the tail-end of the difference curve to bend upwards while over-estimation causes the tail-end to bend downwards. Clearly an error in estimating the steady-state value can drastically influence the remainder of the analysis.

Compounding the analysis problem is noise or variability in the data. Riggs shows, by way of an example, how a small amount of random noise added to the exact values of an exponential curve can influence the results. It is important to note that for small differences, noise in the data is magnified when logarithms are taken, and this increased scatter reduces the accuracy in estimating the exponential term with the longest time constant. Therefore, some form of weighting should be applied in which less importance is given to those points later on in the curve than those which occur at an earlier time.

From this discussion it is clear that there are serious limitations which must be taken into account when applying this graphical method of analysis to multi-exponential curves. Because of these limitations it is virtually impossible to estimate, with any degree of accuracy, more than two exponential terms with non-ideal data. Also, there is no estimate of the errors in the values obtained. Certainly published results that claim to have resolved three or more exponential terms by using this graphical method must be viewed with a great deal of suspicion.

It is possible to use numerical methods of analysis, assisted by a computer, to estimate the exponential terms and the errors in the parameter estimated. A comparative study was made by Worsley (1964) of a variety of numerical techniques for fitting experimental data of the decay type by forms involving the sum of exponentials. The results of this study showed that the values of the fitted parameters are very sensitive to variations in the fitting procedure, and that error bounds can be so large that no confidence can be placed in their values. She suggested that it would probably be best to select a uniform technique both for running the experiments and for analyzing the data. Then, one should consider as significant only relative results between one subject and the next.

APPENDIX C

THE COMPUTER INTERFACE

C.1 Introduction

Before the LINC-8 computer could be used to measure and control the various parameters of an on-line experiment, a means of synchronizing the computer to events in the muscle was required. It appeared best to have a master clock (Devices Digitimer) remote from the computer, and to use this clock to set the rate of stimulation of the muscle and to control both the beginning of the sampling sequence and the sampling interval of the computer.

As the experimental apparatus was some 150 metres from the computer it was necessary to have remote control of, and visual indication of, computer operation. An interactive computer interface was designed and built to meet these requirements.

The interface consisted of a digital and an analog section. The digital section had the function of controlling computer operation and timing, while the analog section set the dc level and range of the analog signals being presented to the computer. Both sections were completely independent, each with its own power supplies.

C.2 Interface Controls and Signals

To obviate the necessity of having to use special computer programming techniques such as program interrupts and all that they entail, the programs were kept at a more elementary level. The twelve external sense lines of the computer were used to convey control information to the computer, while information from the computer was returned to the inter-

face via its six relay outputs.

Since the LINC-8 computer uses negative logic, i.e. a negative voltage represents a logical "1", the digital logic for the interface was made from discrete components rather than from integrated circuits, as they require a positive voltage as a logical "1". The individual logic elements were constructed on plug-in circuit boards (Veroboard VB/C/10723), using the FLIP-CHIP principle of Digital Equipment. Thus all interconnections between logic elements were made at the pins of the individual sockets. This allowed for greater design flexibility of the interface, and if at some future date its functional structure needs to be changed, it can be accomplished quite easily by changing the wiring between the socket pins only. In the interface, -15 V represents a logical "1", and 0 V represents a logical "0".

C.2.1 Interface status lights

The interface status lights had a dual function: they indicated the status of the interface and the computer separately, and the sequence in which the various lights turned on and off gave an indication of either normal operation or computer-interface malfunction. The definition of each of the status lights is given below.

READY — The READY status light is illuminated when the READY flip-flop in the interface is set. It indicates that an EXT SYNC pulse has triggered the interface and that a READY signal has been sent to the computer. Under normal operation the set-reset cycle for the READY flip-flop happens so quickly that the READY status light is never visibly on. If the light does come on it usually means that the interface and the computer are not syn-

chronized. This light can be extinguished manually, by using the RESET function switch, or remotely, by a READY CLEAR signal.

SAMPLE — This light indicates that the SAMPLE flip-flop has been set and that SAMPLE STROBE pulses are being transmitted to the computer - provided that the interface function switches are set for AUTO and RUN. In the MAN mode of operation, the SAMPLE flip-flop and hence the SAMPLE status light are set the first time MAN SAMPLE is pressed. However, only one SAMPLE STROBE pulse is generated each time the MAN SAMPLE button is pressed. When the computer is finished the sampling sequence a SAMPLE CLEAR signal is sent to the interface which resets the SAMPLE flip-flop and extinguishes the SAMPLE status light. The SAMPLE light and flip-flop can be reset manually by pressing RESET.

TAPE END — The TAPE END acts as a warning light that is activated by the computer. When the last block of digital magnetic tape has been written the WARN subroutine is called and it flashes the TAPE END light to warn the operator that the magnetic tape is full.

COMP HOLD — This status light indicates that the computer is "holding-off" the interface, preventing it from being activated by an EXT SYNC or MAN SAMPLE signal. When the light is off, the interface is enabled and can resume normal operation.

C.2.2 Interface function switches

Six illuminated push-button switches (DIALCO, 513-0301-604, two-circuit, momentary contact, with 3/4" square non-rotatable lens caps) act as the function switches of the computer interface. They control the mode of operation of both the interface and the computer. A description of each one of the function switches is listed below, and the interconnections between the switches and the digital control logic is shown in Fig. C.1. It is important to note that the switches used here act both as status lights and function switches.

AUTO — When the AUTO button is pushed the corresponding indicator light is illuminated. In this mode of operation the interface accepts SYNC and CLOCK pulses from the master clock and transmits them to the computer via the external sense lines.

MAN — When this switch is pushed, the AUTO indicator light is extinguished and the MAN light is illuminated. This is because the two controls are interlocked so that only one mode can be operational at a time. In the MAN mode, the control signals from the external clock are disabled and alternate control signals must be sent to the computer via the MAN SAMPLE button.

STOP — When this button is pressed all control information, whether it is generated automatically or manually, is prevented from reaching the computer. While in STOP the interface is completely disabled.

RUN — Pressing RUN cancels STOP as these two functions are interconnected in the same manner as the AUTO and MAN functions. In the RUN mode the interface is enabled and can transmit control signals to the computer.

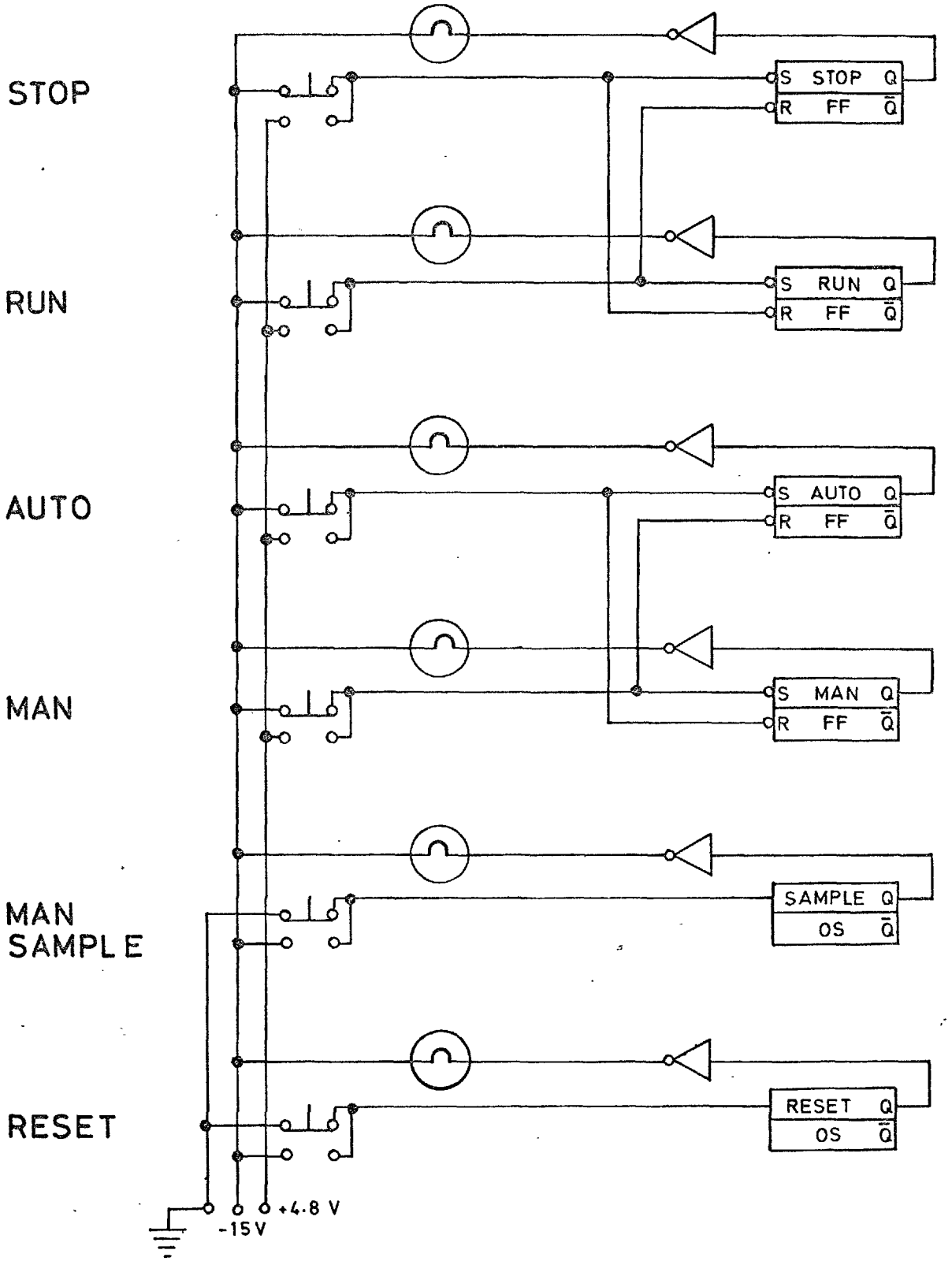

Fig. C.1 The interconnections between the function switches and the interface digital control logic.

RESET — Pressing this button results in a momentary lighting of the RESET indicator lamp. This also generates a RESET signal which resets the READY and SAMPLE flip-flops and extinguishes their respective indicator lamps. This switch is used to re-establish synchronization between interface and computer if they become out of step.

MAN SAMPLE — This switch only functions in the MAN mode of operation. When pressed, the corresponding indicator lamp is momentarily illuminated. Also a signal is generated that sets the SAMPLE flip-flop and sends one STROBE pulse to the computer. Only one STROBE pulse is generated each time the MAN SAMPLE button is pressed. However, the SAMPLE flip-flop remains set until either RESET is pressed, or a SAMPLE CLEAR signal is generated from the computer.

C.2.3 Interface Input/Output Signals

The input/output signals of the interface can be divided into three groups; the clock input signals, the interface output signals, and the computer input signals. Their description and function are listed below.

Clock Input Signals

EXT SYNC — This signal is the leading edge of a negative-going pulse or level which is normally derived from the "O" output of the Digitimer. Provided the interface is in the AUTO and RUN mode, the EXT SYNC pulse sets the READY flip-flop in the interface, which in turn sends a READY signal to the computer.

EXT CLOCK — The EXT CLOCK signal is a train of pulses from the "Continuous Pulse Output" of the Digitimer. When the Digitimer "Time Scale" and "Time Unit" controls are set for 1 ms, these pulses are 0.1 ms in duration and occur once every millisecond. These pulses generate the SAMPLE STROBE pulses that strobe the computer to sample, and they also set the sample rate of 1 kHz.

Interface Output Signals

READY — The READY signal is a -3 V level which appears on external sense line 13_8 when the READY flip-flop is set and it tells the computer to prepare itself for the next sampling sequence. This signal can be disabled by pressing STOP, but the COMP HOLD signal does not have any effect once the READY signal has been generated.

SAMPLE STROBE — The SAMPLE STROBE signal consists of a train of -3 V pulses 50 μs wide that appear on external sense line 12_8. Their rate is set by the EXT CLOCK, and they trigger the computer to sample the analog input line(s). They can also be disabled by pressing STOP. The COMP HOLD signal does not have any effect once the SAMPLE flip-flop has been set.

Computer Input Signals

READY CLEAR — This signal is a -3 V level or pulse that is generated from one of the relay outputs of the computer. The leading negative-going edge of this signal resets the READY flip-flop in the interface. This signal is used by the computer to acknowledge receipt of the READY signal and to indicate that appropriate action is being taken.

SAMPLE CLEAR — When the sampling sequence is ended, as determined by the computer program, the computer sends a SAMPLE CLEAR signal through one of the relay outputs back to the interface. The negative-going edge of this -3 V level or pulse resets the SAMPLE flip-flop which prevents any further SAMPLE STROBE pulses from reaching the computer.

COMP HOLD — This signal is a -3 V level which is used as a remote STOP for the interface. When set, this signal prevents the interface from being triggered by any control signals. However, it does not have any effect on the READY and SAMPLE STROBE signals once their respective flip-flops have been set.

C.2.4 Computer External Sense Line Operation

The output signals from the interface are carried via a 15-way screened cable to the external sense line terminal at the computer. At the interface, the sense lines are brought to the front panel where a series of twelve S.P.D.T. switches control their settings. They are wired such that when a switch is in the "up" position the corresponding external sense line is open circuit and a -3 V level (supplied by the computer) is present on the sense line. Thus when a SXL n (skip on external level) instruction is encountered in the computer program the next instruction in the sequence is skipped. On the other hand, when the switch is in the "down" position the external sense line is earthed and the computer executes the next instruction in the sequence. Therefore, by manual manipulation of the interface sense line switches, control of the computer program can be exercised at a location remote from the computer.

However, there are two exceptions to the above description and they are in external sense line switches 12_8 and 13_8. These two switches are wired so that when in the "down" position the sense lines are connected directly to the digital logic of the interface and they convey the SAMPLE STROBE pulses and the READY signal directly to the computer. In the "up" position, the function is the same as the other switches, i.e. the sense lines are open circuit.

C.2.5 Computer Relay Register Operation

Information from the computer relays is transferred through individual coaxial cables to the interface. These signals can be mechanical (contact closure) or electrical (0 to -3 V) depending upon how the cables are connected at the computer. The electrical signal was chosen for interface activation because it had a rapid rise time and there was no risk of contact bounce generating false signals.

Control of the relays is made via a 6-bit relay register, one bit per relay. To turn on a given relay the corresponding bit is set (made a logical "1") in the accumulator and then the ATR (accumulator to relay) instruction is executed. This transfers the right-most 6-bits of the accumulator to the relay register. Thus a logical "1" represents the relay being "on", and a logical "0" represents "off". The relay register remains in a given state until another ATR instruction is executed to alter its contents.

The computer generated READY CLEAR and SAMPLE CLEAR signals activate the interface on the leading edge of a negative-going pulse or level, and this occurs when the relays are first turned on. The TAPE END and COMP HOLD signals, on the other hand, represent -3 V levels from the computer. As long as their corresponding relays are "on" the status lights are illuminated at the interface.

C.3 Digital Logic

C.3.1 Logic symbology

Before entering into a detailed description of the interface digital control logic it is necessary to define the logic elements and the symbols used to represent them.

The logic elements were constructed using discrete components with -15 V representing a logical "1" and 0 V representing a logical "0". There is one exception to this convention and that is in the signals used to set and reset the flip-flops. These elements require a positive voltage for normal triggering, and as a result, a differentiating network (represented by a small square with a diagonal cross) was required to convert the positive-going edge of a pulse or level change into a positive voltage pulse. In this case the positive voltage represents a logical "1" and 0 V a logical "0". It is important to note that this reversal in polarity is only valid for logic elements contained between the differentiating network and the trigger inputs to the flip-flops. This is indicated by the small open circles at both the inputs and the outputs of the OR gates and the inputs to the flip-flops. The logic elements and their truth tables are shown in Table C.1.

With reference to the logic diagram (Fig. C.2) the following nomenclature has been added for clarity in understanding the operation of the digital logic:

- Some of the inputs to the NAND gates have enabling functions (inputs labelled "e"). When all the inputs are enabled a signal that is presented at the "p" input will pass through the gate.

- The OR gate inputs are labelled "M" or "A". These differentiate between those signals generated in the MAN mode and those generated in the AUTO mode of operation.

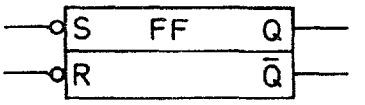

FLIP-FLOP

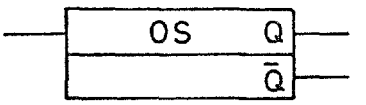

ONE-SHOT

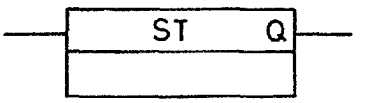

SCHMITT TRIGGER

PULSE INVERTER

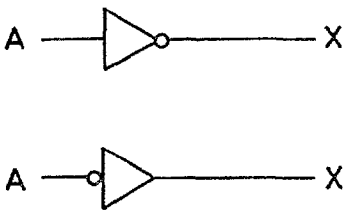

A	X
0	1
1	0

NAND GATE

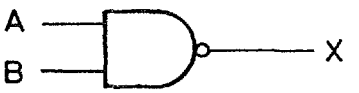

A	B	X
0	0	1
0	1	1
1	0	1
1	1	0

OR GATE

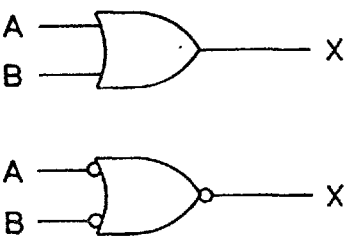

A	B	X
0	0	0
0	1	1
1	0	1
1	1	1

DIFFERENTIATION NETWORK

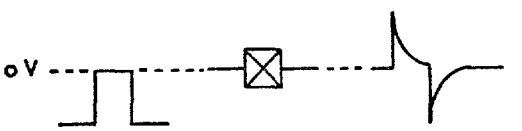

TABLE C.1 Digital logic symbology

- The Q outputs of the flip-flops (FF), one-shots (OS), and Schmitt triggers (ST) are normally at a logical "0" unless set or triggered. The $\overline{Q}$ outputs are always opposite to the Q outputs. The trigger inputs to the flip-flops are labelled "S" for set and "R" for reset. These inputs set Q to logical "1" and logical "0" respectively.

C.3.2 Interface Logic Description and Timing

Initially assume that the interface is in the RUN and AUTO mode. In this mode the RUN and AUTO flip-flops are set and this enables gates AUTO1 and AUTO2; since the MAN flip-flop is off, the MAN gate is disabled. If an EXT SYNC signal occurs the following sequence of events take place in the interface (see logic diagram Fig. C.2 and timing diagram Fig. C.3).

$t = 0$

At this time the EXT SYNC pulse triggers the input Schmitt trigger which passes a pulse through AUTO1 and sets the READY flip-flop and status light. This generates another signal that passes through the READY gate and appears as a READY signal on external sense line 13_8. At the same time, the READY flip-flop triggers the 1.5 ms DELAY one-shot.

$0 < t < 1.5$ ms

Within this interval at some time t (the time depending upon the computer program) the computer senses the READY signal and jumps to the beginning of the sampling sequence in the program. When this point is reached, the computer acknowledges receipt of the READY signal by sending a READY CLEAR signal back to the interface. This signal turns off the READY flip-flop which also extinguishes the READY status light. The computer is now ready to begin sampling the analog input data.

t = 1.5 ms

This time corresponds to the end of the delay cycle of the DELAY one-shot. This delay was built into the interface to allow sufficient time for the computer to reach the beginning of the sampling sequence. Therefore, this 1.5 ms interval can be considered as "dead time" in the interface during which time no SAMPLE STROBE pulses can appear at the output. At the end of this delay the SAMPLE flip-flop is set which enables SAM2 and allows the EXT CLOCK pulses to reach the SAMPLE STROBE one-shot.

t = 2 ms

The first SAMPLE STROBE pulse occurs at this time on external sense line 12_8 (providing the clock pulse interval is 1 ms). The SAMPLE STROBE pulses represent 50 μs windows during which time the computer can be triggered to sample. Since these pulses are so narrow, the possibility of jitter or fluctuations in the sampling interval is reduced.

t = n

At this time (the duration n being controlled by the computer program), the sampling sequence is terminated, and a SAMPLE CLEAR signal is sent back to the interface from the computer. This resets the SAMPLE flip-flop and turns off the SAMPLE status light. Now SAM2 is disabled preventing any further SAMPLE STROBE pulses from reaching the computer.

If the interface is put into the MAN mode, AUTO1 and AUTO2 are disabled. This prevents the READY flip-flop from being set and also prevents

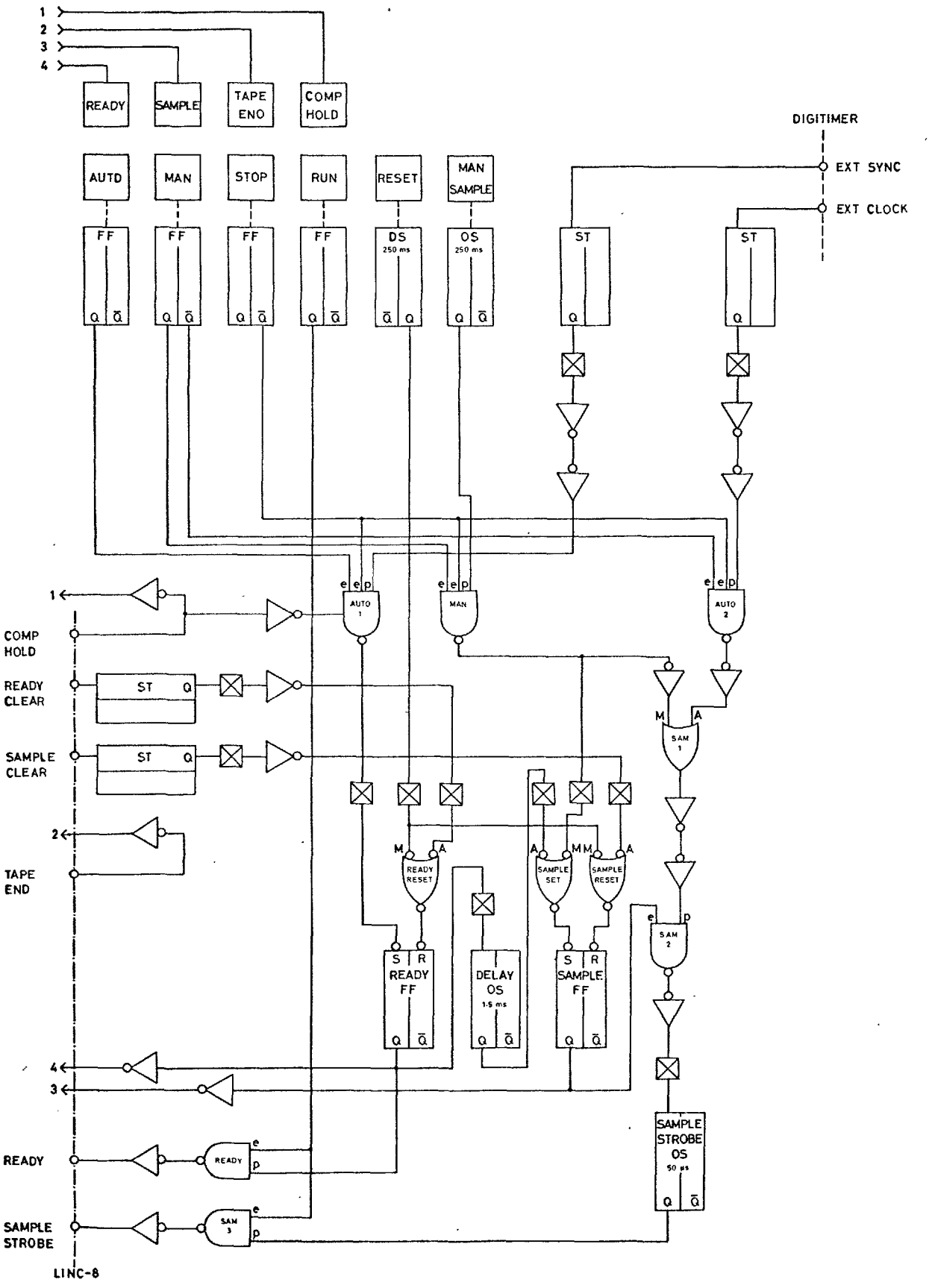

Fig. C.2 LINC-8 INTERFACE LOGIC DIAGRAM

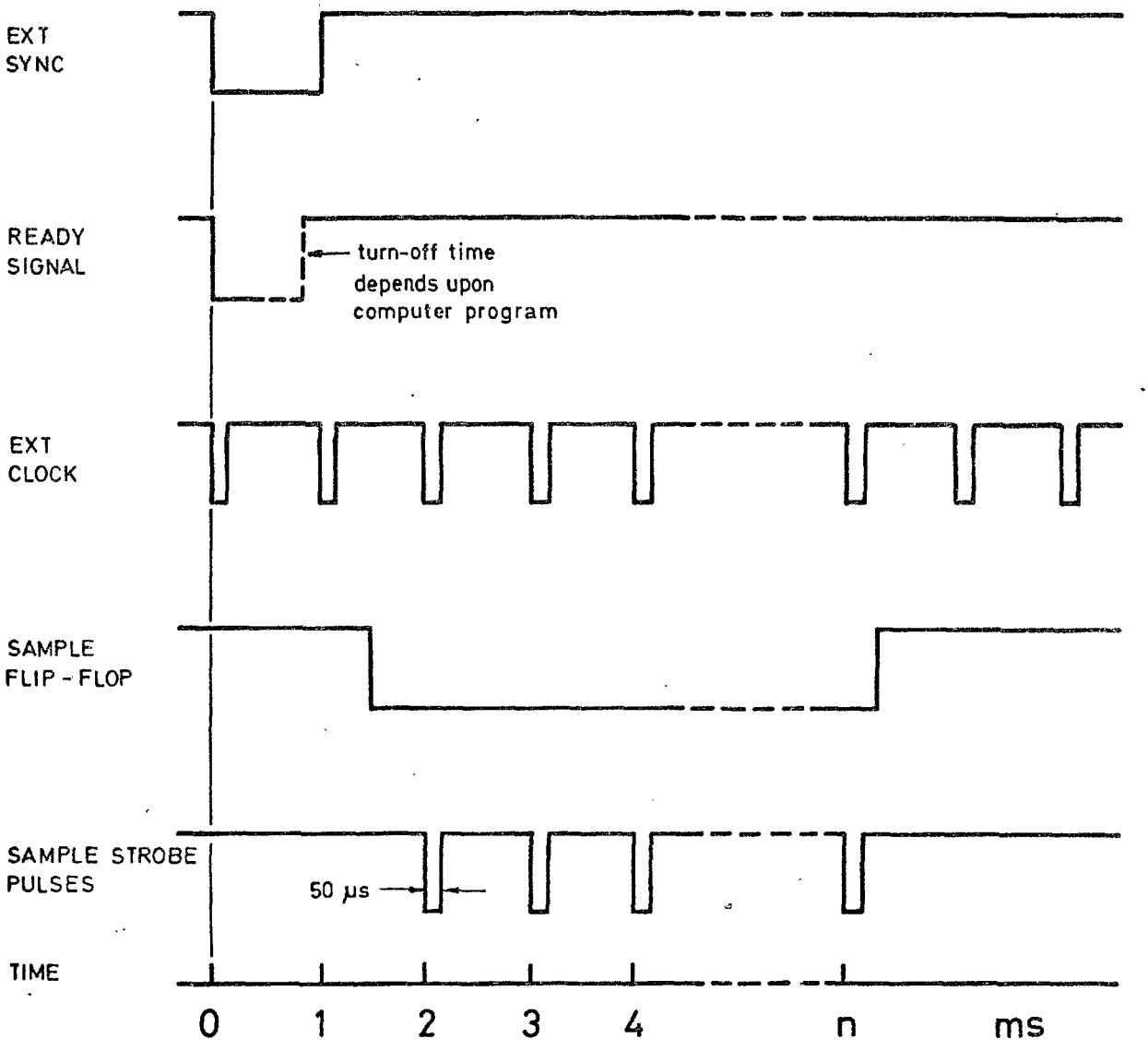

Fig. C-3 LINC-8 INTERFACE TIMING DIAGRAM

any EXT CLOCK pulses from reaching the SAMPLE STROBE one-shot. However, if MAN SAMPLE is pressed, a single 250 ms pulse is generated which passes through MAN and sets the SAMPLE flip-flop on the leading edge of this pulse. This in turn enables SAM2 which passes the MAN SAMPLE signal to the SAMPLE STROBE one-shot. This sequence causes one SAMPLE STROBE pulse to be generated.

If STOP is pressed, the AUTO1, AUTO2, MAN, READY and SAM3 gates are all disabled. This prevents the READY and SAMPLE flip-flops from being set, and if they are already set, their signals are disabled by the READY and SAM3 gates.

C.4 Analog Section

The analog section consists of three operational amplifiers (709-OPA, RS Components Ltd.) mounted on a single plug-in board. Each operational amplifier circuit (Fig. C.4) was designed to convert the 0 V to 1.25 V output from the pen recorder to be compatible with the $\pm$ 1 V analog input range of the computer.

For normal operation the amplifiers were connected in the non-inverting mode (A) so that their outputs were in phase with the input signals. This had the added advantage that the high input impedance did not load down the output of the pen recorder. The amplifiers were designed to have a gain of between 0.5 and 5 in the inverting mode, which then gave a gain of 1.25 and 2.9 in the non-inverting mode.

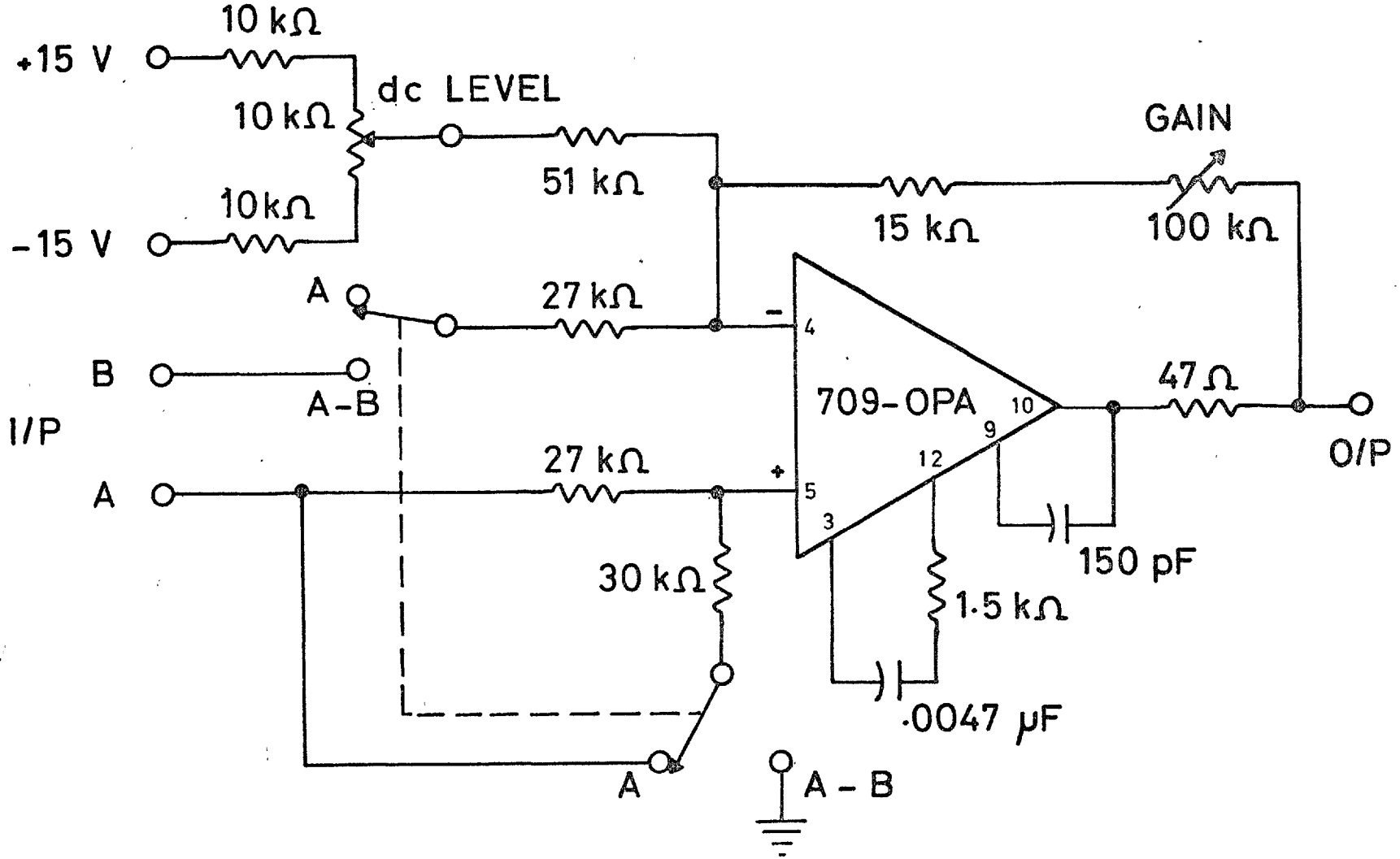

Fig. C.4 INTERFACE ANALOG BUFFER AMPLIFIER

APPENDIX D

DIGITAL SIGNAL PROCESSING

D.1 Introduction

A LINC-8 computer was used as the foundation of the data acquisition and measuring system. The hardware and software of the system were designed so that the computer could be used on-line to measure a number of parameters for each contraction on a beat-to-beat basis (Chapter 3). These measurements were required in real-time, and as the signals of interest were low frequency (< 10 Hz), elementary digital signal processing techniques could be used.

The frequency content of isometric tension and isotonic length signals were measured so that suitable digital filters could be designed to process them. A low pass digital filter was used to smooth the incoming signal before measurements were made, and a high pass digital filter was used to differentiate the filtered signal to obtain rate measurements.

D.2 Spectral Content of Signals to be Processed

Before any digital signal processing can be implemented it is necessary to determine the spectral content of the signals to prevent the attenuation of any important frequency components present in the original signal.

D.2.1 Sampling rate

In order to determine the spectrum of the signals of interest, consideration must be given to the sampling interval, for the Sampling Theorem (as cited by Lathi, 1967, p. 437) states: "A bandlimited signal which has no spectral components above a frequency f_m cycles per second is uniquely determined by its values at uniform intervals less than $1/2f_m$ seconds apart."

If the maximum rate of stimulation of the muscle is taken as 120 per minute, or 2 Hz, and allowing for ten harmonics to be present, the maximum band-width of the signal to be filtered is in the order of 20 Hz. Thus, according to the sampling theorem, a sampling rate of 40 Hz would uniquely define our signal.

However, if this low a sampling rate were used, it would be necessary to reconstruct our sampled signal in order to determine what had occurred in the time between sample points. This is especially true if one is trying to determine peak values, and their time of occurrence. Unfortunately, there is a restriction on the amount of computing time available for interpolation if these measurements are to be made in real-time. Consequently, a higher sampling rate must be chosen to increase the time resolution of the measurements and to reduce the number of computations required by the computer. For our particular system a sampling rate of 1 kHz has been chosen. This high rate will enable the measurement of signals of up to 500 Hz bandwidth, and will give a possible time resolution in our measurements of 1 ms.

D.2.2 Power Spectra of Muscle Contractions

The LINC-8 computer was used in conjunction with a Fast Fourier Transform (FFT) program (FILTERFT, P. Handler, Washington University) to determine the spectral content of unfiltered twitch responses. The FFT program requires 256 sample points upon which it performs its calculations to produce a power spectrum of 128 components.

Fig. D.1a shows a typical unfiltered isometric twitch which lasts for about one second. The muscle temperature was 30°C and the frequency of stimulation was 20/min. The power spectrum associated with this contraction contains a large dc component and a fundamental frequency component at 1 Hz.

In contrast to this, Fig. D.1c shows a typical isotonic length change produced by a muscle. This signal is shorter in duration and is more asymmetrical than the tension signal. As a result, the power spectrum (Fig. D.1d) contains frequency components up to 8 Hz.

These spectral measurements indicate that a sampling frequency of 1 kHz is more than adequate, and that any digital filters applied to the signal must have a bandwidth of not less than 8 Hz.

D.2.3 System Noise

The analog signals that are fed to the computer have noise superimposed on them. This noise originates from two prime sources; wideband noise from the DC-6 pre-amplifiers, and stray 50 Hz mains pickup.

The wideband amplifier noise appears to be characteristic of pen recorder pre-amplifiers and is usually of large amplitude (typically 20 mV peak-to-peak). Although it can be reduced by external filtering, this noise can never be completely eliminated if a reasonable bandwidth is to be maintained. Since the analog-to-digital system of the LINC-8 computer

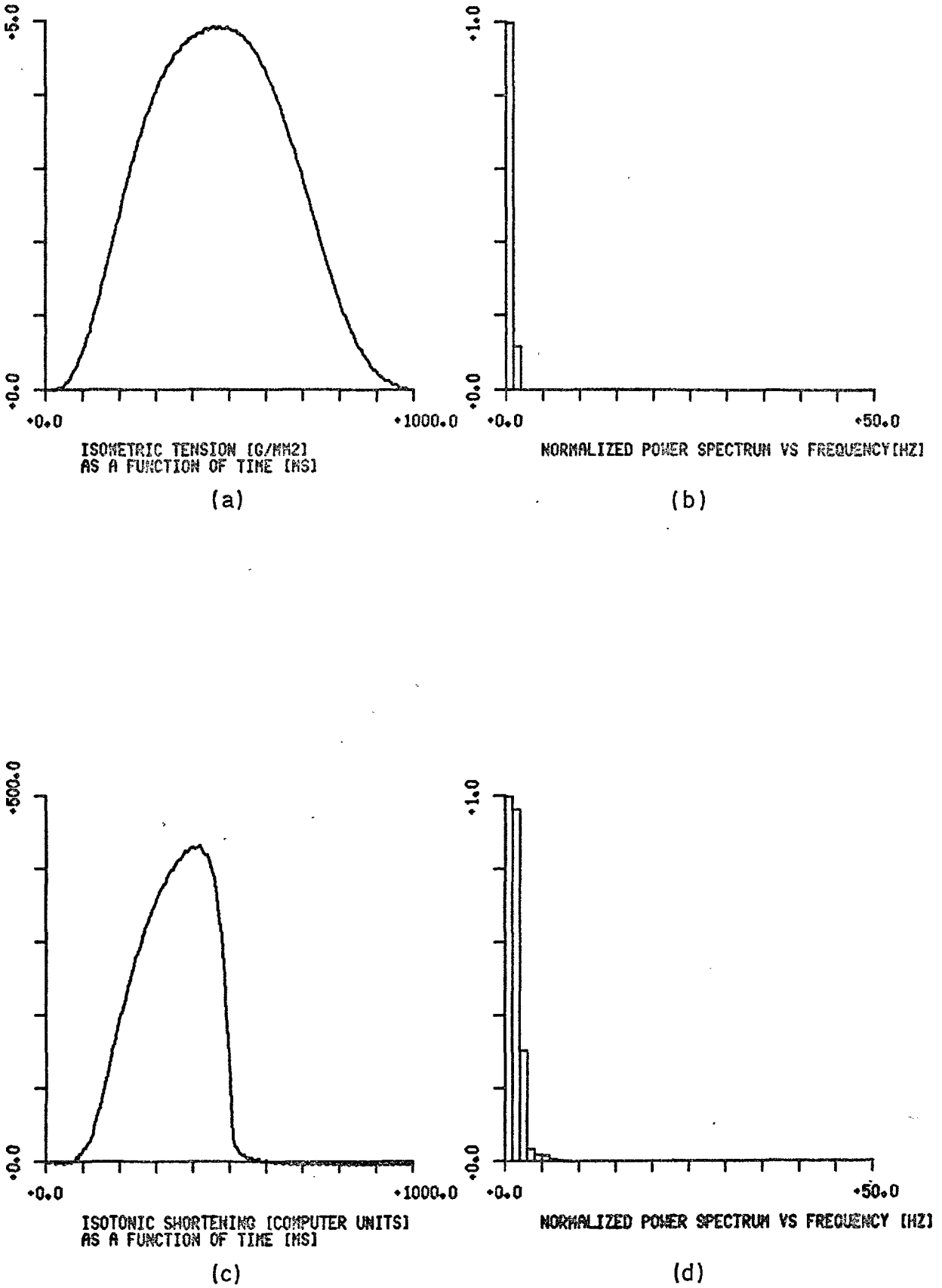

Fig. D-1 Typical transducer signals of papillary muscle contractions.

has a resolution of 3.92 mV this wideband noise can cause fluctuations in a digitized signal of up to 5 computer units (c.u.). The mains interference can be substantially reduced provided adequate precautions are taken in shielding, routing of cables, and prevention of ground loops. However, even with this exercise of care, it is possible that some 50 Hz interference may still be present.

These unwanted fluctuations in the digitized signal due to noise must be reduced if accurate and reproducible measurements are to be made. Thus, by using an appropriately designed digital filter, the signal-to-noise ratio can be significantly increased.

D.3 Digital Filtering

Digital filtering can be considered as a form of numerical analysis, and a digital filter consists of a set of numerical weights that are applied to the signal to be filtered. These weights can be regarded to form a window across which the sampled data passes as it is being filtered. The terms "weighting function" and "window" are interchangeable, and apply to the set of numerical weights.

The total number of weights is determined by the combination of the width of the window and the interval between the individual weights, while the numerical value of the weights is set by the window's shape. The width and profile of the window in turn define the filter's characteristics.

The filtering process consists of multiplying the input data points with the corresponding window weights and summing. This operation produces one output point. This procedure is then repeated with the window shifted by one data point until all the input data has been filtered.

Quite clearly the amount of filtering or smoothing is governed by

the number of data points selected to form the sum in the filtering process; the more points used, the greater is the filtering. This process can be related to low pass filtering in which the higher frequency components are filtered out.

In terms of signal processing this filtering procedure can be related to numerical convolution in the time domain (see for example Skilling, 1965, p. 582 for a more complete description of numerical convolution). The introduction of the concept of convolution implies that others such as Fourier transform, transfer function, and impulse response can also be introduced. Thus the weighting function can be related to the impulse response of the digital filter in the time domain, and its Fourier transform is the frequency response, or transfer function of the filter in the frequency domain.

For the specific signals of interest, namely isometric tension and isotonic shortening, a digital filter is required that has a bandwidth of at least 10 Hz, and if possible, infinite rejection of all other frequencies, and in particular 50 Hz. Within this bandwidth, minimal distortion of the waveform is required if accurate measurements are to be made. In addition, the filter must be easy to implement with a view to on-line, and real-time measurements using the LINC-8 computer. It only remains to find a weighting function which meets as many of these specifications as possible.

D.3.1 Low Pass Digital Filter - Rectangular Window

For a low pass digital filter consider the most elementary weighting function, a rectangular window (Fig. D.2a). The time domain representation of this window has a constant value of A within the interval $t = \pm T_w$, and is 0 outside this range. This window represents the impulse response of the

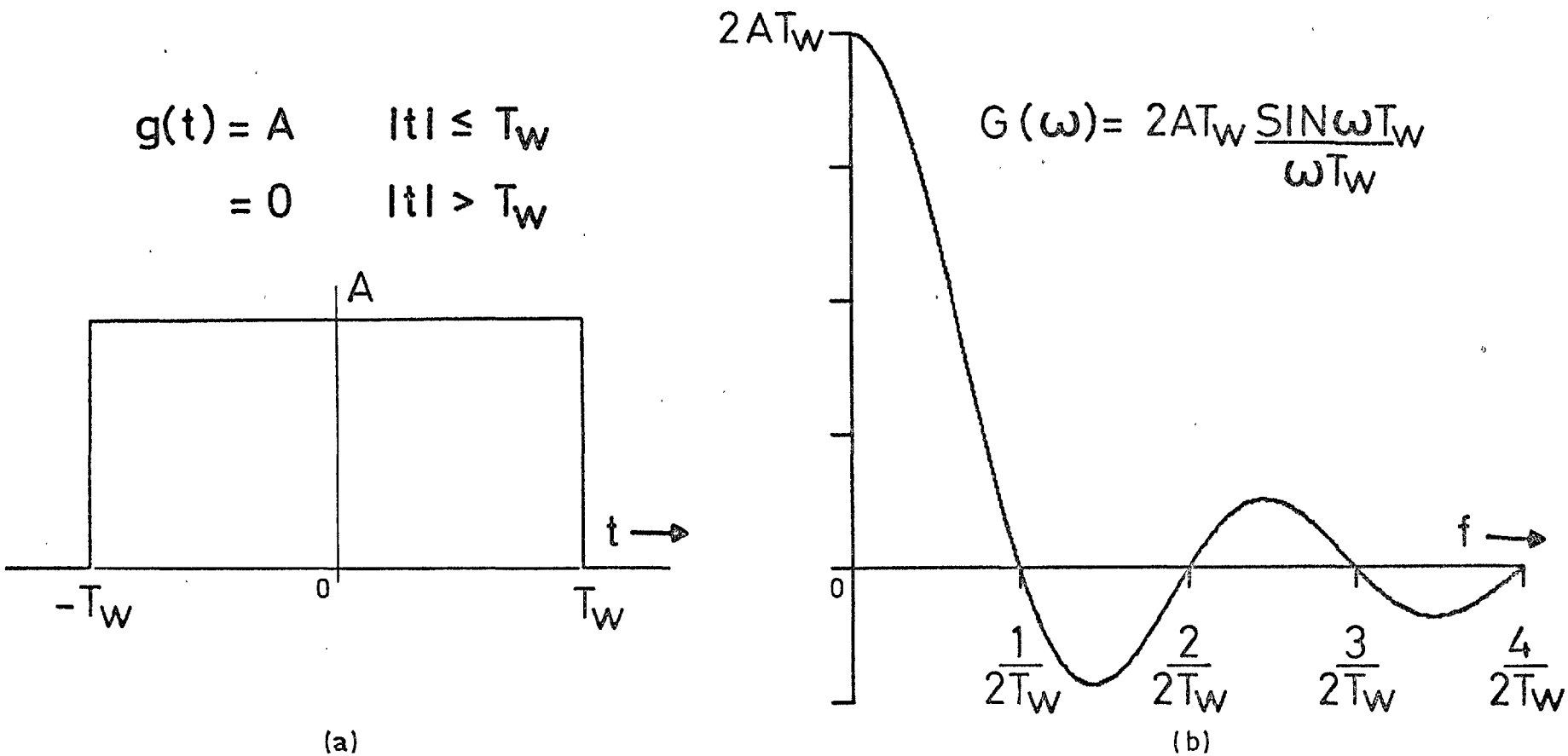

Fig. D.2 Low pass digital filter-rectangular window.

filter, and by applying the Fourier integral (Lathi, Chapter 4) to this window the frequency response of the filter $G(\omega)$ can be determined.

$$G(\omega) = \int_{-\infty}^{\infty} g(t)e^{-j\omega t}dt$$

$$= \int_{-T_w}^{T_w} Ae^{-j\omega t}dt$$

$$= \frac{A}{\omega} \cdot \frac{e^{j\omega T_w} - e^{-j\omega T_w}}{j}$$

$$G(\omega) = 2AT_w \frac{\sin \omega T_w}{\omega T_w}$$

The frequency response (Fig. D.2b) is of the form (sin X)/X with a coefficient of $2AT_w$. This coefficient represents the area under the impulse response curve and is also equivalent to the sum of the total weights used. In addition, it represents the dc gain of the filter. Thus, for unity gain of the filter at dc, it is necessary to have either the sum of the weights equal to 1, or else to divide the output by the sum of the weights used.

Examination of the frequency response curve reveals that infinite rejection of certain frequencies occurs each time the curve passes through zero. The zero points of the filter can be computed by noting that

$$\sin \omega_o T_w = 0 \qquad \text{where } \omega_o = 2\pi f_o$$

when $\omega_o T_w = n\pi$ where $n = 1, 2, 3$-----

Therefore the filter zeros occur at

$$\omega_o = \frac{n\pi}{T_w} \qquad \text{or} \qquad f_o = \frac{n}{2T_w}$$

As a result, it is possible to reject a given frequency and its harmonics by adjusting the window width of $2T_w$.

The Fourier transform of a rectangular window (as shown in Fig. D.2a) is a real function with no imaginary part. Therefore there is no phase shift introduced between the input and output signals within each lobe of the frequency response. However, the fact that the frequency response alters in sign indicates that a 180° phase shift is introduced into the output signal each time the frequency response changes sign.

One disadvantage in using this rectangular window is that the sidelobes are quite large with the first lobe having an amplitude of 21% of the main lobe. This would be a serious drawback if the bandwidth of the input signal extended beyond the first zero of the filter, but in the case under consideration the bandwidth of the signals is much less than the frequency at which the first zero occurs (Section D.4.2), so there is no cause for concern.

In order to make the frequency response of a digital filter more closely resemble an ideal filter, it is necessary to eliminate or drastically reduce the height of the sidelobes. This can be achieved by removing any sharp discontinuities in the window's profile.

There are three other windows in common use which have better frequency response characteristics than the rectangular window. They are the triangular window, the Hanning window, and the Hamming window. The last two have sidelobes which are at most one or two percent of the height of the main lobe. As their profiles are constantly changing, the value of

each weight within the window is different. Consequently, the implementation of these windows as filters is more complex and requires more computing time than does the rectangular window. A more detailed treatment of these windows can be found in Blackman and Tukey, 1959.

D.3.2 High Pass Digital Filter - Digital Differentiation

In addition to making measurements on the filtered input signal, further information about the signal can be gained if the rate of change of the signal is also measured. In order to make these rate measurements, it is necessary to differentiate the signal by passing it through a high pass digital filter.

The differential of a curve is proportional or equal to the instantaneous slope of that curve. In its simplest form, the slope of a curve is the amount that the dependent variable has changed for a unit change in the independent variable. Therefore, by applying this principle to our signals, a continuous differential can be computed by the subtraction to two filtered data points spaced a specified time apart.

The time domain representation of the window required to give a differential is that of two impulses of opposite sign spaced $2T_w$ apart (Fig. D.3a). Thus

$$g(t) = A\delta(t + T_w) - A\delta(t - T_w)$$

The application of the Fourier integral will give the frequency response $G(\omega)$ of the filter.

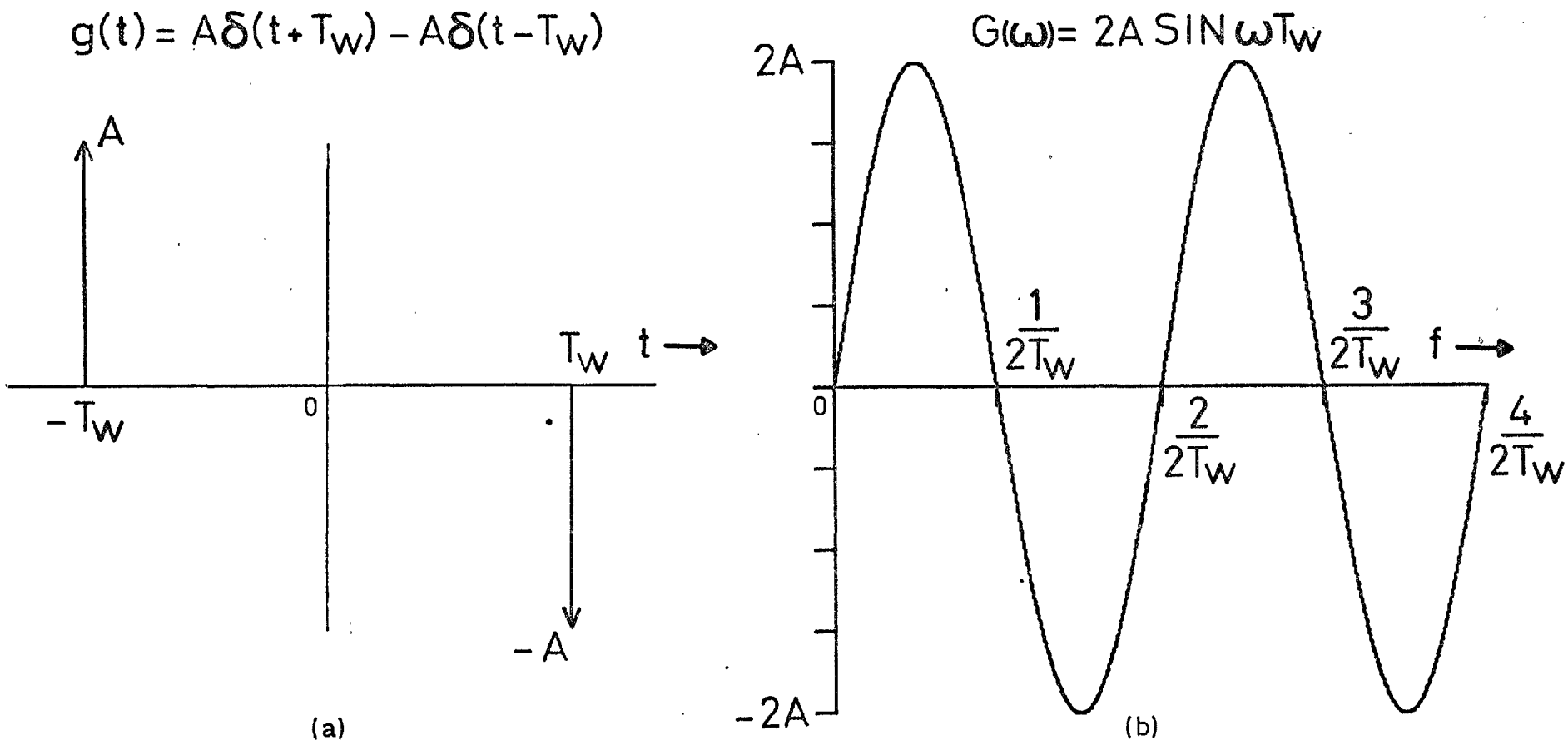

Fig. D-3 High pass digital filter - digital differentiation.

$$G(\omega) = \int_{-\infty}^{\infty} g(t)e^{-j\omega t}\,dt$$

$$= \int_{-\infty}^{\infty} (A\delta(t + T_w) - A\delta(t - T_w))e^{-j\omega t}dt$$

$$= Ae^{j\omega T_w} - Ae^{-j\omega T_w}$$

$$G(\omega) = 2Aj\sin\omega T_w$$

The Fourier transform of this window indicates that the function is imaginary, i.e. it has no real part. This means that the output leads the input by 90°, one of the properties of a true differentiator. The frequency response of the high pass filter is shown in Fig. D.3b.

Before the digital high pass filter is evaluated further, it would be worthwhile to examine the characteristics of an ideal differentiator. Consider a system which has a time constant τ. If this system is an ideal differentiator, the output $y(t)$ is related to the input $x(t)$ by

$$y(t) = \tau \frac{d}{dt} x(t)$$

From this it can be shown (Del Toro and Parker, 1960, p.172) that the sinusoidal steady-state transfer function is

$$H(j\omega) = \frac{Y(j\omega)}{X(j\omega)}$$

$$= j\omega\tau$$

Thus, the magnitude vs. frequency characteristic is a straight line with a slope of τ. This slope also represents the gain of the system. See Fig. D.4a.

Now by converting to a decible scale

$$|H(\omega)| \text{ dB} = 20 \log \omega\tau$$
$$= 20 \log \omega + 20 \log \tau$$

This result is illustrated in Fig. D.4b. The slope of this line is 20 dB/decade, where a decade corresponds to a factor of 10 in frequency.

The intercept of this line at $\omega = 1$ ($\log \omega = 0$) gives the gain of the system in dB, while the point at which the line passes through 0 dB gives the breakpoint of the system ($\omega_b = 1/\tau$).

The magnitude of the frequency response $G(\omega)$ of the high pass digital filter is shown in Fig. D.4c, and can be represented by the equation

$$|G(\omega)| = |2A \sin\omega T_w|$$

At the point about $\omega = 0$ the slope of the magnitude frequency response curve can be considered to be constant and equal to the first differential of the curve. Thus

$$|G'(\omega)| = \frac{d}{dt} |2A \sin \omega T_w|$$
$$= |2AT_w \cos \omega T_w|$$
$$= 2AT_w \text{ at } \omega = 0$$

Thus about $\omega = 0$ the frequency response curve can be represented by the equation

$$|G(\omega)| = 2AT_w\omega$$

This equation is analogous to the linear frequency response curve of the ideal differentiator with $2AT_w$ now representing the gain of the digital filter.

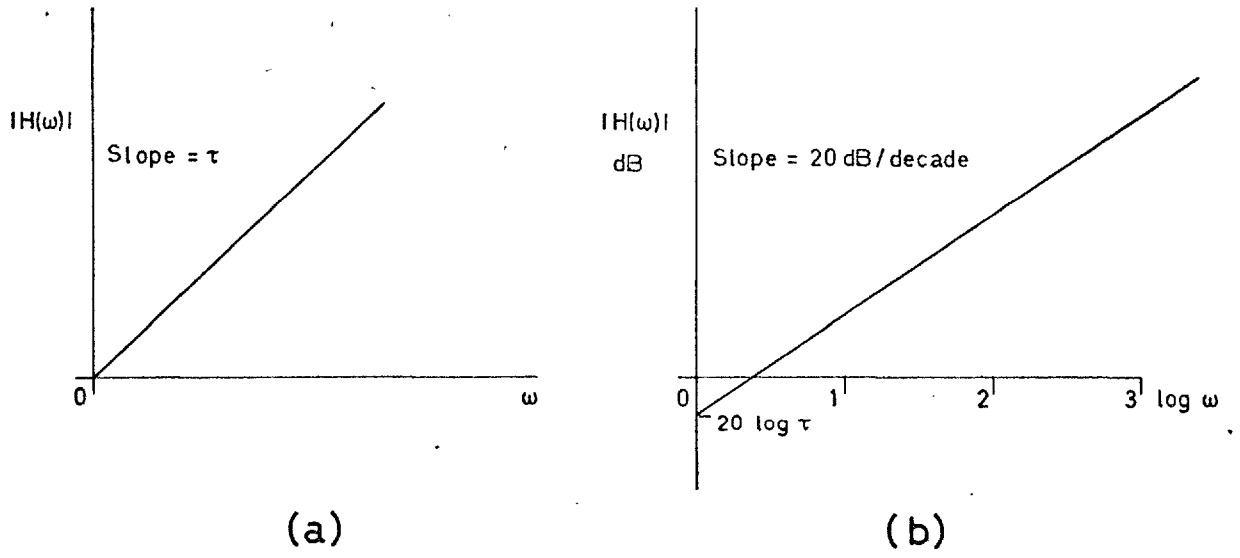

(a) (b)

Ideal differentiator

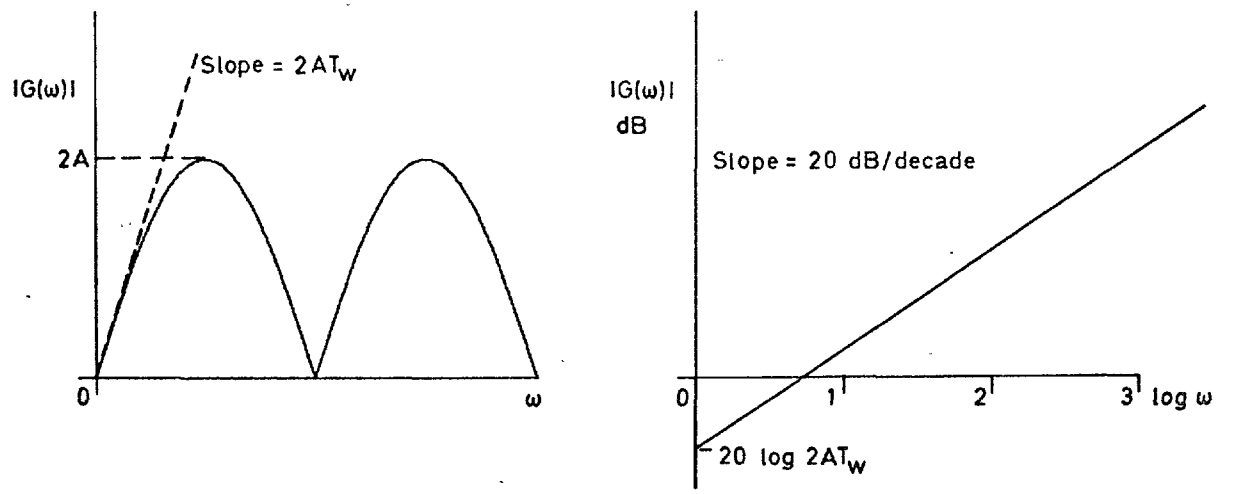

(c) (d)

Digital differentiator

Fig. D.4 Frequency characteristics of an ideal and digital differentiator.

Converting to decibels

$$|G(\omega)|\ \text{dB} = 20 \log 2AT_w\omega$$

$$= 20 \log 2AT_w + 20 \log \omega$$

This equation represents a straight line (Fig. D.4d) which has the slope of 20 dB/decade and an intercept at $\log\omega = 0$ of $20 \log 2AT_w$. This intercept represents the gain of the filter in dB.

The fact that the digital filter, represented on a logarithmic scale, has a slope of 20 dB/decade indicates that the high pass digital filter is behaving as an ideal differentiator in the region about $\omega = 1$. The range over which this relationship holds true will be discussed in Section D.4.4.

D.4 Digital System Evaluation

D.4.1 Analog-to-digital conversion

The analog-to-digital (A/D) system of the LINC-8 computer consists of a multiplexed A/D converter with a sample-and-hold circuit. It will accept any signals within the range of $\pm$ 1 V. The sample-and-hold circuit will accurately track a signal that swings the entire dynamic range in 2 μs, and conversion is completed in 19.5 μs with the result stored in the accumulator.

Upon execution of the "sample" instruction the computer samples the appropriate input analog channel and leaves its numerical value, eight bits plus sign, in the rightmost nine bits of the accumulator.

A +1 V input corresponds to a numerical value of $+377_8 = 255_{10}$, and a -1 V input corresponds to $-377_8 = -255_{10}$. This gives the A/D system a resolution of 3.92 mV.

D.4.2 Low pass digital filter evaluation

The low pass digital filter used in the computer program is a rectangular window of unity height (A = 1), with a window width of 20 ms (T_W = 10 ms). According to Section D.3.1 this results in a low pass filter having a gain of $2AT_W$ = 20 at dc, and a zero at 50 Hz. The normalized frequency response is shown in Fig. D.5a.

Examination of the frequency response curves (Fig. D.5) indicates a gradual attenuation of a signal with increasing frequencies, and the 3 dB point of the filter occurs within the main lobe at about 22 Hz.

By using a rectangular window of unity height, the filtering process can be considered to consist of a series of additions and subtractions. If a running sum is kept, beginning with the first data point, the filtering procedure is reduced to one addition and one subtraction once the first twenty points have been summed. By adding the current sample point to the sum, and subtracting the twenty-first earlier point, the running sum is updated. This new sum is the current filtered value with a gain of 20.

In computing the final filtered output, the updated sum is divided by 4 which gives the filter a gain of 5. The purpose of this is twofold: 1) To keep the amplitude of the filtered signal sufficiently large to increase the resolution of the digital high pass filter, and 2) To keep the numerical value small enough so that they will not overflow a single 12-bit word in the computer.

Since sampling and filtering are being conducted in real-time, the only data points that the filter can operate on are those that have occurred in the past. This means that the filter output is delayed in time by an amount equal to half a window width, T_W. This is equivalent to shifting the window in the time domain by an amount T_W so that it is no longer symmetrical about the t = 0 axis. This time shift introduces a linear phase shift of ωT_W into the output signal. In making time measurements on the filtered signal

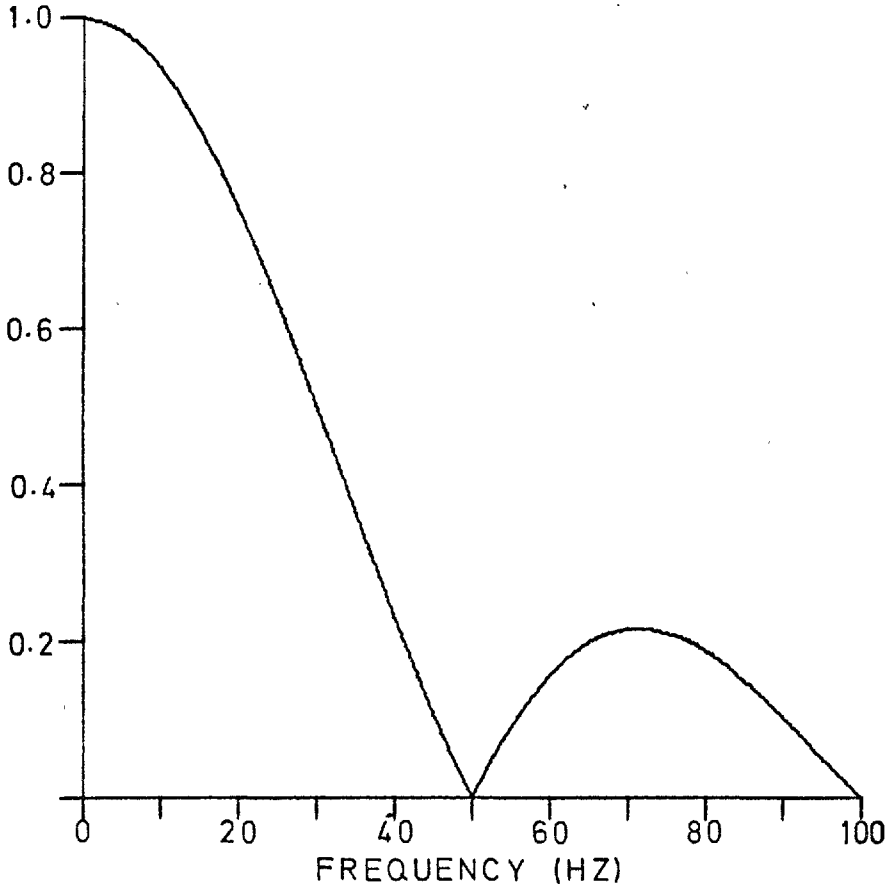

(a) LOW PASS DIGITAL FILTER
NORMALIZED FREQUENCY RESPONSE
20 POINT RECTANGULAR WINDOW

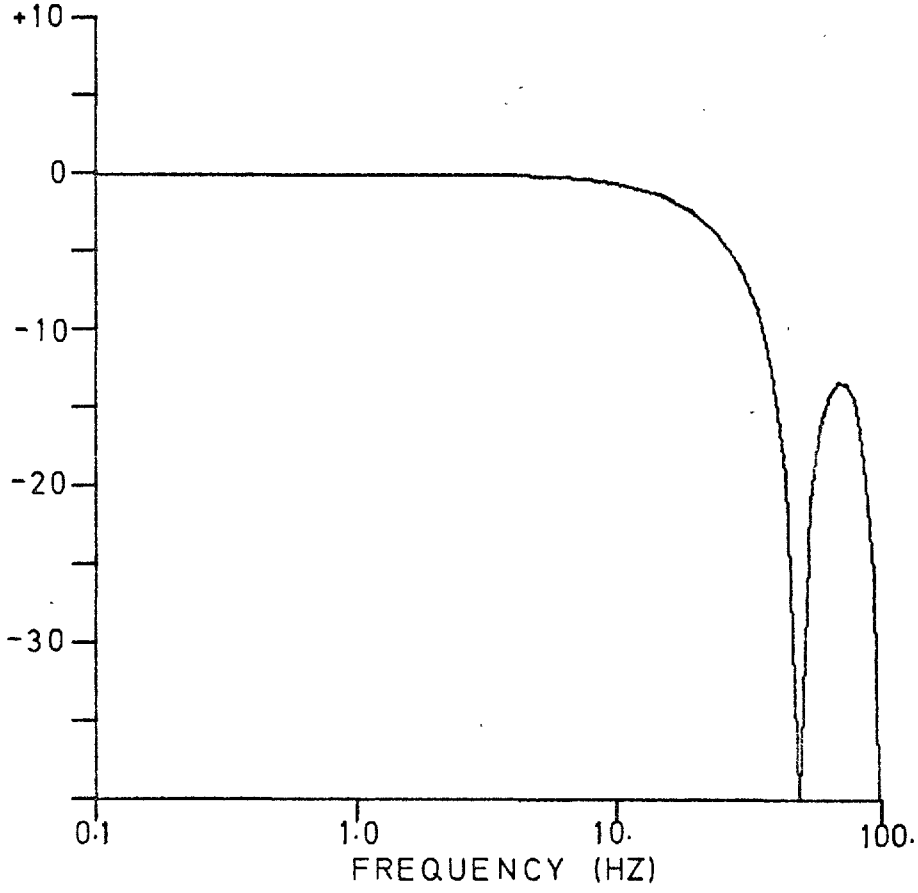

(b) LOW PASS DIGITAL FILTER
DB FREQUENCY RESPONSE
20 POINT RECTANGULAR WINDOW

Fig. D·5

it is important to take this time delay into consideration.

This low pass digital filter meets all the specifications as outlined in Section D.3, namely; infinite rejection at 50 Hz, a bandwidth greater than 8 Hz, no distortion of the waveform, and easy implementation for use in real-time measurements.

D.4.3 High pass digital filter evaluation.

Based on the theoretical considerations of Section D.3.2 a high pass digital filter was designed with T_w = 10 ms. This gave a filter which had infinite rejection at dc, and at 50 Hz and all its higher harmonics. The magnitude frequency response is shown in Fig. D.6a.

The gain (g) of this type of filter was shown to be $2AT_w$ (Section D.3.2). Thus for

$$A = 1$$

and $$T_w = 10 \times 10^{-3} \text{ s}$$

the gain is $$g = 2AT_w$$
$$= 2 \times 10 \times 10^{-3}$$
$$= 20 \times 10^{-3} \text{ s}$$

As the gain is not unity, it is necessary to divide the output of the filter by its gain to obtain the true differential output. Therefore, if the output of the filter is Y computer units (c.u.) the true output Y_t is

$$Y_t = \frac{Y}{g}$$

$$= \frac{Y}{20 \times 10^{-3}}$$

$$Y_t = 50Y \text{ c.u. } s^{-1}$$

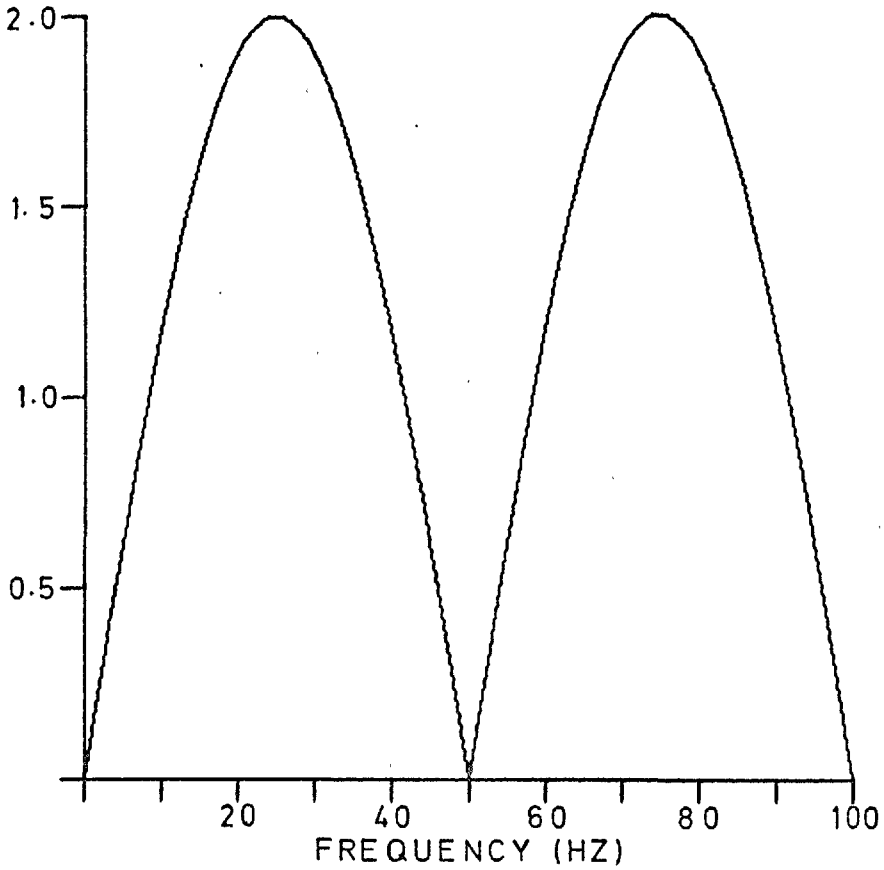

(a) HIGH PASS DIGITAL FILTER
FREQUENCY RESPONSE
2 IMPULSES SEPARATED BY 20 MS

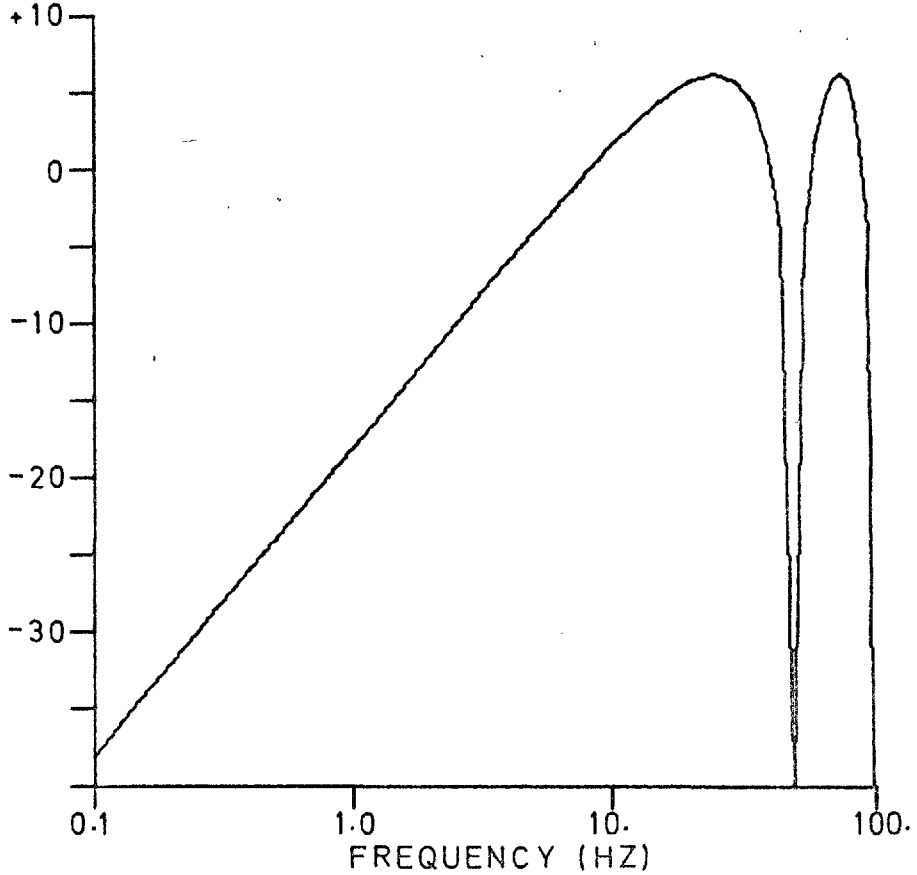

(b) HIGH PASS DIGITAL FILTER
DB FREQUENCY RESPONSE

Fig. D.6

This means that to obtain a true differential it is necessary to multiply the filter output by 50.

The frequency response of the high pass filter (Fig. D.6b) shows that in the region of 0.1 - 1.0 Hz, the slope is constant at 20 dB/decade, and that between 1.0 and 10 Hz the slope does not deviate much from the ideal value. This is discussed in more detail in the next section.

D.4.4 Combined filter characteristics

Up to this point considerable time has been spent in defining the characteristics of the low and high pass digital filters. However it is important to realize that these two filters are in cascade and that the output frequency response of the digital signal processing system is the product of the individual frequency responses. Figure D.7a and b illustrate the linear and logarithmic representation of the two filters in cascade.

In Section D.3.2 it was mentioned that an ideal high pass filter had a frequency response which had a slope of 20 dB/decade. Section D.4.3 confirmed that the slope of the digital high pass filter in the region of 0.1-1.0 Hz was 20 dB/decade. It is of interest to determine over what frequency range this relationship is true for the digital high pass filter.

The amplitude error of the high pass filter was measured by computing the deviation of the linear frequency response of the filter from the ideal response, and expressing this deviation from the ideal as a percentage. These results are shown in Fig. D.8a.

Because the two digital filters are in cascade, the frequency response of the low pass filter will influence the output of the high pass filter. This can be easily seen by comparing Figs. D.6 and D.7. Consequently the differential output is slightly altered from that of the high pass filter

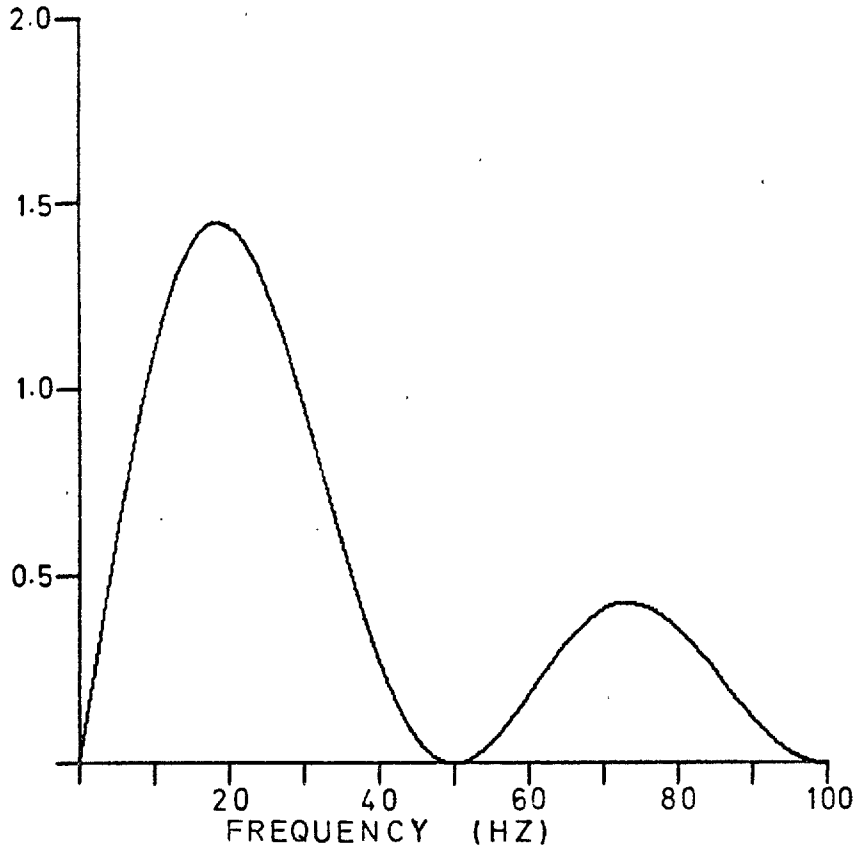

(a) COMBINED DIGITAL FILTERS
FREQUENCY RESPONSE

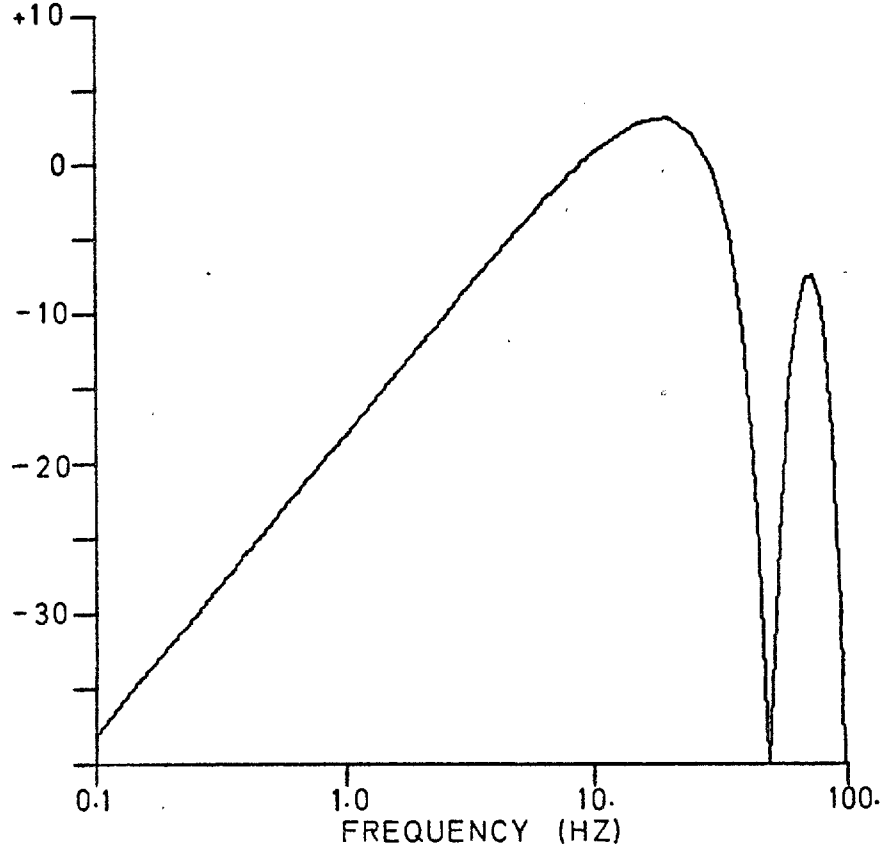

(b) COMBINED DIGITAL FILTERS
DB FREQUENCY RESPONSE

Fig. D.7

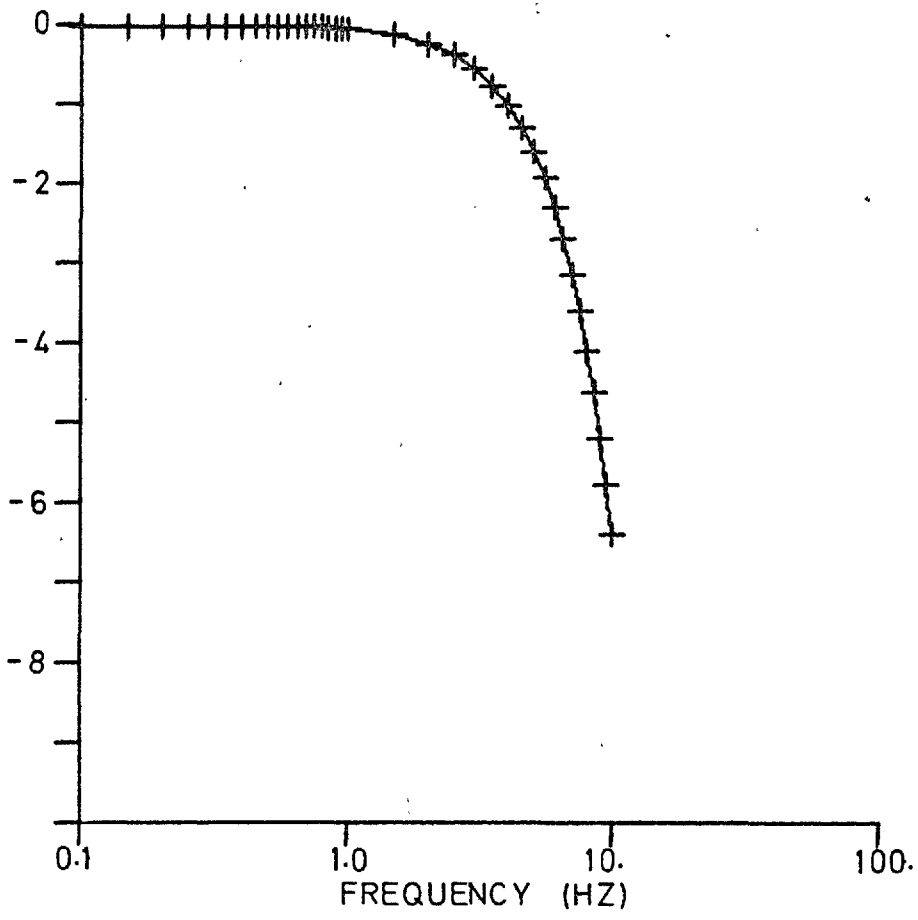

(a) PERCENT AMPLITUDE ERROR
HIGH PASS DIGITAL FILTER

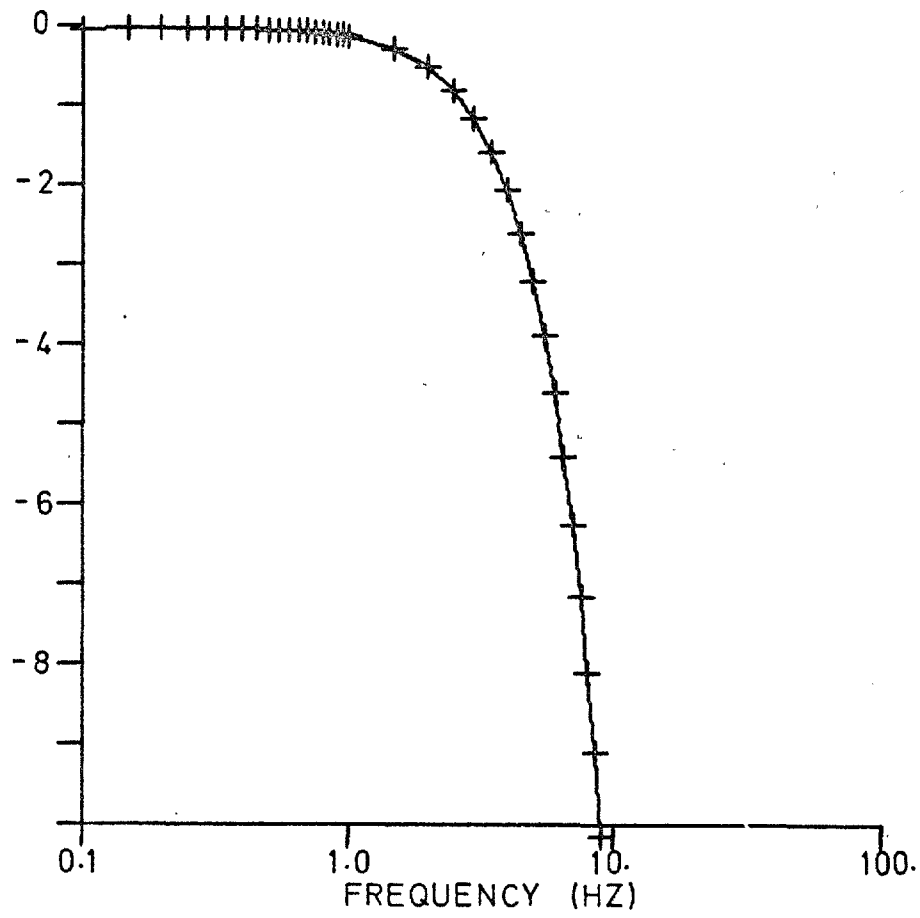

(b) PERCENT AMPLITUDE ERROR
COMBINED DIGITAL FILTERS

Fig. D.8

on its own. Fig. D.8b indicates the percent amplitude error of the differential output from the combined filters as a function of frequency (log scale). This result shows a 10.2% amplitude error at a frequency of 9 Hz. However, as the bulk of the frequency content of the signals of interest is contained in the range of 0-3 Hz one can be assured that the differential output as measured by the computer has an inherent amplitude error of less than 10%.

APPENDIX E

FLOW CHART OF DATA ACQUISITION AND PROCESSING PROGRAM

The language in which this computer program was written was LAP6-3L. This is a low-level LINC language unique to the LINC, LINC-8, and PDP-12 range of computers manufactured by Digital Equipment Corporation.

The program occupies 1K of memory, and requires an additional 2K for data storage. All computations were carried out using integer arithmetic. The filtering was done using double length words, but the results were stored as a single 12-bit word.

The flow charts shown here, and in Appendix F were generated on a CDC 274 Digigraphic console backed by a CDC 6600 computer. The charts were then plotted on a Kingmatic flat-bed plotter. Both the Digigraphics system and the plotter were located at Imperial College of Science and Technology, while the CDC 6600 computer was located at the University of London Computer Centre some five miles away. The flow charting program has been described in a recent paper by Keillor (1972).

MAIN PROGRAM

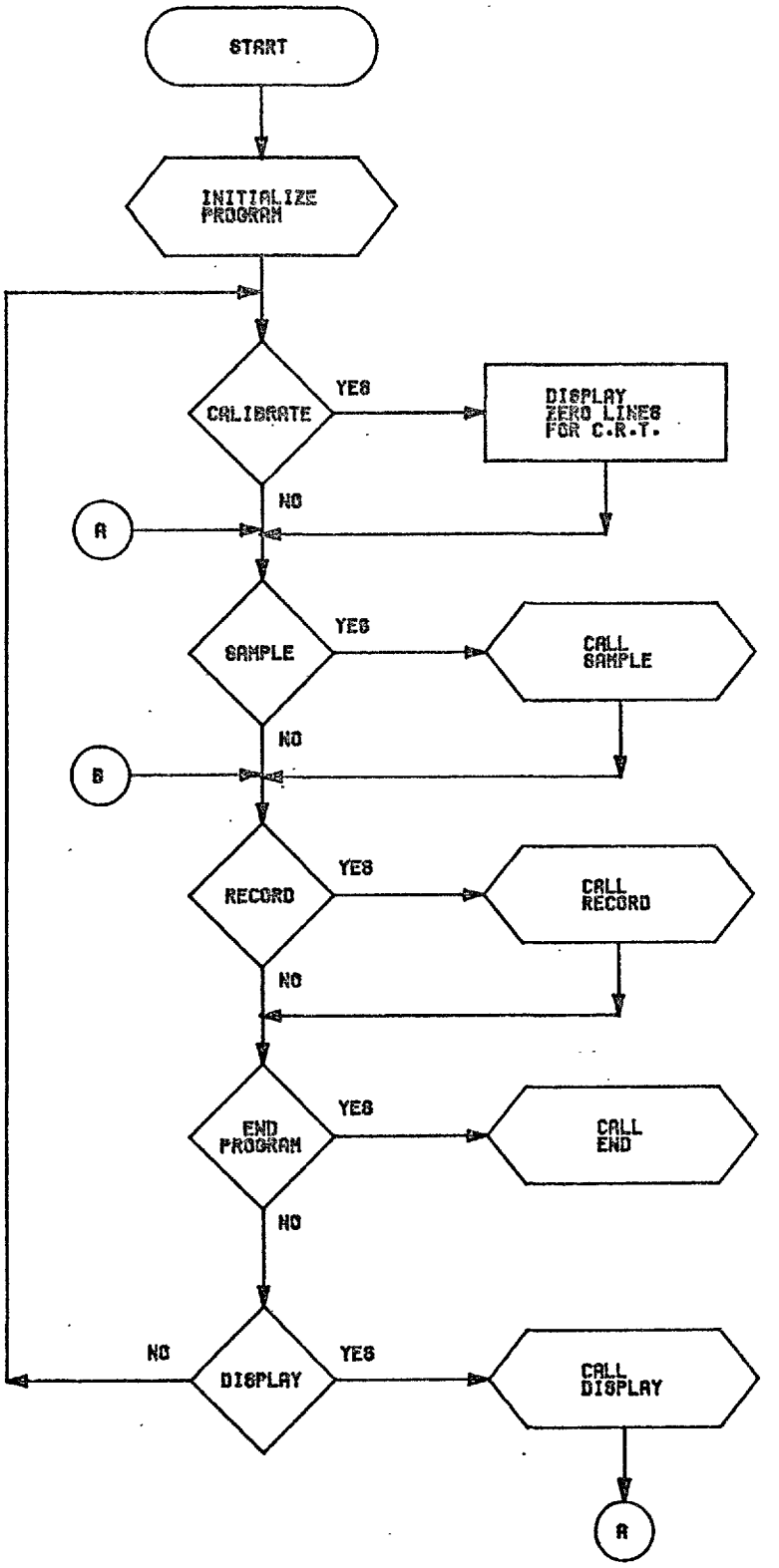

SAMPLE SUBROUTINE

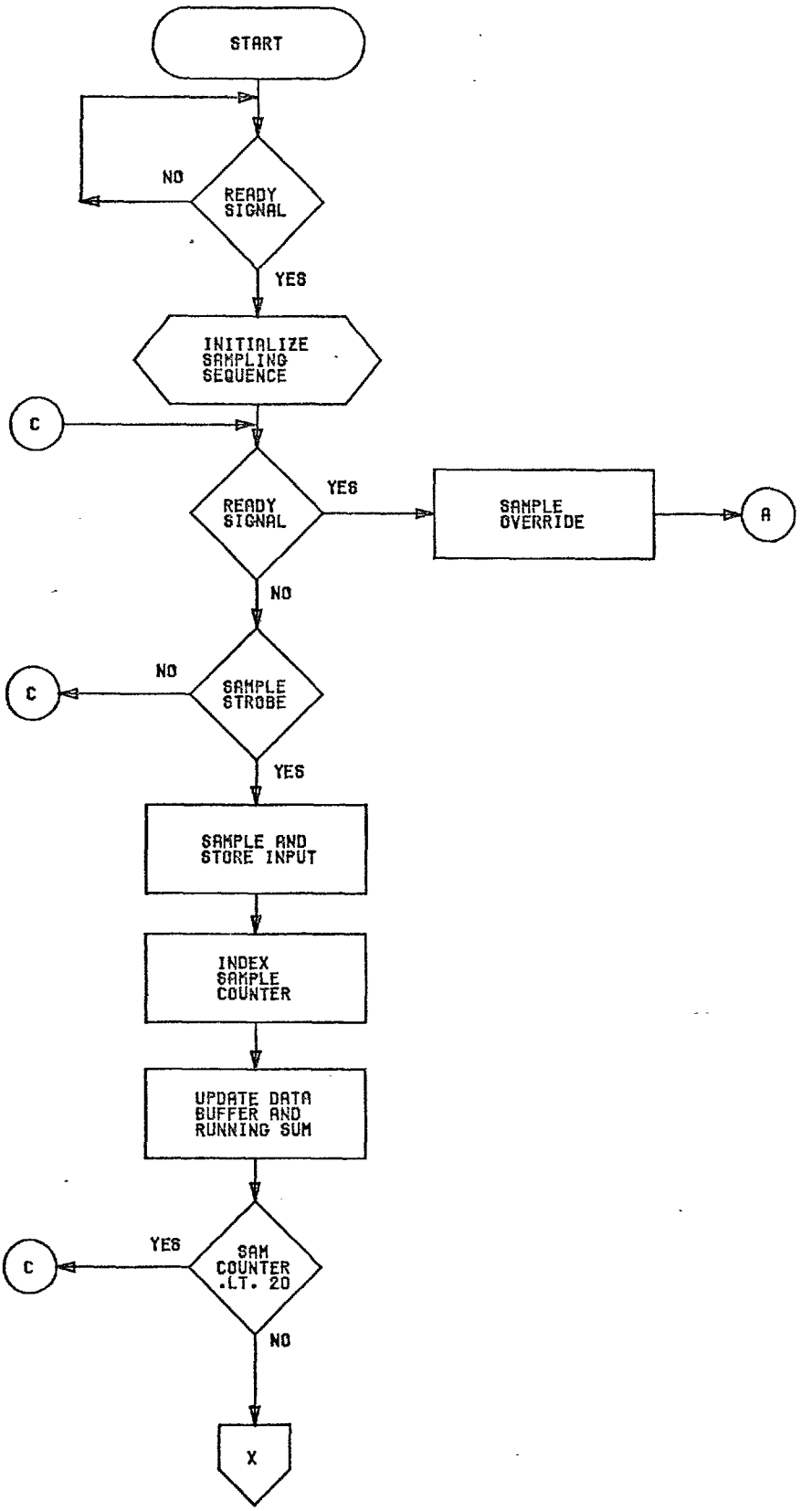

SAMPLE SUBROUTINE (CONTINUED)

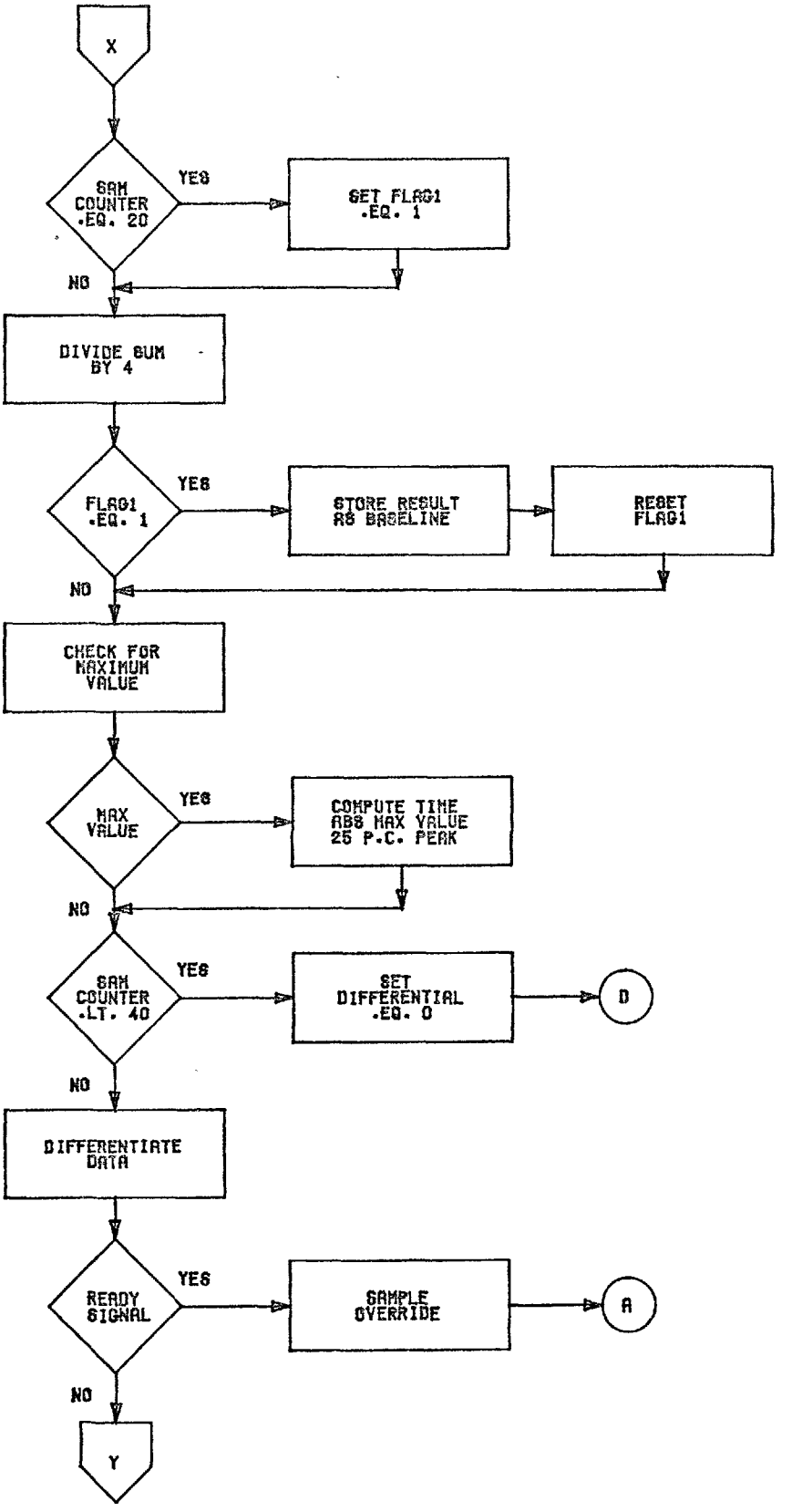

SAMPLE SUBROUTINE (CONTINUED)

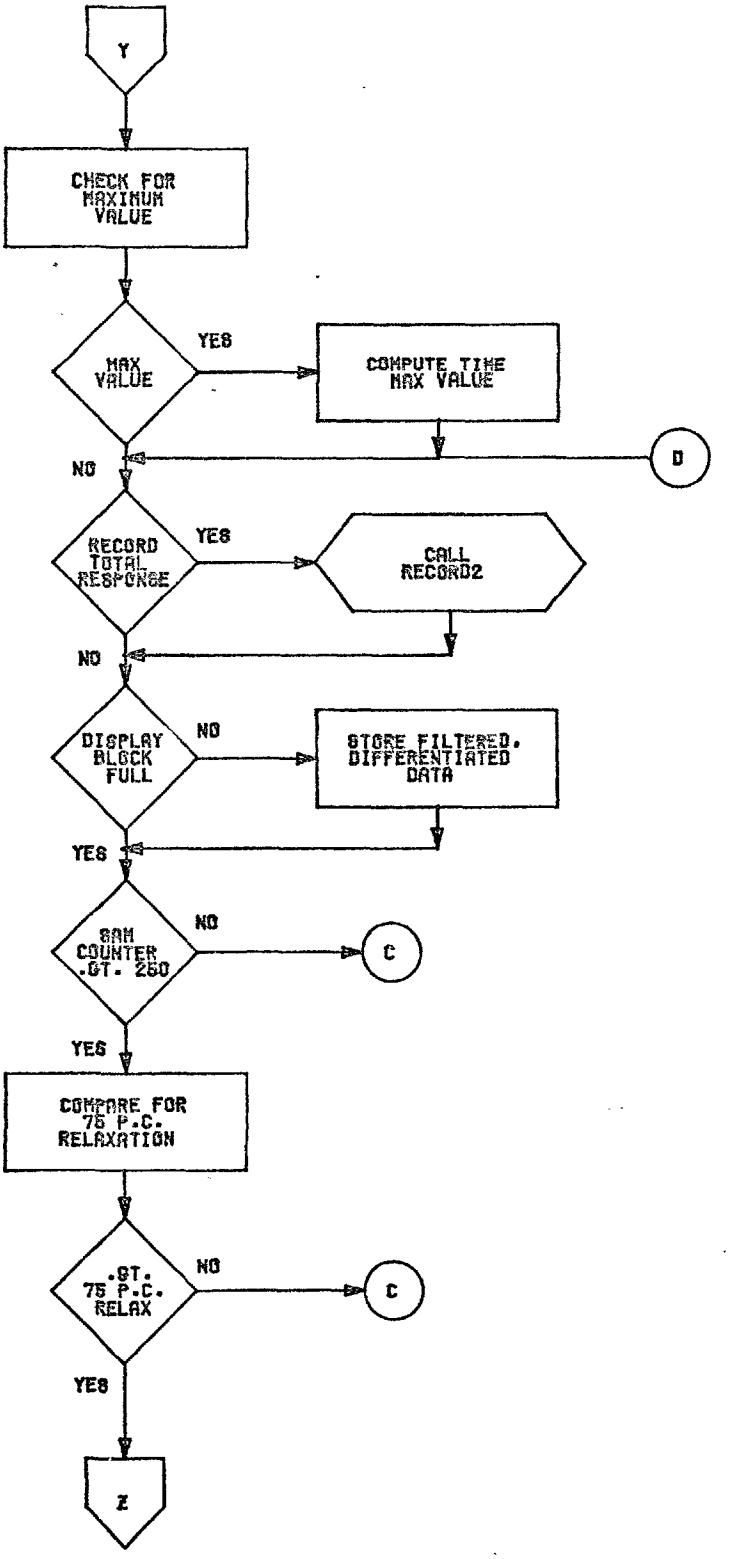

SAMPLE SUBROUTINE (CONTINUED)

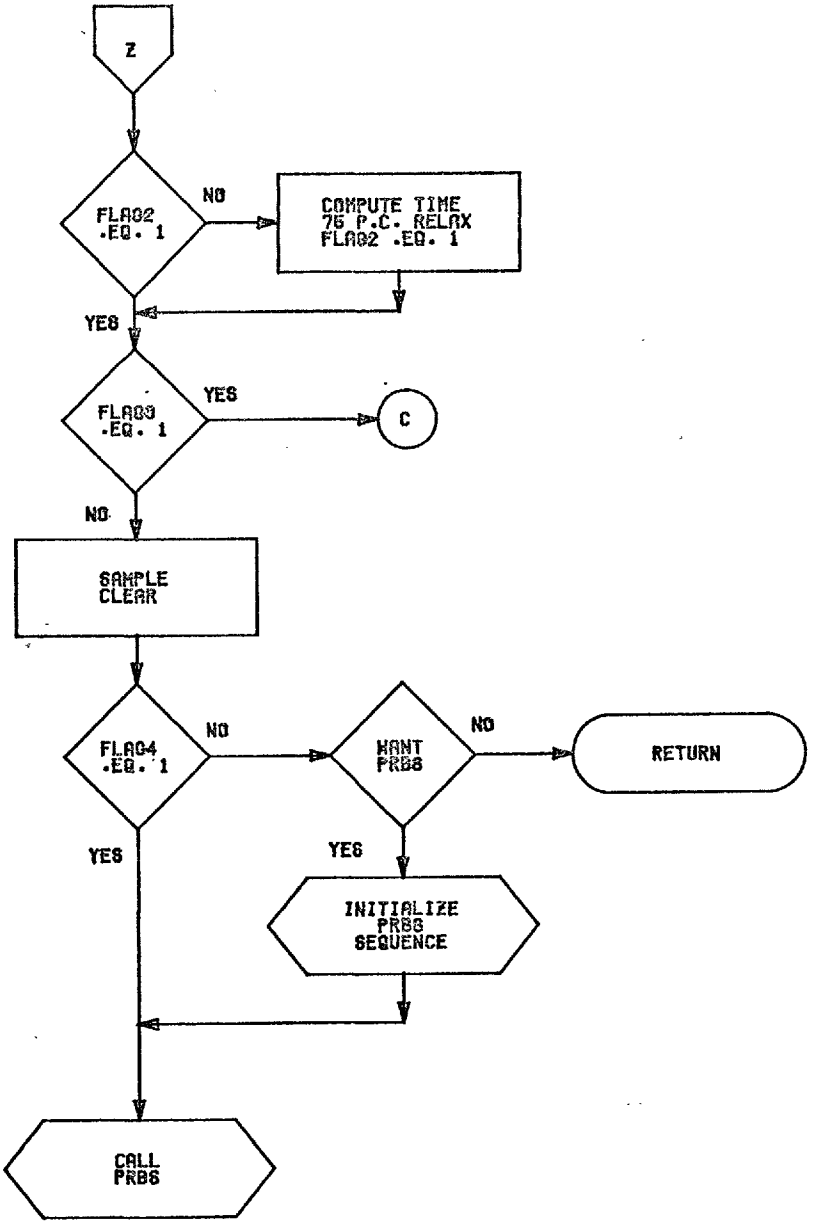

RECORD SUBROUTINE

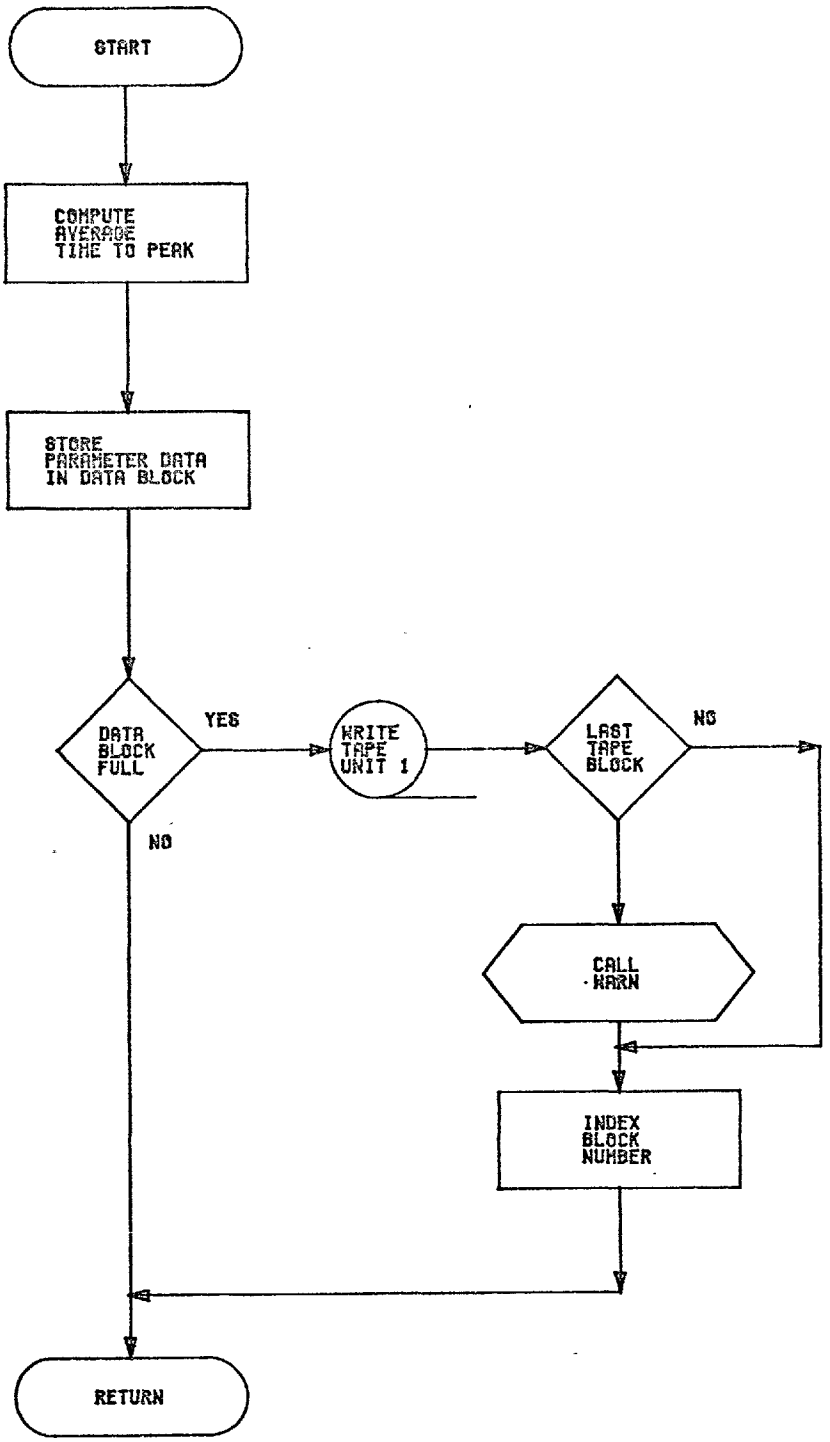

RECORD2 SUBROUTINE

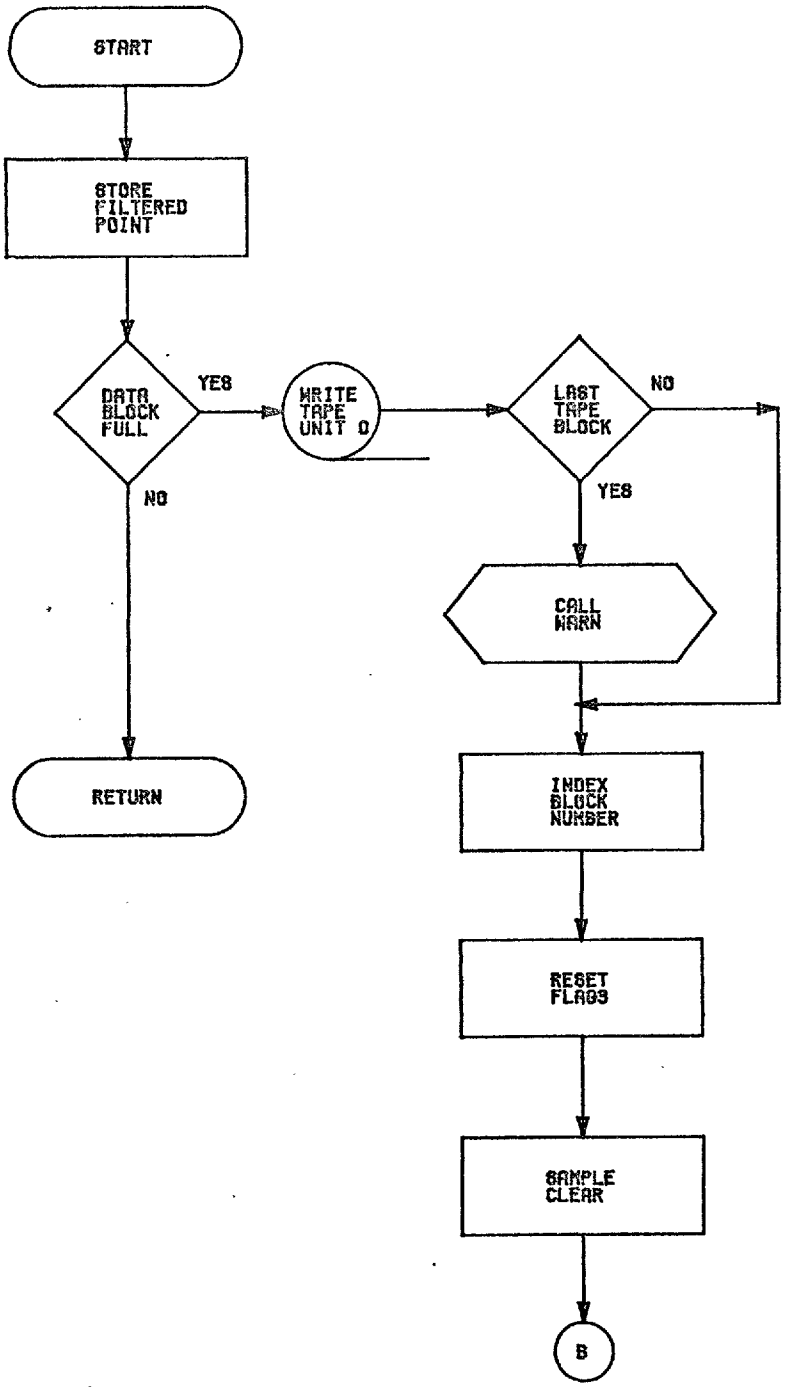

APPENDIX F

PSEUDO-RANDOM SUBROUTINE FLOW CHART

The pseudo-random subroutine was also written in LAP6-3L. It could be called up at any time by raising external sense line switch 3 at the interface. Once the subroutine was entered, all operations - superfusion valve switching and data recording - were carried out automatically by the computer. At the end of the p.r.b.s., the superfusion valves were returned to their initial position with the control solution perfusing the muscle, and the subroutine was then exited. If for any reason the sequence had to be aborted, this could be done by raising external sense line switch 4 at the interface.

Two separate programs were written incorporating the p.r.b.s. subroutines. One was used to generate a 255-point M-length p.r.b.s. (the one described in the flow chart), and the other to generate a 510-point inverse-repeat sequence based on the 255-point sequence. Consequently, if the sequence was to be changed from one to the other, it was necessary to reload the computer with the appropriate program.

In the 255-point subroutine, the sequence was allowed to go through one complete cycle before the data was recorded. With the 510-point sequence, the data was recorded after the subroutine was 100 points into the sequence. Recording was then carried out over 255 and 510 muscle contractions respectively. This initial delay in recording was to allow any start-up transients in the preparation to have decayed before measurements were made (Godfrey, 1969).

The actual p.r.b.s. was coded into the recorded data structure by making the measured absolute maximum value of tension (A.M.V.T.) negative

whenever the p.r.b.s. output was "0", and by leaving it as a positive value whenever the output was "1". Later, in the off-line analysis, the p.r.b.s. was separated from the tension values before the two signals were crosscorrelated.

PSEUDO-RANDOM SUBROUTINE

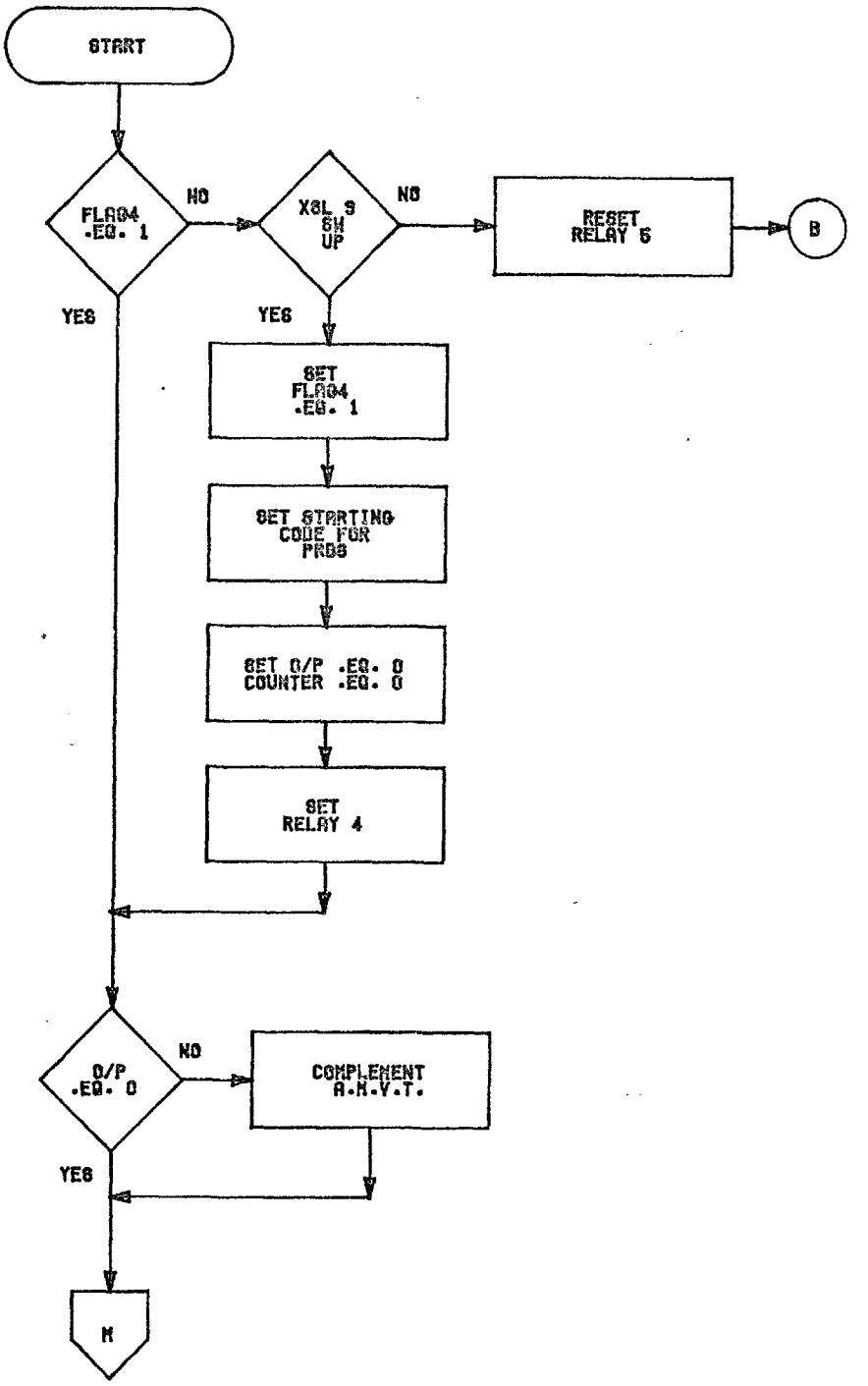

PSEUDO-RANDOM (CONTINUED)

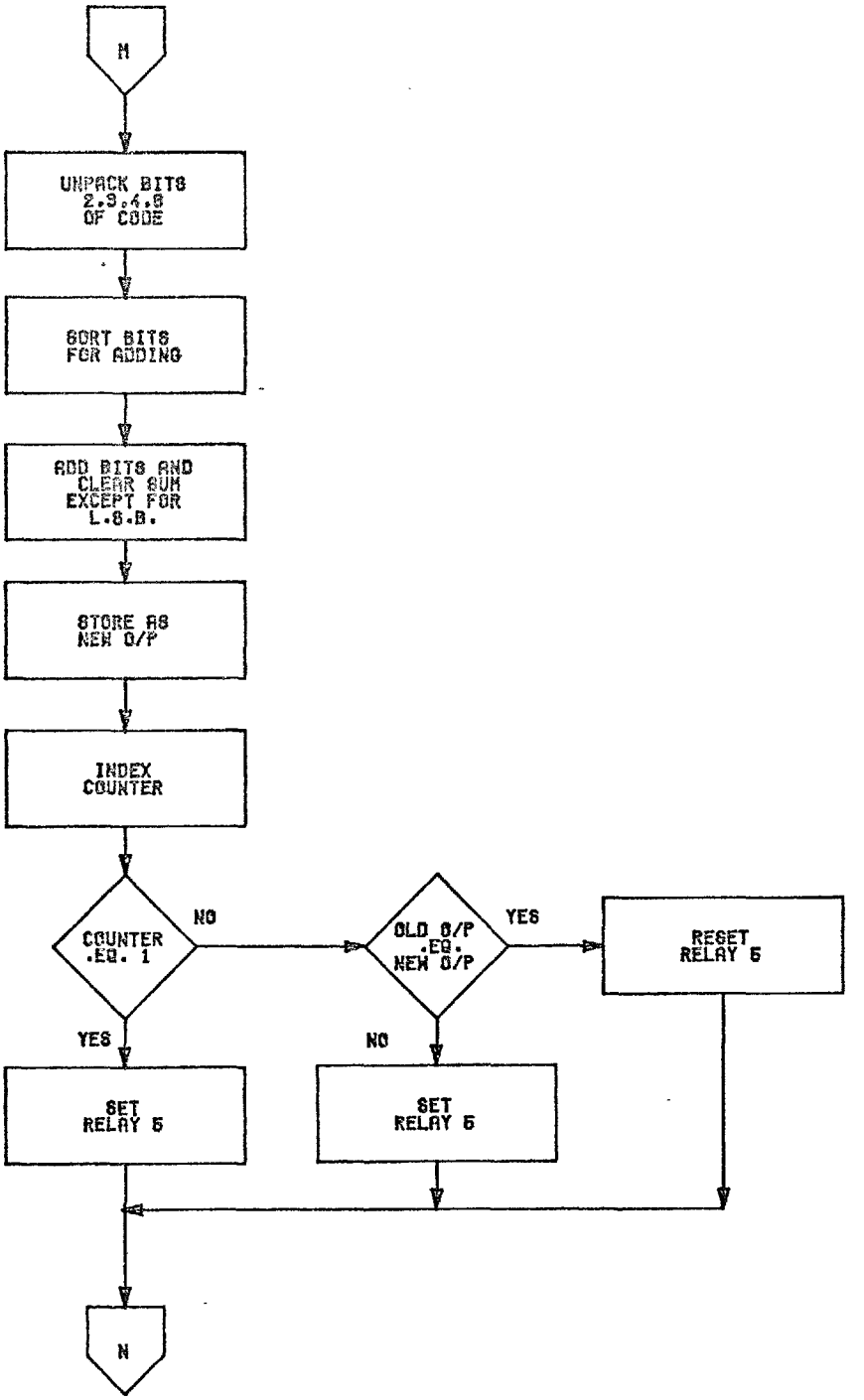

PSEUDO-RANDOM (CONTINUED)

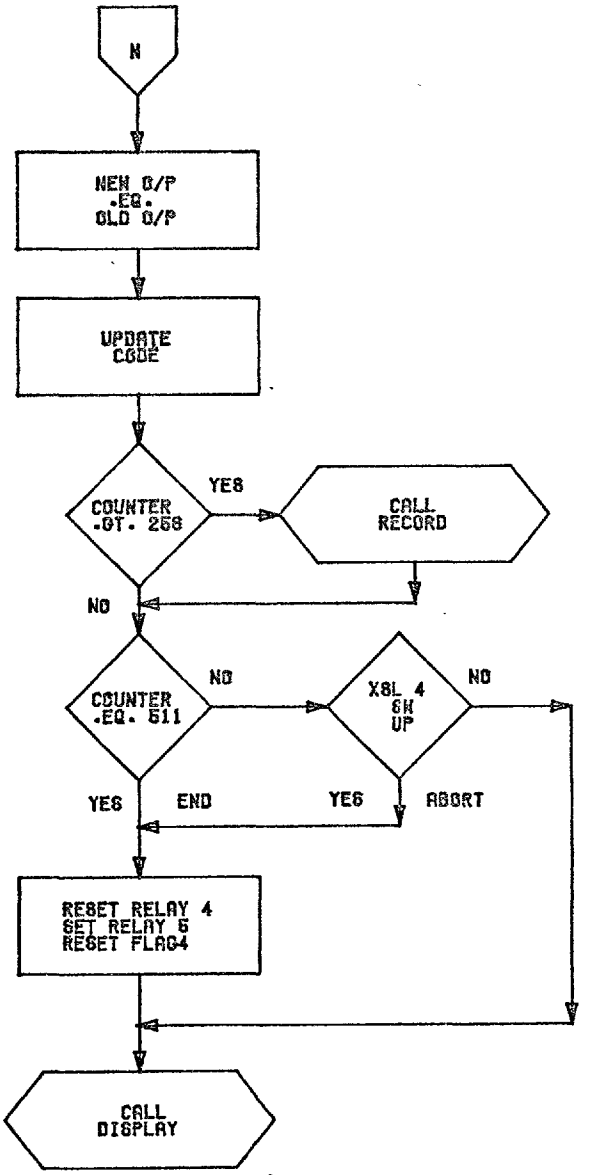

APPENDIX G

SUPERFUSION ELECTRONIC CONTROL SYSTEM

G.1 Introduction

If the superfusion system is to be used for step changes in calcium concentration and pseudo-random studies, then a method of accurately controlling the switching of the superfusion valves is required with facilities for both manual operation and remote computer control. Such a system was designed and will be described in detail in the next section.

There are two unique design features incorporated into the control electronics. One is that the circuit operation is centered around the control of mains voltage using triacs and zero-voltage-switches to eliminate switching transients. The other is the inclusion of an adjustable delay between the time one valve is switched off and another is switched on. This breaks the flow pattern of the perfusate and improves the exchange characteristics of the fluid around the muscle.

G.2 Principle of Operation

With reference to Fig. G.1a, consider the system to be in the following initial condition; the Delay one-shot (OS) is off ($\overline{Q}$ output is a logical "1"); Flip-Flop 1 (FF 1) is on ($\overline{Q}$ output is a logical "0", and Q is "1"); and FF2 is off (Q is "0" and $\overline{Q}$ is "1"). The combined effect of the states of these logic elements is to enable gate G1, and disable gates G2 and G3. As a result, there is a "0" output at point X of Fig. G.1a, and a "1" output elsewhere. This logical "0" enables the CA3079 zero-voltage-switch (Fig. G.1b) so that pulses can occur at pin 4,

each time the line voltage crosses zero. These pulses trigger the one-shots in the triac-drive-circuit which turns on the triac. See Appendix I for a detailed description of this circuit operation.

When a signal is applied to the isolated-input trigger circuit, either by manually pushing the MAN TRIG switch, or by applying a negative voltage pulse or level to the EXT TRIG input, there is a corresponding emission of light from light emitting diode 1 (LED1). This light is detected by a photodiode which in turn triggers the Delay OS. The "0" output from $\overline{Q}$ disables gates G1, G2, and G3 which turns off all the triacs. In addition to acting as a delay, the Q output of the Delay OS also acts as the "clock" pulse for the Master-Slave J-K Flip-Flops.

As J-K Flip-Flops are designed not to be triggered until the trailing edge of the clock pulse, one of two things can happen at the end of the delay time: i) If the J-K lines of FF2 are earthed, either externally, or through the solution-selector switch (switch at SOLUTION 1-2, Fig. G.1a, and also timing diagram Fig. G.2a), then that flip-flop is prevented from changing state. Thus $\overline{Q}$ is still "1" enabling G1 and G2. On the other hand, the J-K lines of FF1 are constantly enabled. Therefore, at the end of the delay, the clock pulse causes FF1 to change states making $\overline{Q}$ a logical "1" and Q a logical "0". Also $\overline{Q}$, of the Delay OS, has returned to a logical "1". Subsequently, gate G2 is enabled while G1 and G3 are disabled. This causes a "0" output at point Y of Fig. G.1a, and the triac for solution 2 is turned on. As long as the J-K lines remain earthed, each time the circuit is triggered the solutions switch alternately between solution 1 and 2 as FF1 shifts from one state to the other.

ii) However, if the J-K lines of FF2 are raised to a logical "1" (selector switch at SOLUTION 3, Fig. G.2b) the next clock pulse has the effect of turning FF2 on. In this state Q is "1" enabling G3, while $\overline{Q}$, which is "0",

disables G1 and G2. The "0" output from G3 (point Z of Fig. G.1a) enables the triac drive-circuit for Solution 3 and turns that valve on.

With the next trigger pulse, the "1" output from Q of FF2 combined with the "1" from the "clock" pulse enables G4. This generates a "clear" signal which resets both FF1 and FF2, i.e. Q is made a logical "0" and $\overline{Q}$ a logical "1".

Now providing that the J-K lines of FF2 remain at a logical "1", the trailing edge of the "clock" pulse turns FF2 on again permitting solution 3 to resume its flow. If, on the other hand, the J-K lines were set to "0" then the effect would be to keep FF2 off, and to turn on FF1, permitting solution 1 to flow.

From this description it is important to note the following points:

1) Each time a trigger pulse occurs, all the superfusion valves are turned off for the duration of the "clock" or delay pulse. The duration of this pulse is governed by the RC time constant of the Delay OS, and it is adjusted to give a delay interval of 100 ms.

2) The solution-selector switch is the key factor in determining which valve is to be turned on. If the switch is set to SOLUTION 1-2, either manually or externally, then the perfusion flow will alternate between those two solutions with each trigger pulse. However, if the switch is set to SOLUTION 3, the flow will return to solution 3, if it was previously at either solution 1 or 2. The flow will then remain at solution 3 independent of any trigger pulse.

3) There is one restraint as to the combination of solutions that can be switched. It is impossible to switch directly from solution 3 to solution 2; all other combinations are possible.

Because three CA3079 zero-voltage-switches were used for controlling the triacs, it was not possible to run these circuits directly from the mains

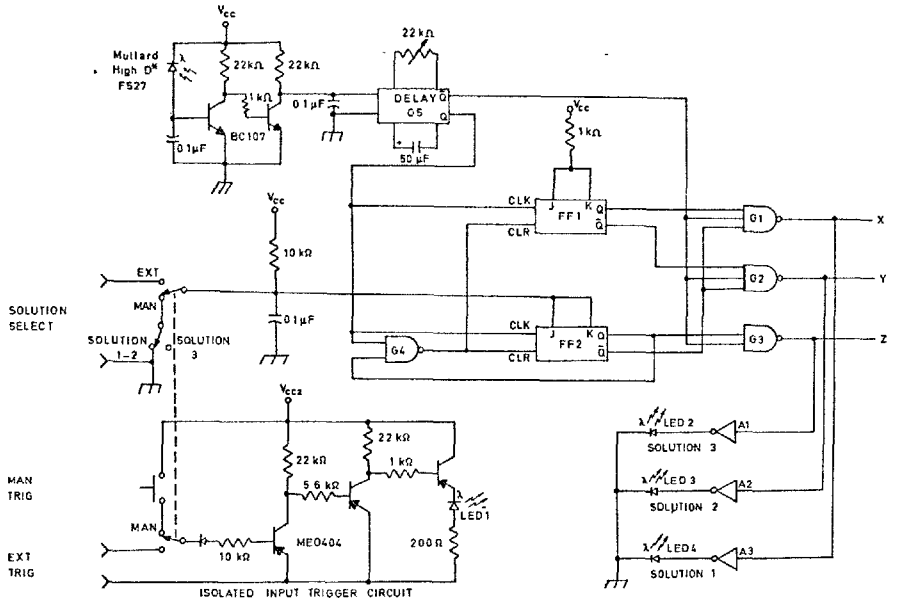

(a) DIGITAL CONTROL LOGIC

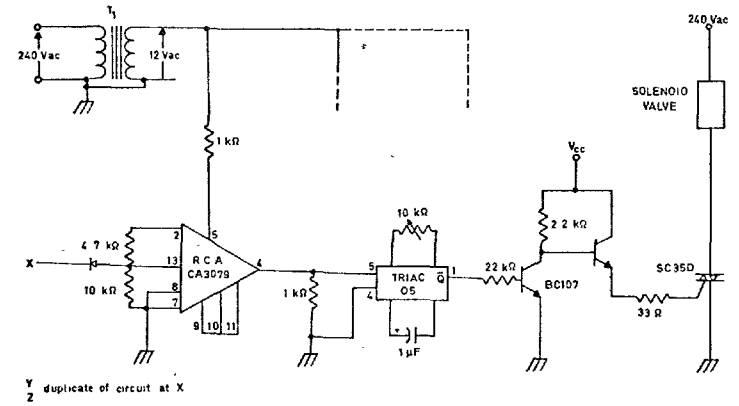

(b) ZERO-VOLTAGE SWITCH AND TRIAC DRIVE CIRCUIT

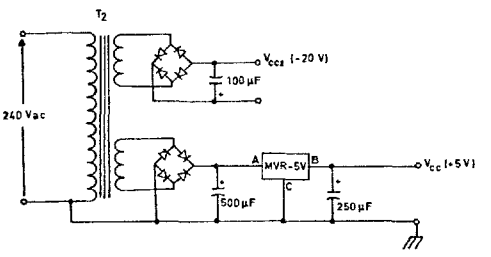

(c) POWER SUPPLY

A1, A2, A3	each 1/6	SN7404
G1, G2	each 1/3	SN7410
G3, G4	each 1/4	SN7400
FF1, FF2	each 1/2	SN7473
DELAY 05		SN74121
TRIAC 05		SN74121
LED1-4		H.P 5082-4403
T1	RS 12 V	sub-miniature mains transformer
T2	RS 12 V	miniature mains transformer

Fig. G.1 SUPERFUSION ELECTRONIC CONTROL SYSTEM

TIMING DIAGRAM FOR SOLUTION CHANGE

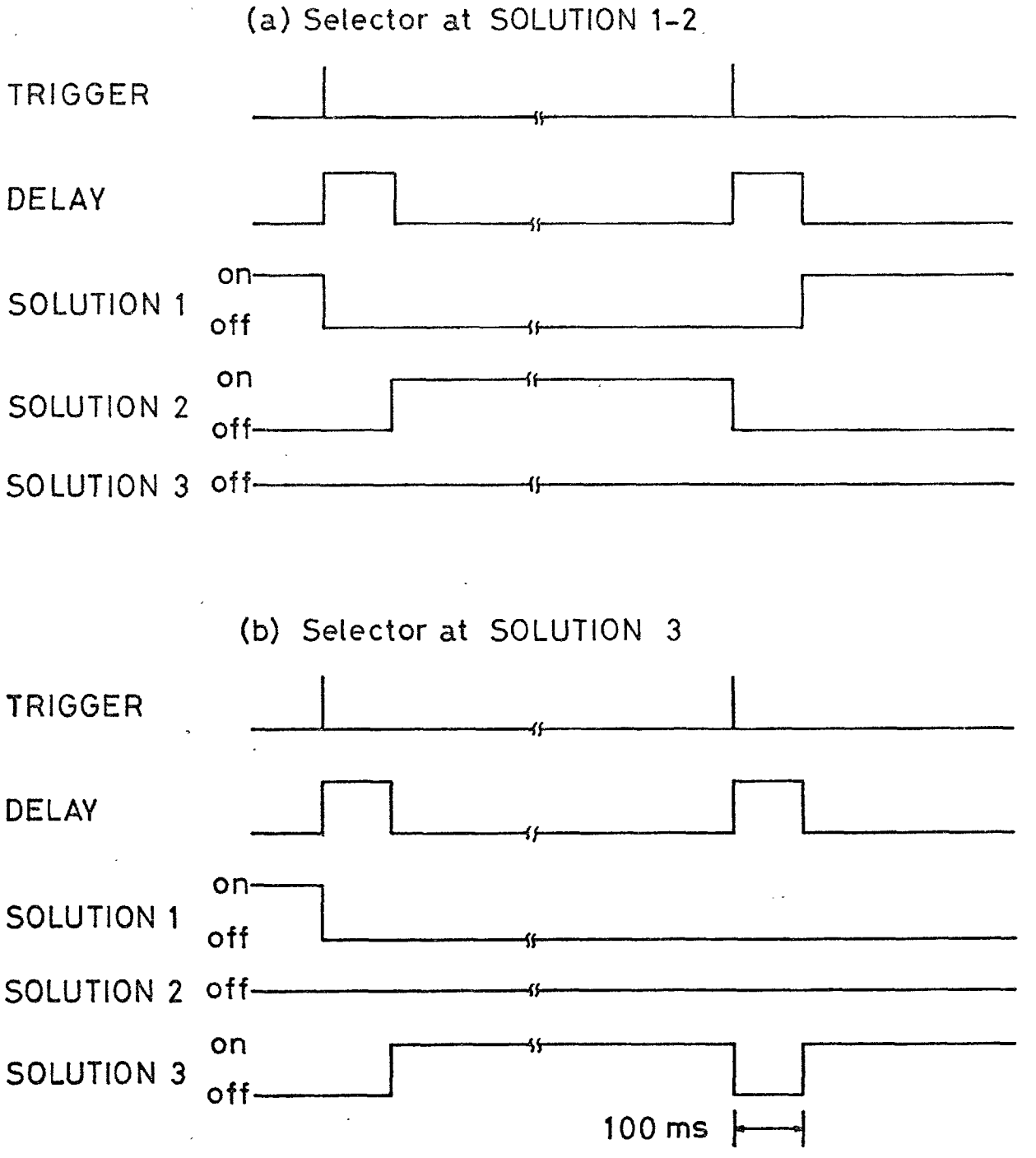

Fig. G.2

voltage as the total power dissipated in the dropper resistors (connected to pin 5) was in the order of 10 W. This generated excessive heat within the housing where this circuit was contained. However, this problem was overcome by dropping the mains voltage to 12 V ac by using a transformer (Fig. G.1b) before powering the CA3079s.

The duration of the pulses from the triac drive-circuit one-shots had to be adjusted individually. This was due to the fact that the impedance of the solenoids varied slightly from one to another, and also the transformer used to drop the mains voltage introduced a slight phase shift between its output voltage and the line voltage. It was found that a pulse width of between 7-8 ms was adequate for all of the solenoids.

The reason for using an optically-coupled input circuit was to isolate the logic circuitry and the triacs, which use the mains neutral as their reference, from the earth of the remainder of the experimental apparatus. It is important to note that the external connector of the solution-selector switch also takes its reference from the mains neutral. Therefore, it is necessary to isolate this connector from the computer lines with an additional relay (Fig. 3.1) for safety.

APPENDIX H

Computer simulation of tension transients

```
      PROGRAM TRY(INPUT,OUTPUT,TAPE5=INPUT,TAPE6=OUTPUT)
      DIMENSION CONCA(10),CONCR(11),ALPHA(20),EXPR(20),ZERO(20),D(11,20)
     1,TENSION(256),RAD(11),AREA(11),TITLE(8)
      READ(5,101)ZERO
      READ(5,101)D
  600 CONTINUE
      READ (5,100) DIFF,RADI,START,END,PMAX,COEF,RC
      IF (DIFF .LE. 0) STOP
      READ (5,105) TITLE
      WRITE (6,104) TITLE
      CONCR(11) =START
      RAD1 =RADI*10.
      AREA(1) =0.
      RAD(1) =0.
      DO 400 I=2,11
      RAD(I) =RAD(I-1) +RAD1/10.
      AREA(I) =3.1415*RAD(I)**2
      AREA(I-1) =AREA(I) -AREA(I-1)
  400 CONTINUE
      DO 500 I=1,20
      ALPHA(I) =-DIFF*10.0**-6*ZERO(I)**2/(RADI**2)
  500 CONTINUE
      STEP = 0.
      T =0.0
      DO 506 K=1,256
      DO 501 L=1,20
      EXPR(L)=EXP(ALPHA(L)*T)
  501 CONTINUE
C     SUM EACH TERM IN DIFFUSION EQUATION AT EACH RADIUS
      DO 503 I=1,10
      SUM=0.
      DO 502 J=1,20
      SUM=SUM+D(I,J)*EXPR(J)
  502 CONTINUE
      CONCR(I)=1.0-2.0*SUM
      CONCR(I)=START+STEP*CONCR(I)
  503 CONTINUE
C     COMPUTE AVERAGE CONCENTRATION FOR EACH ANULUS
      SUM =0.
      DO 504 I=1,10
      CONCA(I)=(CONCR(I)+CONCR(I+1))/2.
C     COMPUTE TENSION FOR EACH ANULUS AND SUM
      TEN =PMAX+COEF*EXP(RC*CONCA(I))
      SUM =SUM +TEN*AREA(I)
  504 CONTINUE
      TENSION(K) =SUM/AREA(11)
      IF (K .EQ. 1) T =2.0
      IF (K .GT. 1) T =T+3.0
      STEP=END-START
      CONCR(11)=END
  506 CONTINUE
      WRITE (6,102) DIFF,RADI,START,END
      WRITE (6,103) TENSION
      GO TO 600
  100 FORMAT (7F10.4)
  101 FORMAT(10F8.5)
  102 FORMAT (1H ,10/,10X,20HDIFFUSION CONSTANT =,F10.4,11HE-6 CM**2/S/
     1       10X,8HRADIUS =,F10.4,3H CM/10X,
     2        24HSTARTING CONCENTRATION =,F10.4,11H MILLIMOLAR/10X,
     3       19HNEW CONCENTRATION =,F10.4,11H MILLIMOLAR)
  103 FORMAT (10/,10(2X,F10.4))
  104 FORMAT (1H1,5/,8A10)
  105 FORMAT (8A10)
      END
```

APPENDIX I

Med. & Biol. Eng. Vol. 10, pp. 532–535. Peter Peregrinus Ltd., 1972. Printed in Great Britain

AN ISOLATED TRANSIENT-FREE SOLID-STATE A.C. POWER SWITCH*

M. O. TOLL
Department of Physiology, University College, London, England

Abstract—An inexpensive electronic a.c. power switch has been developed for use in environments where switching transients cannot be tolerated. Transient suppression is achieved by using a zero-crossing voltage detector to gate a thyristor into conduction whenever the line voltage is zero. Optical coupling is used electrically to isolate the input-trigger circuit from the thyristor-gating circuit. An additional feature of this circuit is that highly inductive loads can also be switched without generating any transients.

1. INTRODUCTION

THE USE of mechanical means to switch a.c. power to a load can result in the generation of radio-frequency interference (r.f.i.) which can be propagated through the power lines or be radiated directly through the equipment. It is this type of interference that appears as noise in radio receivers, and as artefacts on oscilloscope traces. In addition, it may falsely trigger equipment.

With mechanical devices, this interference can be reduced by placing capacitor–resistor combinations across the contacts, but often the switching transients cannot be entirely eliminated. Semiconductor thyristors, however, offer a decided improvement over mechanical switches since, by their very nature, they eliminate two of the most common sources of r.f.i. generation—contact bounce and arcing.

2. PRINCIPLE OF OPERATION

2.1 *Transient suppression using a thyristor and a zero-voltage switch*

The main component of the device described here is a zero-voltage switch (z.v.s.) integrated circuit. This circuit contains a zero-voltage-crossing detector that generates an output pulse during each passage of the line voltage through zero. This output pulse can be applied directly to the gate of the thyristor to trigger it into its conduction state so that it applies power to the load. A fail-safe circuit and a differential amplifier are also contained within this integrated circuit to inhibit the output pulses when power is to be removed from the load.

When there is no power applied to the load, there cannot be any current flowing through it. Therefore, if the thyristor is triggered into its conduction state at a time when the line voltage is zero, no current can flow and, as a result, no switching transient will result.

Once conducting, the thyristor will commutate itself (turn off) as soon as the current passing through it is zero. Thus, with the removal of the gate trigger pulse, the thyristor will automatically turn itself off, and hence remove power from the load as soon as the instantaneous load current reaches zero. To sustain conduction, the thyristor must be triggered every halfcycle of the line voltage.

2.2 *Electrical isolation of the input-trigger circuit from the power switch*

A disadvantage of using thyristors to control

* *Received 17th October 1971*

KLINENBERG, J. R. and KIPPEN, I. (1970) The binding of urate to plasma proteins determined by means of equilibrium dialysis. *J. Lab. Clin. Med.* **75**, 503–510.
LIDDLE, L., SEEGMILLER, J. E. and LASTER, L. (1959) Enzymatic spectrophotometric method for determination of uric acid. *J. Lab. and Clin. Med.* **54**, 903–913.
LONSDALE, K. (1968) The formation of urinary calculi. *Brit. J. Hosp. Med.* 243–246.
LONSDALE, K. and SUTOR, D. J. (1968) Composition of urinary calculi by X-ray diffraction. *Brit. J. Urology* **XI**, 402–411.
LONSDALE, K. and SUTOR, D. J. (1968) Composition of urinary calculi by X-ray diffraction. *Brit. J. Urology* **XL**, 23–36.
PETERS, J. P. and VAN SLYKE, D. D. (1946) Quantitative clinical chemistry. 2nd edn. Vol. 1. Interpretations pp. 949–955. Williams & Wilkins, Baltimore.
PIERCE, W. C. and HAENISCH, E. L. (1948) Quantitative analysis. 3rd edn., p. 196. Wiley, New York.
PORTER, P. (1963) Physico-chemical factors involved in urate calculus formation: I-solubility. *Res. Vet. Sci.* **4**, 580–591.
PRIGOGINE, I. and DEFAY, R. (1954) Chemical thermodynamics. p. 131. Longmans, Green & Co., London.
RINGER, W. E. (1910) Über der Bedingungen der Ausscheidung von Harnsäure und Harnsäuren salzen aus ihren Losungen. *Z. Physiol. Chem.* **67**, 348–403.
RINGERTZ, H. (1965) Optical and crystallographic data of uric acid and its dihydrate. *Acta Cryst.* **19**, 286–287.
ROBERTS, W. (1892) The chemistry and therapeutics of uric acid gravel and gout. *Brit. Med. J.* **II**, 6–11.
SEEGMILLER, J. E. (1965) The acute attack of gouty arthritis. *Arthritis Rheum.* **8**, 714–725.
SEEGMILLER, J. E. (1966) Toward a unitary concept of gout. *Hospital Practice* **1**, 33–39.
SEEGMILLER, J. E. and HOWELL, R. R. (1962) Old and new concepts of acute gouty arthritis. *Arthritis Rheum.* **5**, 616–623.
SEEGMILLER, J. E., HOWELL, R. R. and MALAWISTA, S. E. (1962) The inflammatory reaction to sodium urate. *J. Am. Med. Assoc.* **180**, 469–475.
SEEGMILLER, J. E., LASTER, L. and HOWELL, R. R. (1963) Biochemistry of uric acid and its relation to gout. *New England J. Med.* **268**, 712–716, 764–773, 821–827.
STRICKLAND-CONSTABLE, R. G. (1968) Kinetics and mechanism of crystallization. Academic Press, London.
SUTOR, D. J. (1968) Difficulties in the identification of components of mixed urinary calculi using the X-ray powder method. *Brit. J. Urology* **XL**, 29–32.
SUTOR, D. J. (1968) Identification standards for human urinary calculus components, using crystallographic methods. *Brit. J. Urology* **XL**, 22–28.
YOUNG, E. G. and MUSGRAVE, F. F. (1932) The formation and decomposition of urate gels. *Biochem. J.* **26**, 941–953.
VON KANITZ, A. (1921) Die Bedeutung der zweiten Dissociationskonstante der Harnsäure für die Gleichgewichte der Monouratlösungen. *Z. Physiol. Chem.* **116**, 96–106.

SOLUBILITE DE L'ACIDE URIQUE ET DU MONOURATE DE SODIUM

Sommaire—On donne un traîtement théorique compréhensif des facteurs régissant la solubilité de l'acide urique et du monourate de sodium. On évalue les constantes diverses paraissant dans le traîtement, en fonction de la température, de la force ionique, en faisant usage à la fois des données existantes et des données expérimentales. La solubilité de l'acide urique augmente avec l'augmentation du pH, alors que la solubilité du monourate de sodium a un minimum de près de pH 7,7 à 37°C. Le produit de solubilité du monourate de sodium augmente avec la force ionique.

DIE LÖSLICHKEIT DER HARNÄSURE UND DES MONO-NATRIUMURATS

Zusammenfassung—Eine umfassende theoretische Behandlung der Faktoren, die die Löslichkeit der Harnsäure und des Mono-Natriumurats beherrscht, wird angeführt. Die verschiedenen Konstanten in der Behandlung als Funktionen der Temperatur und ionischen Stärke werden mit der Verwendung von bestehenden und neu-experimentellen Daten ausgewertet. Die Löslichkeit von Harnsäure vermehrt sich mit wachsendem pH, während die Löslichkeit von Mono-Natriumurat ein Minimum in der Nähe von pH 7,7 bei 37°C hat. Das Löslichkeit-Produkt des Mono-Natriumurats vermehrt sich mit wachsender ionischer Stärke.

power to a load is that the associated trigger circuitry requires the neutral power line as its common or reference line. This presents a problem when the thyristor circuit is to be triggered from an external source whose reference is independent of the neutral power line.

This difficulty is overcome by electrically isolating the input-trigger circuit from the thyristor-drive circuit with optoelectronics. Coupling between the two circuits is achieved by using a light-emitting diode in the input-trigger circuit, and a light-activated switch in the thyristor-drive circuit.

2.3 *Switching of inductive loads*

The previous description has been related mainly to resistive loads. If the load is highly inductive, some additional circuitry is required in order to maintain power to the load. As previously described, when power is first applied to the load, both the load voltage and current are zero. However, as the applied voltage begins to increase sinusoidally, the instantaneous current will increase in a predictable manner depending on the impedance of the load. Thus, if the load is inductive, a phase shift is introduced between the voltage and the current. This means that, when the load voltage reaches zero on completion of the first halfcycle, the load current can still have a substantial value. Now, since the voltage is zero, a gate-trigger pulse is generated by the z.v.s. to turn on the thyristor for the next halfcycle but, because the current has not yet reached zero, the thyristor is already on. By the time the current does reach zero, the gate trigger pulse has been removed and the thyristor is left off during the next halfcycle

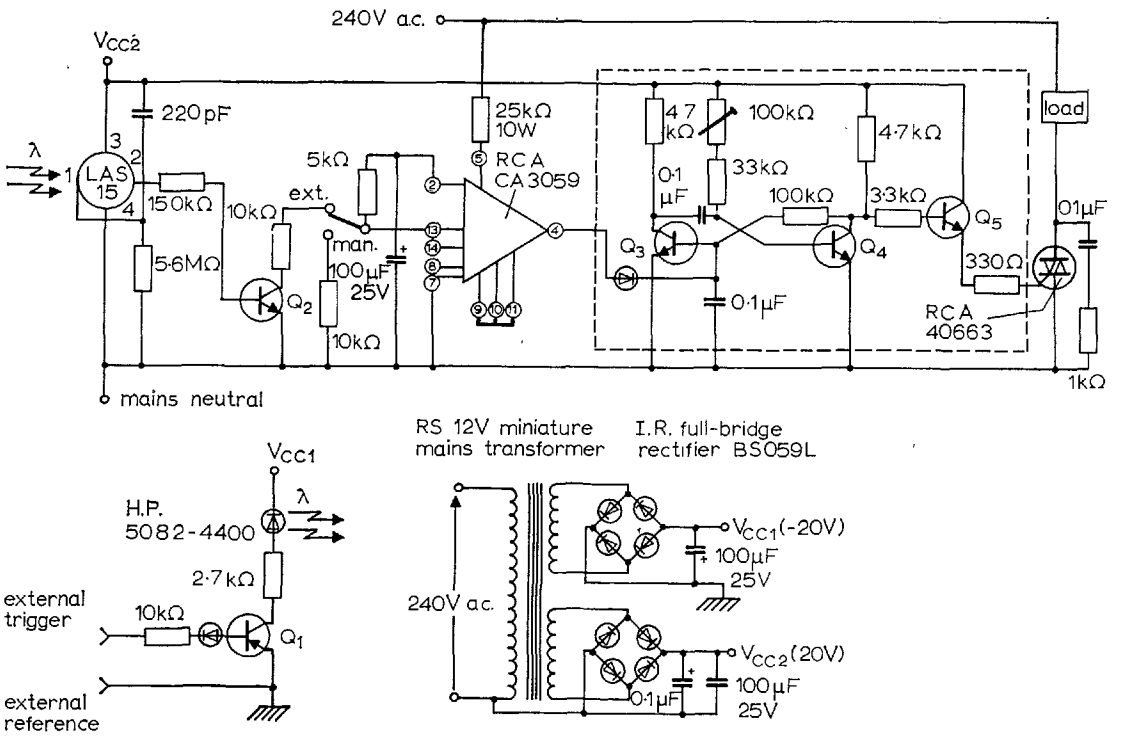

FIG. 1. Schematic of the isolated transient-free solid-state a.c. power switch. If the load is resistive, the circuit within the dotted box can be omitted. All resistors are 10%, 0·25 W unless otherwise stated. Q_1 ME0404; Q_2–Q_5 BFX52.

owing to self commutation. As a result, power is applied to the load only for half of the line-voltage cycle.

To overcome this problem, it is necessary to stretch the original gate-trigger pulse from the z.v.s. from its original 100 μs duration to a pulse approaching 5 ms. With the insertion of a univibrator between the z.v.s. output and the thyristor gate, phase shifts of up to 90° can be accommodated.

3. CIRCUIT DESCRIPTION

3.1 *Input-trigger circuit*

The input-trigger circuit (Fig. 1) is optically coupled to the thyristor-drive circuit by the use of a light-emitting diode (Hewlett-Packard 5082-4400), and a light-activated switch (RS Components Ltd. LAS 15). These two components are housed in a $1{\cdot}2 \times 2$ cm phenolic rod which has been drilled out to accommodate the two units. This ensures minimal interference from ambient lighting, and also complete electrical isolation between the two circuits to eliminate any possible shock hazard.

The main advantages of a light-emitting diode over an incandescent bulb are its high reliability, low drive power (less than 15 mW), and fast switching time (10 ns). The light-activated switch is a medium-speed (20 kHz frequency response) Schmitt trigger type of integrated circuit whose sensitivity to light levels can be adjusted by changing the values of an external capacitor-resistor combination. With the component values shown in Fig. 1, the trigger circuit is activated with a negative input d.c. level or pulse as low as 2 V.

3.2 *Thyristor-drive circuit*

The thyristor-gate-trigger pulses are derived from a zero-voltage switch (RCA-CA3059) integrated circuit. The output pulses can be inhibited or enabled depending upon the voltage level present on pin 13 of the CA3059. If the voltage is greater than +6 V, the output is inhibited, but, if it is between +3 and 5 V, the output is enabled. To set the mode of operation, an s.p.d.t. switch is used to select either external triggering or manual triggering of the circuit.

If only resistive loads are used, the output of the CA3059 (pin 4) can be connected directly to the gate of the thyristor (RCA 40663 triac). However, if inductive loads are to be used, a univibrator must be connected between pin 4 and the thyristor gate. The power supply for this univibrator is the same as that used to supply the LAS 15.

4. CIRCUIT PERFORMANCE

The maximum a.c. power that can be delivered to a load is limited by the current rating of the thyristor. In the case of the RCA 40663 thyristor and a line voltage of 240 V a.c., the maximum power is 7·2 kW. For most experimental applications the load being switched is

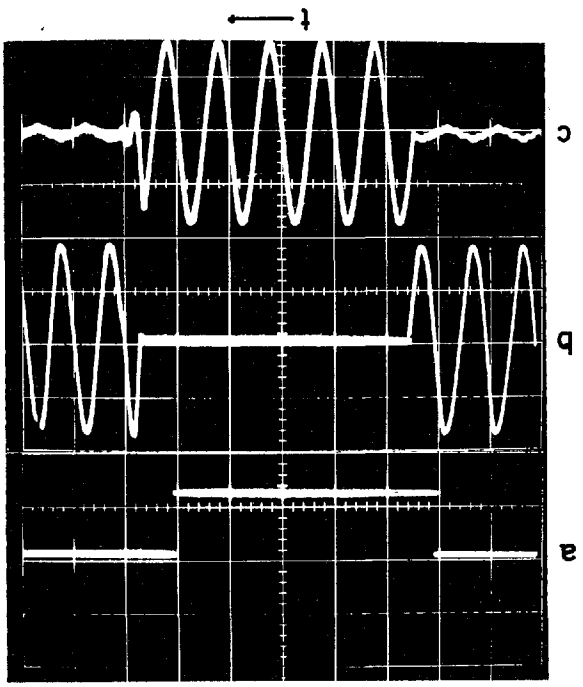

FIG. 2. Typical response of a.c. power switch as related to an input-trigger pulse.

Horizontal scale is 20 ms/division
a Input-trigger pulse (10 V/division)
b Triac voltage (200 V/division)
c Load voltage (200 V/division)

less than 1 kW, so that a thyristor of lower rating can replace the one used here.

Although there is no delay in the activation of the input-trigger circuit, there can be a delay of up to half a voltage cycle (i.e. 10 ms for a 50 Hz line frequency) before power is supplied to the load. This is due to the absence of any form of synchronisation between the input signal and the time the line voltage passes through zero. If the input signal is applied later than 50 μs after the line voltage reaches zero, no output pulse will appear from the CA3059, and the thyristor will have to wait for the next halfcycle before it can be switched on.

The removal of the gate-trigger pulses will result in the thyristor turning off as soon as the load current passes through zero. Thus, with highly-inductive loads, a turnoff-delay time of up to 5 ms can occur. A typical response of the circuit to an input signal is shown in Fig. 2. If there is a large phase shift present, a large voltage can be applied instantaneously across the thyristor at the time of commutation. This sudden rise of voltage can cause the thyristor to break down and continue to conduct. A series resistor–capacitor network is therefore required across the thyristor to limit the rate of rise of voltage.

5. CONCLUSIONS

The use of mechanical devices to control a.c. power to a load can result in enormous switching transients being generated. At best, these transients are annoying and, at worst, they can be hazardous. To overcome this difficulty, an isolated, transient-free, solid state, a.c. power switch has been developed for use in environments such as hospitals and laboratories where switching transients cannot be tolerated. Using inexpensive, readily available components, this device can be made small enough to be held in the hand.

In a hospital environment, this switch could be used as part of a fault detector to isolate faulty equipment before a fatal shock situation could develop. It could also be used in an explosive atmosphere, where a spark generated by normal mechanical switching could cause an explosion.

In our laboratory, this power switch has replaced a relay that controlled power to a solenoid valve. As a result, false triggering of equipment and artefacts due to switching transients have been eliminated.

Acknowledgment—The author is the holder of a Canadian Heart Foundation Fellowship. The work was carried out with the aid of the British Heart Foundation.

UN COMMUTATEUR ISOLE NON-TRANSITOIRE ETAT-SOLIDE COURANT ALTERNATIF

Sommaire—On a développé un commutateur électronique à courant alternatif bon marché pour usage dans des milieux où les commutateurs transitoires ne peuvent pas être tolérés. L'antiparasitage transitoire est obtenu par l'usage d'un détecteur de voltage zéro-croisant qui barre un thyristor en conduction dès que le voltage de ligne est zéro. Un couplage optique est utilisé pour isoler électriquement le circuit du déclencheur d'entrée de courant du circuit barreur du thyristor. Un autre trait de ce circuit est qu'il est possible de commuter des charges fortement inductives sans générer des transitoires.

EIN EINZELNER, EINSCHWINGFREIER, ALL-TRANSISTOR WECHSELSTROMNETZSCHALTER

Zusammenfassung—Ein billiger elektronischer Wechselstromnetzschalter ist entwickelt worden für den Gebrauch in Umgebungen wo Schaltstöße nicht geduldet werden können. Die Unterdrückung der Schaltstöße wird erreicht durch die Verwendung eines Nullkreuzung-Spannungsdemodulators, der einen Thyristor anschaltet, wenn die Leitungsspannung bei Null liegt. Optische Kopplung wird für die elektrische Isolation der Eingangstrigger-Schaltung von der Thyristor-Auswertung Schaltung verwendet. Eine zusätzliche Eigenschaft dieser Schaltung besteht aus der Tatsache, daß hochinduktive Lasten auch umgeschaltet werden können, ohne Schaltstöße zu erzeugen.

Med. & Biol. Eng. Vol. 10, pp. 536–541. Peter Peregrinus Ltd., 1972. Printed in Great Britain

ADVANTAGES OF SYMMETRICAL ISOLATION TRANSFORMERS IN THE REDUCTION OF PATIENT HAZARDS*†

A. M. KLOMP and J. H. M. LUCAS
Medical Systems Division, N. V. Philips Gloeilampenfabrieken, Eindhoven, Netherlands

Abstract—A brief outline is given of the various advantages and disadvantages of using isolation transformers in conjunction with equipment connection to patients. Particular attention will be paid to the use of symmetrical isolation transformers.

IN RECENT years, the subject of isolation transformers used in medical practice has received a lot of attention in the technical literature. Their use has been advised and rejected, both on technical grounds and for economic reasons. Nevertheless, their use has been recommended in a few national standards dealing with safety in medical practice such as: VDE 0107/3.68 (W. Germany), NFPA 76 BM 1971 (USA), Règlement de Sécurité U 58 (France) and IEC SC62A–WG2 (Secr.) 16th August 1971 (Draft).

Fig. 1 shows the usual isolation-transformer circuit supplying power to portable medical electrical equipment provided with a mains input transformer.

It provides a floating power source for medical equipment via a permanently installed isolation transformer with double insulation between the coils. Shown here is a circuit with one piece of equipment connected to it. More equipment may be connected to an isolation transformer but an insulation breakdown from one of the power conductors to the protective earth will then cause all the equipment, instead of just one unit, to be supplied from a nonfloating power source. Moreover, finding the location of the insulation breakdown becomes more difficult.

Usually, the floating circuit is provided with an insulation-monitoring device.

This evaluates the insulation condition of the floating circuit with respect to earth and, when a certain limit is reached, a visual and/or an audible alarm signal is given.

The main advantage of using isolation transformers is in maintaining continuity of the supply of electric power to vital equipment in the case of a first failure in the insulation of the intermediate circuit to earth.

Such vital equipment may be, for example, life-supporting equipment such as heart–lung machines, equipment in the operating theatre, intensive-care and coronary-care units.

It must, however, be pointed out that this advantage is not as great as it may seem. First, it covers only one of many possible failures which may interrupt the supply of power to equipment and, secondly, the likelihood of an insulation failure may be reduced substantially by careful, periodic inspection and the use of double or reinforced insulation in the mains circuit.

In some older hospitals, it may be difficult to achieve potential equalisation in critical areas by connecting all conductive parts, such as water and gas pipes and equipment, to a protective-

* *Received 20th October 1971*

† This paper is based on a paper given by the author to the EUROCON 71 conference held at Lausanne, Switzerland, from the 18th to 22nd October 1971